Instituto Universitario de Ciencia de Materiales Nicolás Cabrera

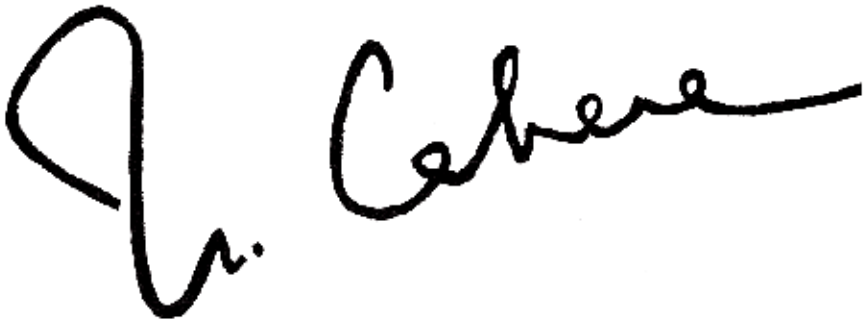

Campus Internacional de excelencia UAM CSIC

UAM UNIVERSIDAD AUTÓNOMA DE MADRID

FACULTAD DE CIENCIAS
UNIVERSIDAD AUTÓNOMA DE MADRID

INSTITUTO NICOLÁS CABRERA

Índice

Madrid, 15 de julio de 2013

Estimado lector:

En estas páginas encontrará una recopilación de los artículos de D. Nicolás Cabrera.

La ocasión del centenario de su nacimiento en 1913 nos ha parecido adecuada para re-editar este grupo de artículos, compilado hace casi dos décadas por el entonces equipo directivo del Instituto Nicolás Cabrera.

La mayoría de los actuales miembros del Instituto no tuvimos la suerte de conocer al Profesor Cabrera. Gracias a su trabajo y al de sus colaboradores, hemos tenido la ocasión de contagiarnos de la pasión por la Física que le caracterizaba, y de beneficiarnos de su tarea como organizador. Los éxitos de la Física en la Autónoma son el fruto del trabajo inteligente de los que crearon estructuras técnicas y administrativas que facilitan el trabajo del investigador. Nuestro reto es modernizar estas estructuras, impulsando la excelencia y el conocimiento. Volver a leer los trabajos del Profesor Cabrera y transmitirlos a nuestros estudiantes es sin duda una buena forma de comenzar. Y no somos los únicos, algunos de los trabajos que recogemos aquí han sido citados más de 500 veces entre 2009 y 2012, y siguen influyendo en temas de la mayor importancia tecnológica, como la oxidación de superficies o el crecimiento de cristales.

Le deseo una lectura agradable de estos artículos, y espero que le sean útiles en su trabajo como profesor e investigador.

Hermann Suderow
Director del Instituto de Ciencia de Materiales Nicolás Cabrera

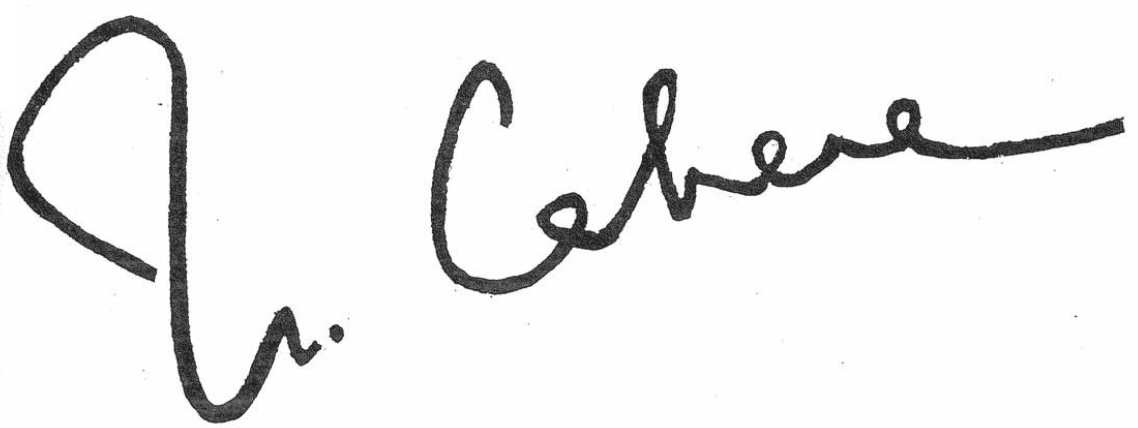

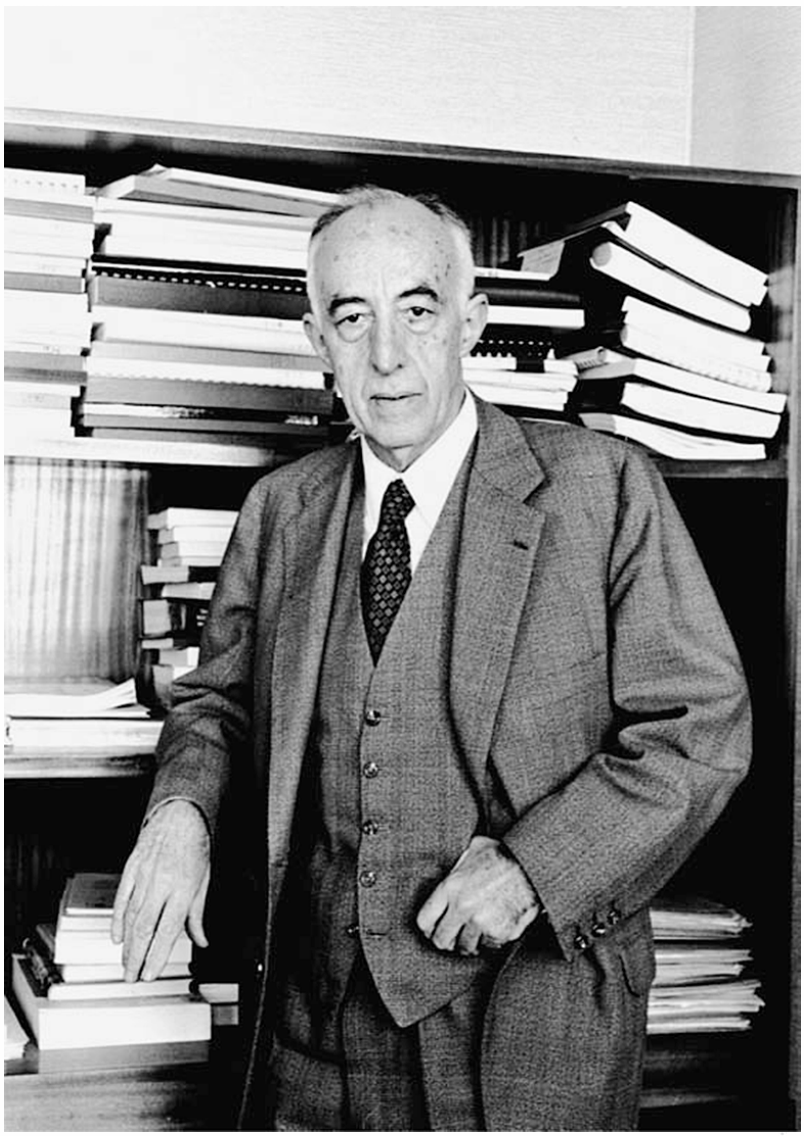

1

CABRERA N.
SUR L'OXIDATION DE L'ALUMINIUM ET L'INFLUENCE DE LA LUMIÈRE.
COMPTES RENDUS 220, 111 (1945).

Note de M. **Nicolas Cabrera**, présentée par M. Albert Pérard.

1. On sait qu'il se forme sur l'aluminium une couche d'oxyde (Al^2O^3) dont l'épaisseur croît d'abord très rapidement, ensuite lentement, pour arriver après trois mois à $\simeq 7^{m\mu}$ avec une vitesse de croissance de $0^{m\mu},2$ à $0^{m\mu},3$ par mois. Mott (1) a donné une théorie en admettant que l'oxydation est commandée par le passage des électrons libres du métal à la bande de conductibilité de l'oxyde (différence d'énergie Φ), suivi de leur diffusion jusqu'à la surface oxyde-air. L'accroissement rapide du début est dû à ce que, pour des épaisseurs faibles, les électrons peuvent traverser cette barrière de potentiel directement par *effet tunnel* quantique. Dans le tableau ci-dessous (I) nous donnons, en fonction de Φ, les épaisseurs x calculées, pour lesquelles $dx/dt = 0,25$ mμ/mois $\simeq 10^{-7}$ mμ/sec.

Épaisseurs calculées (*en* mμ) *pour lesquelles* $dx/dt = 10^{-7}$ mμ/sec (observées $\simeq 7$ mμ).

	I. Effet tunnel.	II. Effet thermique.			III.
Φ eV.		T = 300° K.	T = 400° K.	T = 500° K.	Effet photoél. (10^{-4} rayonn. sol.).
1	4,0	5.	5.10^4	10^7	5.10^2
1,5	3,4	10^{-10}	10^{-2}	10^2	10^2
2	3,0	5.10^{-17}	10^{-8}	10^{-3}	5.10
2,5	2,7	10^{-25}	10^{-14}	10^{-8}	10

On voit que l'effet tunnel n'est pas suffisant pour rendre compte des épaisseurs limites observées.

2. A la température ambiante et au-dessus, et pour des valeurs faibles de Φ, l'énergie thermique est suffisante pour faire passer les électrons du métal à la bande de conductibilité de l'oxyde. La théorie de ce mécanisme conduit à une loi de la forme

$$(1) \qquad \frac{dx}{dt} = \frac{n\Omega D}{x}, \qquad n = \frac{2(2\pi mkT)^{\frac{3}{2}}}{h^3} e^{-\frac{\Phi}{kT}},$$

où n est le nombre d'électrons par cm³ dans la bande de conductibilité de l'oxyde, en équilibre avec le métal à la température T, Ω le volume d'oxyde par électron libéré ($\simeq 10^{-22}$ cm³), et D la constante de diffusion des électrons ($\simeq 0{,}25$ cm²/sec). D'après le tableau (II), et pour obtenir à T $\sim 300°$ K. des épaisseurs de $\sim 7^{m\mu}$, il suffit d'admettre que $\Phi \sim 1$ eV; c'est ce qu'a supposé Mott. Or, d'après ce même tableau, et avec $\Phi \sim 1$ eV, il suffirait de monter au-dessus de la température ambiante pour avoir des épaisseurs énormes (50^{μ} à 400° K., 1^{cm} à 500° K.), qui ne correspondent pas à la réalité. En effet nous avons étudié, dans des expériences préliminaires, la formation de la couche d'oxyde à ces températures. Après 9 jours, les épaisseurs obtenues ont été de ~ 4, ~ 12 et $\sim 20^{m\mu}$ aux températures de 300°, 400° et 500° K. Nous devons en conclure que la température joue un rôle secondaire dans le mécanisme de l'oxydation, ce qui conduit à supposer $\Phi \gtrsim 2$ eV.

3. Il y a un autre mécanisme possible, pour faire passer les électrons à travers le saut de potentiel Φ, c'est l'effet photoélectrique des radiations de fréquence supérieur à Φ/h. Nous allons voir que l'effet photoélectrique théorique de la radiation ambiante est suffisant pour obtenir l'ordre de grandeur des couches observées. La formule (1) est toujours valable, n (plutôt n_λ) étant maintenant le nombre d'électrons par cm³ en équilibre avec le métal illuminé par un rayonnement permanent de longueur d'onde λ. La théorie de l'effet

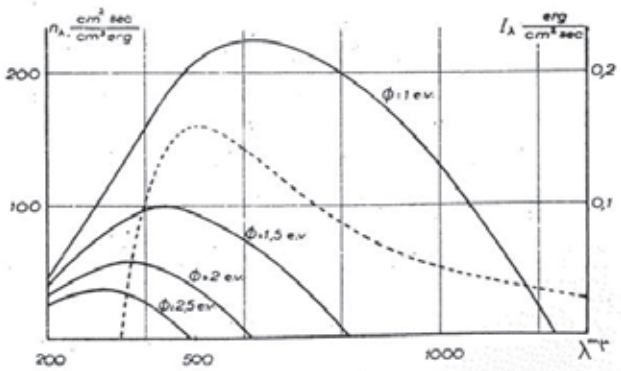

photoélectrique permet de calculer au moins l'ordre de grandeur du nombre P d'électrons émis par unité d'énergie incidente; n_λ est donné par la formule $n_\lambda = 4P/\bar{c}$, $\bar{c}$ étant la vitesse moyenne d'émission des électrons, que nous avons

pris $\simeq 0,8\sqrt{2(h\nu - \Phi)/h}$. La figure donne n_λ en électrons par cm³, et erg d'énergie incidente par cm² et sec, en fonction de λ et pour diverses valeurs de Φ.

Nous avons admis dans le calcul, pour la largeur de la bande de conductibilité de l'aluminium, la valeur 16 eV, tirée des expériences sur l'émission de rayons X. Sur la même figure nous avons reporté la distribution spectrale du rayonnement moyen existant dans un laboratoire, en erg/cm² sec, admettant, pour sa valeur absolue 10^{-5}, celle du rayonnement solaire au-dessus de l'atmosphère. Par une intégration graphique, on obtient alors les $n = \int I_\lambda n_\lambda d\lambda$ correspondant à chaque valeur de Φ, d'où les épaisseurs pour lesquelles $dx/dt \sim 10^{-7}$ mμ/sec, qui sont écrites dans le tableau (III). On obtient ainsi, pour $\Phi \sim 2,5$ eV, l'ordre de grandeur des épaisseurs observées. Nous sommes d'ailleurs en présence d'une nouvelle méthode d'oxydation, que nous appellerons *photoélectrique* et qui permettrait d'obtenir facilement des couches assez épaisses. D'après la figure et admettant $\Phi = 2,5$, le rayonnement le plus efficace serait le proche ultraviolet. Avec $\lambda \sim 300^{m\mu}$ et une énergie de 10^4 erg/cm² sec (lampe à Hg ordinaire à 30^{cm}) on obtiendrait, au bout de 10 jours, une couche d'oxyde de $50^{m\mu}$, qui correspond à $30^{m\mu}$ de Al, c'est-à-dire une couche presque opaque.

2

CABRERA N., MOTT N.F.
THEORY OF THE OXIDATION OF METALS.
REPORTS ON PROGRESS IN PHYSICS, LONDON XII, 163 (1949).

THEORY OF THE OXIDATION OF METALS

By N. CABRERA and N. F. MOTT
H. H. Wills Physical Laboratory, University of Bristol

CONTENTS

§ 1. INTRODUCTION

Recent theoretical and experimental work on the oxidation of metals has provided a general theoretical frame into which it may be possible to fit the complicated phenomena observed. While this scheme is by no means complete or proved at all points, it seems worth while to publish it in its present stage, in the hope that it may act as a guide to future experimental work.

In this Report the phenomena observed will be classified as follows:

1.1. *Formation of stable films at low temperatures.* Recent experimental work indicates that many metals, perhaps all which oxidize readily, show very similar behaviour when exposed to oxygen at a sufficiently low temperature. Oxidation is initially extremely rapid, but after a few minutes or hours drops to very low or negligible values, a stable film being formed 20–100 A. thick. Aluminium behaves like this at room temperature; copper, iron, barium and other metals do the same at the temperature of liquid air. An explanation of this behaviour was first given by Mott (1947 a), and depends on the hypothesis that a strong field is set up in the oxide film, due to a contact potential difference between metal and adsorbed oxygen, which enables the metal ions to move through it without much help from temperature; the theory gives a logarithmic growth law of the type

$$1/X = A - B \ln t,$$

X being the thickness at a time t. This mechanism is discussed in § 4 of this Report.

In many cases there is strong evidence that these films have a pseudomorphic form, are thus not in thermodynamic equilibrium, and are in fact highly compressed. The theoretical basis for understanding this phenomenon has been given by Frank and van der Merwe (1949 a, b) and van der Merwe (1949). According to these authors, the question whether the film will be pseudomorphic depends on the degree of fit or misfit between the lattice in the face of the metal crystal exposed and the spacing of the metal atoms in the oxide. They consider that a monolayer

of oxygen atoms will be formed very rapidly (say in 10^{-2} sec. at a pressure of 10^{-4} mm. Hg); for purposes of calculation they then discuss a metal covered by a monolayer of oxide. They then ask whether or not this monolayer of oxide will take up the lattice parameter of the metal underneath. The answer depends, of course, on the assumptions made about the forces between the oxide layer and the metallic substrate, and also on the elastic constants of the oxide layer itself; the more compressible the oxide, the more likely it will be to take up the distorted form. Making reasonable assumptions, Frank and van der Merwe find that, if the degree of misfit is less than about 15%, the film will, in its state of lowest energy, take up the lattice parameter of the substrate; if it is greater than 15%, it takes up very nearly its own unstrained lattice parameter.

In the latter case an oxide layer will be formed which, while it may have one crystal plane parallel to the surface layer of the crystal, will *not* have its crystal parameter distorted. In the former case, however, once a monomolecular layer of oxide is formed *all over* the surface, it must continue to grow with the same lattice parameter, even though, as soon as the layer thickens, the equilibrium becomes unstable. Provided that the surface is completely covered, the film can only assume its unstrained lattice parameter either by breaking away from the surface through plastic deformation or by recrystallization.

1.2. *Region of intermediate temperatures.* The discussion of the previous paragraph shows that a stable film will grow until it reaches a limiting thickness and will then stop, if the temperature is low enough for the following conditions to be satisfied: (*a*) metal ions cannot cross the film without the aid of a strong electric field, which only exists in *thin* films; (*b*) in the case of films compressed to fit the metal substrate the temperature at which crystallization occurs is not reached.

Recrystallization is a phenomenon which depends on the formation of one or more nuclei, and is thus a process likely to involve a long induction period. Figure 1, which gives results obtained at Bristol by Mrs. Garforth (1949) on the growth rate of oxide on an evaporated copper film determined with a quartz microbalance, shows a phenomenon probably to be explained by the recrystallization of a pseudomorphic film. It would appear from the curve that the recrystallized oxide can pass metal ions without the help of a strong field, so the curve will eventually go over into one of the forms described in paragraph 1.3 below; if the recrystallized material were still opaque, one would expect the logarithmic growth law of the type first described by Evans (1946) for films a few 100 A. thick (not to be confused with the mechanism described under 1.1 above).

For metals for which the original oxide film is not fitted to the metal substrate (aluminium), and perhaps for recrystallized films too, another intermediate region can be recognized, that in which the temperature is high enough for ions to diffuse without the help of a strong field, but in which the thickness is not great enough, in the times used in the experiment, for the parabolic law ($X^2 = 2At$) to be valid (see 1.3 below). In this region it is possible to find theoretical justifications for various laws, a parabolic law with a different constant A, a cubic law $X^3 = 3At$ (cf. the work of Campbell and Thomas (1947) on copper), a roughly linear law $X = At$ (cf. Gulbransen and Wysong (1947) for Al). A brief discussion of these laws will be given in § 3.

1.3. *Parabolic law.* For sufficiently high temperatures, *and* sufficiently thick films, the oxidation should conform to the parabolic law. The derivation of this

law ($X^2 = 2At$) depends on the following assumptions. Either metal or oxygen is soluble in the oxide; local thermodynamic equilibrium exists at the metal–oxide interface and at the oxide–air interface; the concentrations of metal (or oxygen) at the two faces are therefore different; metal or oxygen thus diffuses through the oxide layer under a concentration gradient which is proportional to $1/X$; the rate of growth dX/dt is thus proportional to $1/X$, and integration gives the parabolic law.

Oxides such as those of zinc and aluminium do not dissolve oxygen; they can, however, dissolve metal (thereby becoming excess semiconductors). For such oxides, then, one can assume a vanishing concentration of metal at the oxygen–air interface even for low pressures of oxygen; the rate of oxidation is thus independent of oxygen pressure. Oxides such as those of copper and iron dissolve oxygen

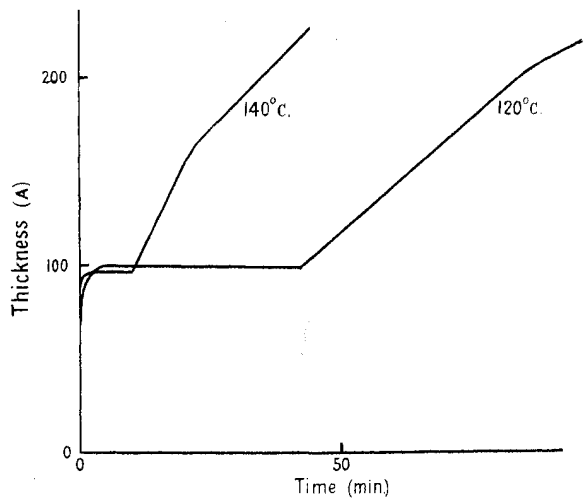

Figure 1. Rate of growth of oxide layer on evaporated copper film at 120° c. and 140° c., at a pressure of oxygen of 1–3 mm. Hg. The weights of oxygen taken up were determined by the microbalance, and converted to thicknesses using the known density of the oxide.

(thus becoming defect semiconductors); the concentration gradient of oxygen thus varies with oxygen pressure, as does also the rate of oxidation. Nevertheless, it is not the oxygen which diffuses, but the metal, as has been proved by the use of radioactive tracers in the case of copper (Bardeen, Brattain and Shockley 1946). This is because the oxygen is taken up in such a way as to form vacant cation sites, which diffuse away from the oxide–air interface.

In trying to estimate the value of the constant A, one must remember that the dissolved metal atoms are almost completely dissociated, e.g. into interstitial ions and electrons. The value of A will depend on whether the pure (stoichiometric) oxide is an insulator at the temperature considered. If this is the case, we shall show in the next section that

$$A = 2\Omega D_i n, \qquad \ldots\ldots(1)$$

where Ω is the volume of oxide per metal ion, D_i the diffusion coefficient for an interstitial ion and n the concentration of dissolved atoms (ions and electrons) at the interface.

The derivation of this formula is valid only if the film is so thick that the concentrations of ions and electrons are equal throughout most of its thickness.

Actually at each boundary there will be layers where they are unequal, and where, in consequence, a space charge is set up, giving rise to a double layer. The thickness of this layer is of order $X_0 = \sqrt{(\kappa \boldsymbol{k} T/8\pi n \boldsymbol{e}^2)}$, where κ is the dielectric constant. This constant is of course very sensitive to temperature. As will be shown in §3, in practice, in experiments lasting a few hours, if the thickness X has grown to 10^{-4} cm., then $X \gg X_0$, and the condition for the parabolic law is satisfied.

For films of thickness less than X_0 the space charge set up in the material, if the concentrations of ions and electrons are unequal, has very little effect. One can thus discuss the motion of ions and electrons separately. The much more mobile electrons will probably pass freely through the film and set up a constant potential difference V between the metal and the adsorbed oxygen layer. The field in the oxide film is thus V/X. If, then, n_i is the concentration of metal *ions* in solution and v_i their mobility, the current is $n_i v_i V/X$ ions/cm^{2}sec., and it is easily seen that a parabolic law follows with

$$A = \Omega v_i V n_i. \qquad \ldots\ldots (2)$$

This value of the constant A is quite different from that given by (1), and for thicknesses of the order X_0, and thus in the transition regions between the two laws nothing in the nature of a parabolic law is to be expected.

Case 1.1 above arises when n_i is vanishingly small; this is discussed in §4.

§2. THE PARABOLIC LAW FOR THICK FILMS

2.1. The mechanism by which oxides (and sulphides and halides) can take up excess metal or excess oxygen is now well understood. Excess metal can be taken either interstitially, when the metallic ion goes into an interstitial position and the electron moves round it through the lattice in an "orbit" probably extending over many lattice parameters, or as an F-centre (site from which the anion is missing and is replaced by an electron). Excess oxygen is taken up through the formation of vacant cation sites, a positive hole (missing electron) being located on an adjacent ion.

An oxide containing excess metal (or oxygen) quenched to a temperature at which the interstitial ions or vacant sites are not mobile behaves of course as an electronic semiconductor*; at low temperatures the electrons are bound to their interstitial ions, but as the temperature is raised an increasing proportion becomes free. When, however, an oxide is in thermodynamic equilibrium with its metal, at a temperature at which the interstitial ions are mobile, the dissolved atoms will nearly all be dissociated into interstitial ions and electrons. It will be assumed throughout this Report that dissociation is complete.

2.2. We have then to discuss the contact between a metal and an oxide capable of accepting excess metal, and to determine the concentration n_i of interstitial ions and n_e of electrons in the oxide at a distance x from the interface, when the whole system is in thermodynamical equilibrium. If x is large enough, n_i and n_e become equal, but this is not so for small x, so that a space charge is set up at the boundary. At the boundary we envisage a situation such as that shown in Figure 2; the process of solution of an ion in the oxide is typically the removal of the ion at P from its position in the surface layer of the metal into an interstitial position of the oxide. If the energy required to do this is denoted by W_i, then W_i may be described as the heat of solution of a metallic ion.

* For a recent eview of the theory of semiconductors see Mott (1949 a).

We may also introduce the energy ϕ required to remove an electron from the metal into the conduction band of the oxide; for oxide grown chemically on the metal we may expect this to have a characteristic value, adsorbed gas layers being absent from the interface.

The usual diagram for an insulator in contact with a metal is shown in Figure 3; ϕ will in general be less than the work function of the metal against vacuum.

The quantity $\phi + W_i - \epsilon$ is the heat of solution of the metal atom in the oxide; here ϵ is the energy with which an electron is bound to the interstitial ion in the oxide. Thus, while ϕ and W_i may individually depend on which crystal face of the metal is exposed, $\phi + W_i$ will not.

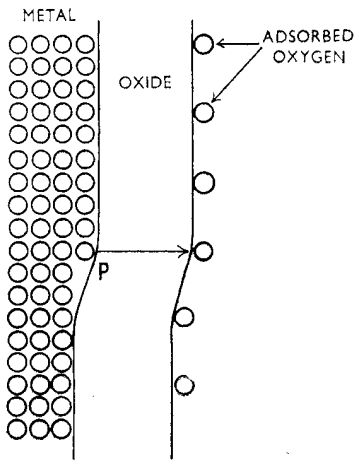

Figure 2. Showing the mechanism by which ions leave a metal and pass through oxide layer (Mott 1947 a).

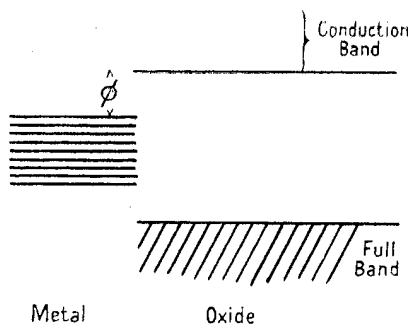

Figure 3. Metal in contact with insulating oxide.

It is easily shown that, if ϵ is less than both ϕ and W_i by at least several multiples of $\boldsymbol{k}T$, the dissociation is almost complete; this will be assumed in what follows.

Immediately at the interface the concentration $n_i(0)$ of interstitial ions is given by

$$n_i(0) = N_i \exp(-W_i/\boldsymbol{k}T), \qquad \ldots\ldots(3)$$

where N_i is the number of interstitial positions per unit volume in the oxide. Similarly the number $n_e(0)$ of electrons is

$$n_e(0) = N_e \exp(-\phi/\boldsymbol{k}T), \qquad \ldots\ldots(4)$$

where $N_e = 2(2\pi \boldsymbol{m}\boldsymbol{k}T/\boldsymbol{h}^2)^{3/2}$. Also if $n_i(x)$, $n_e(x)$ are the numbers at any distance x from the interface, the product $n_i(x)n_e(x)$ must be constant; thus at large distances $n_i(x)$ and $n_e(x)$ are equal, say, to n, where

$$n = \sqrt{(N_i N_e)} \exp\{-\tfrac{1}{2}(W_i + \phi)/\boldsymbol{k}T\}. \qquad \ldots\ldots(5)$$

At intermediate distances these quantities can be deduced from Boltzmann's law:

$$n_i(x) = n \exp(-\boldsymbol{e}V/\boldsymbol{k}T);$$

$$n_e(x) = n \exp(\boldsymbol{e}V/\boldsymbol{k}T),$$

where V is the electrostatic potential, and from Poisson's equation

$$\frac{d^2V}{dx^2} = \frac{4\pi e}{\kappa}\{n_i(x) - n_e(x)\}.$$

It is assumed here that ions carry unit charge.

Substituting for n_i, n_e, this gives

$$\frac{d^2V}{dx^2} = \frac{8\pi n}{\kappa} e \sinh\left(\frac{eV}{kT}\right). \qquad \ldots\ldots(6)$$

An exact solution satisfying the boundary conditions (3), (4) can easily be obtained (cf. Mott 1947 b), but is not necessary for our purpose. We need only examine the form of equation (6) when x is large and V consequently small; it then becomes $d^2V/dx^2 = V/X_0^2$, where

$$X_0 = \sqrt{\{\kappa kT/8\pi n e^2\}}. \qquad \ldots\ldots(7)$$

The solution is $V = \text{const.}\exp(-x/X_0)$. This shows that our treatment of the problem will differ according as the thickness X of our growing film is or is not greater than X_0. If $X \gg X_0$ we may, throughout the bulk of the film, treat n_e, n_i as equal; this assumption will be made throughout the rest of this section. The other extreme case, $X \ll X_0$, will be treated in § 4.

Other interesting examples of double layers in the vicinity of the metal–oxide interface can be given. If the solubility of oxygen in the metal is high and the energy required to take an oxygen ion from the oxide and to put it into the metal is not too big, vacant anion sites will be produced near the metal–oxide interface, with the corresponding electrons in the conduction band of the oxide. These vacant anion sites will diffuse through the oxide during the oxidation processes. This is probably the mechanism by which Ag and also Cu absorb oxygen at high temperatures without the growth of a thick layer of oxide, as long as the saturation concentration of dissolved oxygen in the metal has not been reached.

2.3. The case of an oxide in equilibrium with the oxygen gas, and the formation of a double layer near the oxide–air interface, can be treated in a similar way. Let us consider the case of an oxide (Cu_2O) absorbing oxygen through the formation of vacant cation sites (concentration n_i) and positive holes (concentration n_e) in the full band of the oxide. Far from the oxide–air interface both concentrations are equal to n, given by (see Mott and Gurney 1948, p. 260)

$$n = \sqrt{(N_i N_e)}\left(\frac{n_g}{N_g}\right)^{1/2s} \exp(-E/2skT), \qquad \ldots\ldots(8)$$

where N_i and N_e are as in § 2.2, and

$$N_g = (2\pi MkT/h^2)^{3/2};$$

M is the mass of an oxygen molecule, n_g the number of oxygen molecules per cm^3 in the air and E the energy required for the absorption of one of them and the formation of s vacant cation sites and s positive holes ($s = 4$ in the case of Cu_2O). The concentration n will therefore be proportional to $p^{\frac{1}{s}}$, where p is the pressure.

The calculation of the concentrations $n_i(0)$ and $n_e(0)$ near the oxide–air interface requires more careful consideration. Figure 4 represents the electronic levels of the oxide and those of the adsorbed oxygen layer (we assume for simplicity that the levels of the adsorbed layer correspond to the same energy). As we shall see in § 4, the adsorbed levels may be below the top of the full band (ψ might be negative), particularly in the case of Cu_2O.

Let N_0 and N be the number of empty and full levels in the adsorbed layer per cm². Then it is easy to see that $n_e(0)$ is given by

$$n_e(0) = N_e(N_0/N)\exp(-\psi/\boldsymbol{k}T),$$

where the factor N_0/N is due to the different ways in which the N occupied levels can be distributed among the total number $N_0 + N$ of levels. On the other hand, the vacant cation sites will be produced *only* in the neighbourhood of the N adsorbed oxygen ions, requiring an energy W_i, according to Figure 5. Therefore $n_i(0)$ will be given by $n_i(0) = N_i(Na^2)\exp(-W_i/\boldsymbol{k}T)$, where Na^2 represents the proportion of the oxide–air interface occupied by oxygen ions.

The presence of the factor (a^2N) in the formula above can be seen by an application of the principle of detailed balancing. The number of vacant cation sites created per second will be proportional to (a^2N); the adsorbed oxygen ion is then neutralized and another one is produced somewhere else in order to keep N constant. On the other hand the number of vacant cation sites disappearing per second will be proportional to $n_i(0)/N_i$ and independent of (a^2N), because this process *does not* require the vicinity of an adsorbed oxygen ion.

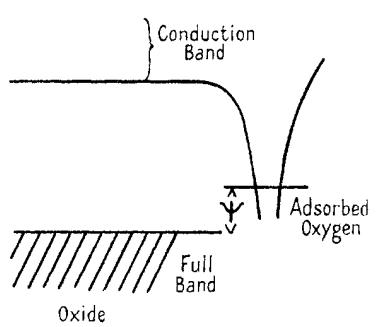

Figure 4. Insulating oxide in contact with oxygen.

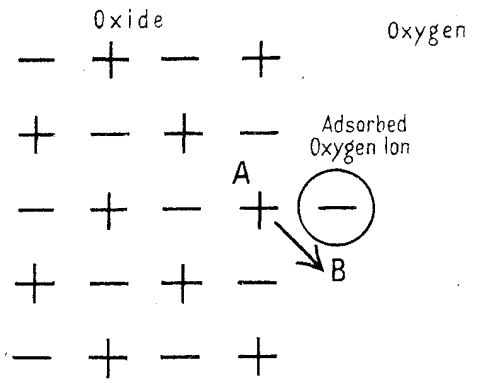

Figure 5. Showing the process by which a vacant cation site is created in the vicinity of an adsorbed oxygen ion.

As $n_e(0)n_i(0) = n^2$, we deduce that the proportion of the oxide–air interface covered with adsorbed neutral oxygen is

$$N_0a^2 = \left(\frac{n_g}{N_g}\right)^{1/s}\exp\left\{-\left(\frac{E}{S} - \psi - W_i\right)\Big/\boldsymbol{k}T\right\},$$

obviously a function of pressure. On the other hand the number N of adsorbed oxygen ions will be equal to the total space charge near the oxide–air interface, and, therefore, also a function of pressure.

Throughout this discussion it has been assumed that the oxide of stoichiometric composition is an insulator i.e. it has no intrinsic electronic or ionic conductivity, or these conductivities are small compared with that due to the dissolved atoms.

2.4. *Calculation of rate of growth of oxide film.* In the oxide film, we denote by D_e, v_e the diffusion coefficient and mobility of an electron and D_i, v_i the same

quantities for an interstitial ion. Then if F is the field in the film, the current i_e carried by electrons is (in units of $\boldsymbol{e}$)

$$j_e = -D_e \frac{\partial n_e}{\partial x} + F n_e v_e,$$

and the current j_i carried by the ions

$$i_i = -D_i \frac{\partial n_i}{\partial x} - F n_i v_i.$$

In a steady state these are equal and opposite; thus, putting both equal to j (number of atoms crossing unit area per unit time), we see on eliminating F between the two equations,

$$j\left\{\frac{1}{n_e v} + \frac{1}{n_i v_i}\right\} = -\frac{\boldsymbol{k}T}{\boldsymbol{e}} \frac{\partial}{\partial x} \ln (n_e n_i). \qquad \ldots\ldots (9)$$

In deriving this equation use has been made of the Einstein equation $D/v = \boldsymbol{k}T/\boldsymbol{e}$.

We may certainly assume that $v_e \gg v_i$. In the case of an oxide which is an insulator in the absence of dissolved metal or oxygen, and for which $X \gg X_0$, we may further assume that $n_i(x) = n_e(x) = n(x)$, say, throughout the film, except for the boundary zone, which we neglect. The equation (9) thus becomes

$$j = -2D_i \frac{\partial n}{\partial x},$$

or, on integrating throughout a film of thickness X,

$$jX = 2D_i[n(0) - n(X)].$$

The rate of growth is thus $dX/dt = A/X$, whence $X^2 = 2At$, where

$$A = 2D_i \Omega [n(0) - n(X)]. \qquad \ldots\ldots (10)$$

The parabolic law is thus satisfied. The quantity in the square brackets is the difference between the concentrations of dissolved atoms at the surface metal–oxide and at the surface oxide–oxygen.

A further case in which equation (9) can be solved is that in which oxide (or halide) is a good ionic conductor in the pure state, and the electronic conductivity, due to the addition of metal, is small in comparison. This may be the case for the halides. We may then set $n_e v_e \ll n_i v_i$ and take n_i as constant throughout the film. The equation then becomes

$$j = -v_e \frac{\boldsymbol{k}T}{\boldsymbol{e}} \frac{\partial n_e}{\partial x},$$

so the parabolic law is satisfied with

$$A = D_e \Omega [n_e(0) - n_e(X)].$$

Returning to (10), the usual assumption is that, for oxides which form excess semiconductors (ZnO, Al_2O_3), the concentration $n_e(X)$ of dissolved metal at the oxide–air interface is zero (except for very small pressures of oxygen), so that the oxidation constant becomes

$$A = 2D_i \Omega n(0). \qquad \ldots\ldots (11)$$

Note that here D_i is the diffusion coefficient of the interstitial ions and $n(0)$ the concentration of metal *atoms* (dissociated or otherwise) in the oxide in equilibrium with metal. For oxides such as Cu_2O on the other hand we assume that $n(0)$,

the concentration of vacant sites in equilibrium with the metal, is small compared with that, $n(X)$, in equilibrium with the air; thus, approximately,

$$A = 2D_i \Omega n(X), \qquad \ldots\ldots (12)$$

where $n(X)$ is the concentration of vacant cation sites in the oxide in equilibrium with oxygen, and D_i the diffusion coefficient for one of these sites. Note that in the former case the oxidation rate is almost independent of oxygen pressure p, unless this is very low; in the latter case, according to (8), it should vary as $p^{\frac{1}{2}}$.

2.5. *Experimental results at high temperatures.* Putting in formulae (11) or (12) the usual expression $D_i \sim a^2 \nu \exp(-U/\boldsymbol{k}T)$ for the diffusion coefficient of defects in the oxide, a being the interatomic distance, $\nu (\sim 10^{12}\,\mathrm{sec}^{-1})$ the atomic frequency of vibration and U the activation energy for movement between two equilibrium positions of the defect, and using formulae (5) or (8) for n, we get, for the constant A in the parabolic law, an expression of the form

$$A = A_0 \exp(-B/\boldsymbol{k}T), \qquad \ldots\ldots (13)$$

where

$$A_0 = 2a^2 \nu \Omega \sqrt{(N_i N_e)}, \qquad B = \tfrac{1}{2}(W_i + \phi) + U \text{ or } E/2s + U.$$

The factor $(n_g/N_g)^{1/2s}$ appearing in (8) is of the order unity and can be disregarded. Taking $a \sim 3 \times 10^{-8}$ cm., $\nu \sim 10^{12}\,\mathrm{sec}^{-1}$, $\Omega \sim a^3$, $N_i \sim 10^{22}\,\mathrm{cm}^{-3}$, $N_e \sim 10^{18}\,\mathrm{cm}^{-3}$, we obtain $A_0 \sim 10^{-5}\,\mathrm{cm}^2/\mathrm{sec}$. In this evaluation we have disregarded the change of vibrational frequencies of the solid due to the presence of defects and the change of the activation energy B with temperature. This may, however, introduce a factor which can be of the order of a few powers of 10 (see Mott and Gurney 1948, p. 29), and which seems to be larger for the vacancy type of defect than for interstitial ions.

Table 1 gives the constants A_0 (in $\mathrm{cm}^2/\mathrm{sec}$.) and B (in ev.), determined experimentally during the oxidation of several metals in the range of temperature indicated. In some of these cases the oxide layer is complex.

Table 1. Values for the Constants A_0 and B in Formula (13) and governing Rate of Oxidation

	Temperature range	A_0 (cm^2/sec.)	B (ev.)
Fe	700° to 900° c.	1·0	1·6
Cu	700° to 1000° c.	0·2	1·5
Ni	800° to 1000° c.	0·1	2
Pb	470° to 626° c.	0·2	1·4
Zn	600° to 700° c.	0·002	1·5

For Fe there are three layers (FeO, Fe_3O_4, Fe_2O_3, going from metal to air). The values given in Table 1 correspond to the thickness of FeO (Bénard and Coquelle 1946), which in the range of temperatures considered forms 90% of the total thickness. It is believed that the diffusing elements are mostly vacant cation sites formed at the FeO–Fe_3O_4 interface. For Cu, at pressures below 100 mm. Hg at 1,000° c., there is only Cu_2O and no CuO. Assuming that the diffusing elements are also vacant cation sites produced at the Cu_2O–air interface, one expects from formula (8) that A_0 should be proportional to $p^{\frac{1}{2}}$; this was proved to be the case by Wagner and Grünewald (1938). The values given in Table 1 are extrapolated to $p = 1$ atm. For Ni, vacant cation sites are also responsible for the diffusion of the metal, and, therefore, A_0 is also a function of the pressure, as was proved by Wagner and Grünewald. The values quoted in

Table 1 are deduced from data given by Evans (1948, p. 144). The values for Pb and Zn were observed by Krupkowski and Balicki* (1937), who studied the formation of solid oxide layers on the surface of liquid metals. It is well known that the diffusing elements in ZnO are interstitial ions formed at the metal–oxide interface; therefore one expects the constant A_0 to be independent of the pressure, as was shown by Wagner and Grünewald (1938).

Bénard and Talbot (1948) have studied also the oxidation of single crystals of copper at 900° c. Figure 6 represents the increase of weight as a function of time on different faces of a copper crystal. These differences were also reported earlier by Gwathmey and Benton (1940) on copper at 1,000° c. It is known from the work of Wagner and Grünewald (1938) that in the case of copper the con-

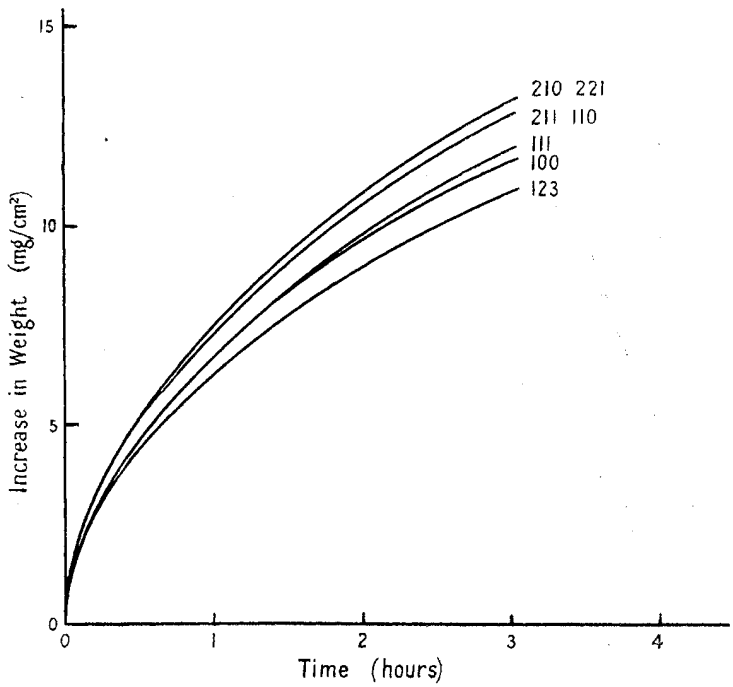

Figure 6. Oxidation of different faces of copper at 900° c. (Bénard and Talbot 1948).

centration of vacant cation sites in the oxide near the metal–oxide interface $n(0)$ is not quite negligible in comparison with their concentration near the oxide–air interface $n(X)$. Therefore formula (10) has to be used. On the other hand, the diffusion coefficient D_i cannot be a function of direction in a cubic crystal such as Cu_2O; therefore, Bénard and Talbot's results show that $n(0)$ or $n(X)$, or perhaps both, are not equal to the equilibrium concentrations, which of course would not depend on the crystal surfaces exposed. As the differences depend on the orientation of copper surface we expect that $n(0)$ will not be equal to the equilibrium concentration, but will be higher for the faces for which the rate of oxidation is lower.

One of us (Cabrera 1949 b) has advanced the following hypothesis to explain this. As long as there are enough positions such as P (Figure 2) on the metal

* These authors observed also the oxidation of liquid Cu (1,100° to 1,200° c.) and Ag (1,000° to 1,035° c.), for which they obtained an initial linear increase of weight without the formation of a thick oxide layer, due to the absorption of oxygen in the liquid metal.

surface, the concentration of vacant cation sites near the metal will be maintained equal to the equilibrium concentration, in spite of the constant arrival of new vacant cation sites; but when the evaporation into the oxide of a new atomic layer of the metal has to be started, a larger activation energy will be required for the formation of a "hole" on the metal surface, such as is illustrated in Figure 7, and, therefore, the concentration of vacant cation sites in the oxide will grow.

This point of view assumes that the metal surface has a practically perfect structure, and one can deduce that the order of increasing rate of oxidation should be the same as the order of decreasing density of metal atoms on the surface: that is to say (111), (100), (110), (311), (331), which is not in agreement with the experimental results represented in Figure 6. Actually the metal surface is not

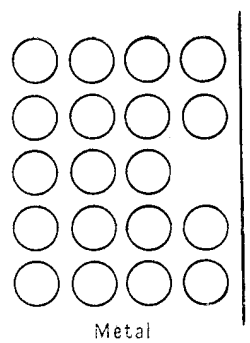

Figure 7. First step in the evaporation of a new layer of metal into the oxide.

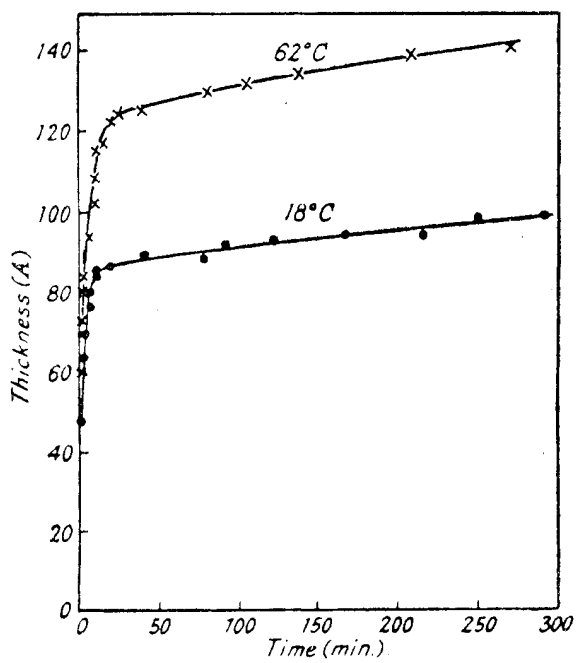

Figure 8. Growth curves for Cu_2O on Cu determined by Miley and Evans by an electrometric method.

even microscopically perfect; according to an idea put forward by Frank and others (Burton, Cabrera and Frank 1949, Frank 1949) a certain type of "dislocation" in the body of the metal produces positions such as P (Figure 2) on the metal surface, which are *not* destroyed when the entire atomic layer is evaporated; therefore the rate of oxidation on different crystal surfaces will depend on the concentration of these dislocations per unit area of each crystal surface. Just how this will depend on the crystal face is not at present clear.

§ 3. THEORY OF FORMATION OF THIN FILMS

In this section we outline the theory of the rate of growth of thin films. By thin we mean of thickness X small compared with X_0 defined by (7), so that the concentrations of positive ions and electrons diffusing across the layer can become unequal without any important space charge being set up. In practice most of the films that we shall discuss are of thickness 100 A. or less.

No attempt will be made here to survey all the available experimental material. A survey of all but the most recent material is given in the book by Evans (1948); Figure 8 shows results, taken from p. 65 of this book, on the oxidation of copper, measured by an electrometric method. As an example of more recent work Figure 9 represents the rate of oxidation of thin films of aluminium at 10° c.

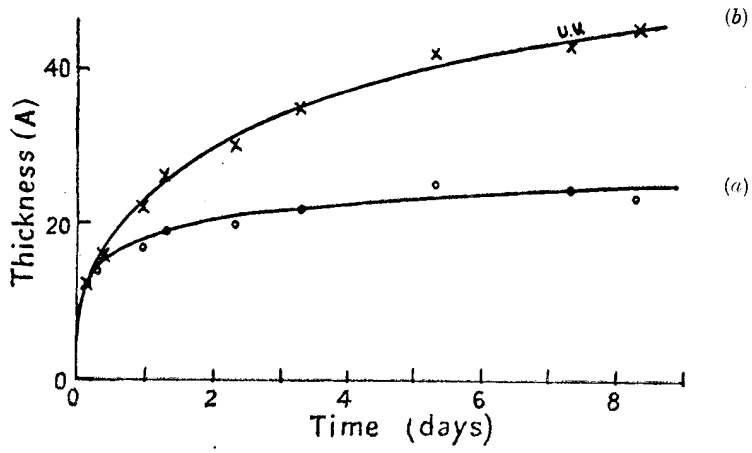

Figure 9. Rate of oxidation of aluminium (Cabrera *et al.* 1947) (*a*) in the dark, (*b*) under ultra-violet illumination.

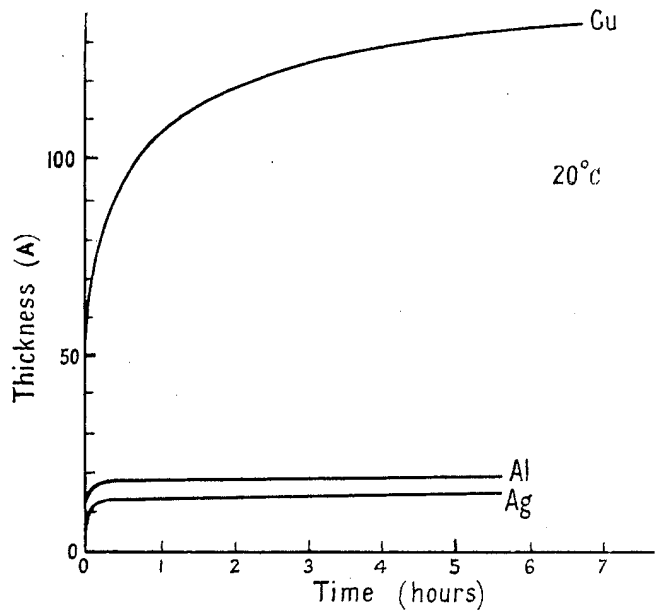

Figure 10. Oxidation at room temperature and pressures of oxygen between 10^{-4} and 10^{-2} mm. Hg (Garforth 1949).

These results were obtained by Cabrera, Terrien and Hamon (1947) from the increase in the transparency of the film during oxidation, a method first used by Steinheil (1934). The upper part of the curve represents the influence on oxidation of ultra-violet light, which will be discussed later. Figure 10 shows the oxidation of copper, aluminium and silver at room temperature and oxygen

pressure of 10^{-4} to 10^{-2} mm. Hg measured recently in this laboratory by Mrs. Garforth (1949) using a quartz microbalance.

The general result of all this work is that all metals investigated show in principle a similar behaviour. If the temperature is low enough, they show, when exposed to oxygen, an initial very rapid growth, followed by a remarkable slowing down, and for some critical thickness X_L of order 100 A. or less growth stops or nearly stops. This behaviour is rather insensitive to the pressure of oxygen.

In this section and the next, then, we shall discuss the mechanism by which these very *thin* films of oxide grow. Consideration of the mechanism by which the first monolayer is formed is deferred until § 5, as is also the related question of whether or not the film is pseudomorphic (strained). Here we suppose that a thin layer of oxide exists in the metal and is growing; we require to know how fast it grows. As in § 2, the oxide is supposed to be an insulator when of stoichiometric composition but to be capable of dissolving metal ions; in contradistinction to the case considered in § 2, it is here supposed that the film is so thin that the effect of any space charge set up by the dissolved ions is negligible, so that the movements of ions and of electrons can be considered independently. In other words, the film is thin compared with the quantity X_0 defined by (7).

It will be worth while to consider again the condition that this should be the case. Suppose that n_i is the number of interstitial ions per unit volume in the oxide when in equilibrium with metal, and let q be the charge on each ion. Then Poisson's equation gives for the potential energy V of an ion in the oxide layer $d^2V/dx^2 = 4\pi n_i q^2/\kappa$. On integrating we see that the contribution to the potential due to the space charge alone is $V = 2\pi n_i q^2 x^2/\kappa$, where x is measured from the mid-point of the film. Thus for a film of thickness X the maximum variation of V is $\frac{1}{2}\pi n_i q^2 X^2/\kappa$. This is negligible if small compared with $\boldsymbol{k}T$. Thus, omitting numerical factors, the condition that the field is negligible is $X \ll \sqrt{(\kappa \boldsymbol{k} T/n_i q^2)}$. This is the same as the relation (7) already obtained.

We consider then a film of oxide on the metal exposed to oxygen. A layer of oxygen will be adsorbed to the surface of the oxide; this oxygen will be assumed to be atomic. We assume further that electrons can pass through the oxide layer from the metal to the oxygen by some mechanism (thermionic emission or tunnel effect), and that the electronic motion is rapid compared with the ionic motion. Some of the adsorbed oxygen atoms will then be converted into ions O^-, setting up a field across the oxide layer, until a state of quasi-eqilibrium is set up between the metal and the adsorbed oxygen, in which, in a time short compared with that in which the metal ions diffuse, as many electrons pass in one direction as the other. The electrostatic potential V set up across the layer will clearly be independent of the thickness, so that the field F is given by $F = V/X$.

The electronic levels in the metal, the oxide and in the adsorbed oxygen layer are shown in Figure 11. Figure 11(*a*) shows the state of affairs before any electrons have passed through the film; in the oxygen atoms there are energy levels *below* the surface of the Fermi distribution in the metal*; the quantity $\boldsymbol{e}V$ already introduced is the amount by which they are lowered. Electrons will pass through the film until the quasi-steady state in Figure 11(*b*) is reached, when as many electrons pass through the film in one direction as in the other. Since V in practice is of the order of one or two volts, its variation with temperature can be ignored.

* These energy levels are probably the surface states described by Bardeen (1947) in his work on rectifiers, cf. Mott (1949 b).

A very rough numerical estimate of V can be given. If E is the electron affinity of O and W_{bind} the adsorption energy of an oxygen ion O^- on the surface of oxide, then $eV = E + W_{\text{bind}} - \phi_0$, where ϕ_0 is the work function of the metal against vacuum. We do not know very much about W_{bind}; if one considers the oxides as ionic solids, the calculations of Lennard-Jones and Dent (1928) suggest that $W_{\text{bind}} \sim 0{\cdot}1e^2/2r$, where r is the radius of the ion O^-. This gives $W_{\text{bind}} \sim 1$ ev. if $r \sim 1$ A. This value is probably too low by a factor 2 or 3, because of the covalent forces existing in the oxides. Taking (Bates and Massey 1943) $E = 2{\cdot}2$ ev. and $\phi_0 = 4{\cdot}6$ ev. for copper, or $4{\cdot}3$ ev. for aluminium, we get values for V of the order of 1 volt.

The growth of the film is due to the strong field set up in this way, which pulls the interstitial metal ions through it. These fields may be very strong; thus for a film 50 A. thick they may be of the order 10^7 v/cm. For these fields the diffusion velocity of a positive interstitial ion is no longer proportional to the field. The condition that the diffusion velocity shall be proportional to the field F is $qaF \ll kT$, where q is the charge on the ion, a the distance between interstitial

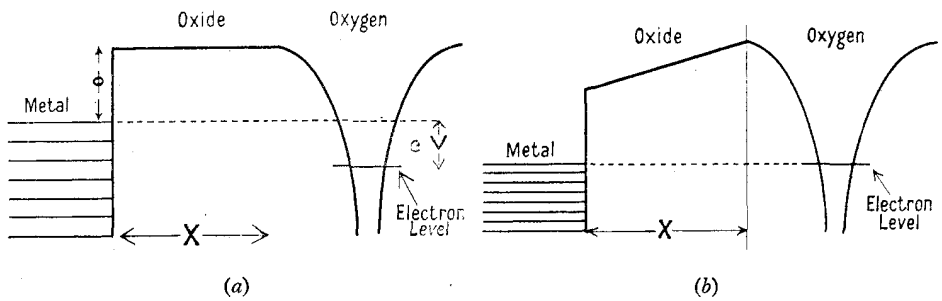

Figure 11. Electronic levels in the metal, oxide and adsorbed oxygen: (*a*) before electrons have passed through the oxide, (*b*) when equilibrium is set up.

positions. This will be the case for films of thickness X large compared with X_1, where $X_1 = qaV/kT$. X_1 is of order 50–200 atomic layers at room temperatures.

We treat first the case when $X \gg X_1$ (though less than X_0 defined by (7)). The number of ions crossing unit area per unit time is

$$n_i v_i F = n_i v_i V/X,$$

where v_i is the mobility of an ion. The rate of growth is thus $dX/dt = A/X$, where

$$A = n_i v_i V\Omega = n_i D_i \Omega(eV/kT). \qquad \ldots\ldots(14)$$

The film thus grows according to the parabolic law. Actually Gulbransen and Wysong (1947) have observed for aluminium a parabolic law between 350° and 450° C., which corresponds very probably to the case considered above. It is, of course, always assumed that electrons can pass freely through film, by either thermionic emission or tunnel effect. If ϕ (Figure 3) is too great for thermionic emission and the film too thick for tunnel effect (*c.* 30 A., cf. Mott 1940), these formulae may be expected to break down and the film to stop growing. Whether this corresponds to any case observed in practice is not known.

It is to be emphasized that the constant A given by (14) is quite different from that derived for $X \gg X_0$ (formula (11)). It depends on n_i, and thus on the exponential factor $\exp(-W_i/kT)$ instead of on $\sqrt{(n_e n_i)}$ and thus on $\exp\{-\frac{1}{2}(W_i + \phi)/kT\}$.

If, for instance, W_i is larger than ϕ, then in the transition region where $X \sim X_0$ the value of A in the parabolic equation increases. It is likely that an increase of this type may account for the apparent linear law observed by Gulbransen and Wysong (1947) for aluminium in the region around 500° c.

It is easy to make a rough estimate of whether the thickness X of an oxide film is greater or less than the thickness X_0 above which the densities of electrons and positive ions can be taken as equal. Let us suppose a film to be growing according to a parabolic law

$$\tfrac{1}{2}X^2 = a^2 \nu t \exp\{-(W+U)/\boldsymbol{k}T\}, \qquad \ldots\ldots(15)$$

where W is the heat of solution of an atom or ion and U the activation energy for motion. We want to know whether X^2 is greater or less than X_0^2 where

$$X_0^2 \sim (a^3 \boldsymbol{k}T/\boldsymbol{e}^2) \exp(W/\boldsymbol{k}T),$$

and thus whether

$$\exp(-W/\boldsymbol{k}T) \lesseqgtr a^3 \boldsymbol{k}T/\boldsymbol{e}^2 X^2.$$

Substituting for $\exp(-W/\boldsymbol{k}T)$ from (15), the condition becomes

$$(X^2/2a^2\nu t)^{\gamma} \lesseqgtr a^3 \boldsymbol{k}T/\boldsymbol{e}^2 X^2, \qquad \gamma = W/(W+U),$$

and thus

$$\frac{X}{a} \gtreqless \left(\frac{a\boldsymbol{k}T}{\boldsymbol{e}^2}\right)^{1\,2(\gamma-1)} (\nu t)^{\gamma\,2(\gamma+1)}.$$

γ is probably about 2/3; the factor $(\boldsymbol{k}Ta/\boldsymbol{e}^2)^{1/2(\gamma+1)}$ is then about 4, so that $X/a \gtrsim 4(\nu t)^{1/5}$.

For experiments lasting a few hours ($t = 10^4$ sec.), and with $\nu = 10^{12}$ sec^{-1}, we see that the critical thickness X is about $6 \times 10^3 a$, or about 2×10^{-4} cm. If in a few hours the film has grown to this thickness the mechanism is that of § 2; if not, it is the mechanism of § 3.

Up to this point the theory has been developed for metals whose oxides form excess semiconductors, e.g. Zn, A. For these metals n_i depends on the metal–oxide equilibrium, and is, of course, independent of thickness. For the oxides of copper, iron, and so on, which take up excess oxygen, the position is rather different. n_i will then refer to the number of places where a cation is missing. These can be formed wherever an oxide ion is adsorbed to the surface by the process shown in Figure 5; W_i now represents the energy required to move the positive ion from A to B. It is clear, then, since $n_i = (N/a)\exp(-W_i/\boldsymbol{k}T)$, that the concentration n_i is proportional to the number N of such negative ions per unit area.

On the other hand N is related to the field F by the Coulomb formula

$$N = \frac{\kappa F}{4\pi \boldsymbol{e}} = \frac{\kappa V}{4\pi \boldsymbol{e}} \frac{1}{X},$$

showing that N is proportional to X^{-1}; therefore n_i in formula (14) is now proportional to X^{-1}. This leads to an oxidation law of the type

$$X^3 = 3At, \qquad \ldots\ldots(16)$$

where the constant A is proportional to $\exp\{-(W_i+U)/\boldsymbol{k}T\}$, W_i being the energy to form a vacant cation site and U the activation energy for its

diffusion in the oxide. Cabrera (1949 a) has used this formula to explain the cubic law observed by Campbell and Thomas (1947) on copper between 100° and 250° c. Their results can be expressed by a formula such as (16), where the constant A is given by

$$A \sim 10^{-7} \exp(-B/\boldsymbol{k}T)\,\mathrm{cm}^3/\mathrm{sec.}, \qquad B = W_i + U \sim 1{\cdot}1\,\mathrm{ev}.$$

As noticed before (§ 2), the differences in the rate of oxidation for different crystal faces, for films of thickness X great compared with X_0 ($c.\ 10^{-4}$ cm.), can be explained only on the basis of a surface nucleation process occurring at the metal–oxide interface, because $W_i + \phi$, the heat of solution of metal, cannot depend on the crystal face. When $X \ll X_0$, the same surface nucleation process will play a rôle, but we expect also to have differences in the rate of oxidation due to the fact that W_i and ϕ (or V) may well depend on the crystal face. Gwathmey and Benton (1942) have observed differences in the rate of oxidation on a spherical single crystal of copper at 200° c. The metallic crystal faces, ordered according to a decreasing rate of oxidation, are (100), (210), (111), (110), (311). The fact that this order is different from that reported by Bénard and Talbot (1948) on copper at 900° c. suggests that the rate-determining factor at low temperatures is the difference in W_i.

§ 4. FORMATION OF VERY THIN FILMS

For very thin films the field is so strong that the velocity of drift of the ions is no longer proportional to it. In this case the motion can be treated as follows (Mott 1947 a). Suppose that an ion has to go over a potential barrier U in order to move from one interstitial site to the next. In the absence of a field the chance per unit time that an ion will do this is $\nu \exp(-U/\boldsymbol{k}T)$ with $\nu \sim 10^{12}\,\mathrm{sec}^{-1}$. The field will, however, lower the barrier by $\frac{1}{2}qaF$ for motion in the direction of the field, increasing the probability of movement to $\nu \exp\{-(U - \frac{1}{2}qaF)/\boldsymbol{k}T\}$. In the opposite direction the chance of movement is decreased by the same factor. Thus the velocity u of drift becomes

$$u = \nu a \exp(-U/\boldsymbol{k}T)\{\exp(\tfrac{1}{2}qaF/\boldsymbol{k}T) - \exp(-\tfrac{1}{2}qaF/\boldsymbol{k}T)\}.$$

For small values of F this reduces to

$$u \sim (\nu a^2 q/\boldsymbol{k}T)F \exp(-U/\boldsymbol{k}T),$$

which is proportional to the field. For large values, on the other hand,

$$u \sim \nu a \exp(-U/\boldsymbol{k}T) \exp(\tfrac{1}{2}qaF/\boldsymbol{k}T),$$

giving an exponential dependence.

It will be seen that, when the field is strong, the motion of the ions is overwhelmingly in one direction; there is, therefore, no question of any local equilibrium between metal and oxide, since equilibrium is only set up when there is a continual exchange of ions. Thus every ion which escapes from the metal is pulled right across the film, and none recombine with the metal. It follows that the rate of oxidation, for these strong fields, is determined only by the rate at which ions escape from the metal. This we must now calculate.

The potential energy of an ion in the surface layer of the metal is plotted in Figure 12. The diagram is intended to describe the state of affairs for an ion in the position P of Figure 2, that is, an ion ready to move into the oxide as the surface layer of metal dissolves. P represents the energy of the ion at rest at

this point; Q_1, Q_2 ... are interstitial positions in the oxide and S_1, S_2 ... the tops of the potential barriers separating these points. The heat of solution W_i for a positive ion and the activation energy for diffusion U are shown in the diagram. It is convenient to set $W = W_i + U$.

Then the chance per unit time that the atom will escape over the barrier to Q_1 is, in the absence of a field $\nu \exp(-W/\boldsymbol{k}T)$. In the presence of the field it is

$$\nu \exp(-W/\boldsymbol{k}T) \exp(qa'F/\boldsymbol{k}T),$$

where a' is the distance from P to the top of the barrier. The rate of growth of the film is thus

$$\frac{dX}{dt} = N'\Omega\nu \exp(-W/\boldsymbol{k}T) \exp\left(\frac{qa'F}{\boldsymbol{k}T}\right), \qquad \ldots\ldots(17)$$

where N' is the number of ions per unit area surface in sites such as P (Figure 2). This may be contrasted with the similar formula for weak fields (cf. equation (14)),

$$\frac{dX}{dt} = \frac{n_i D_i \Omega q F}{\boldsymbol{k}T}.$$

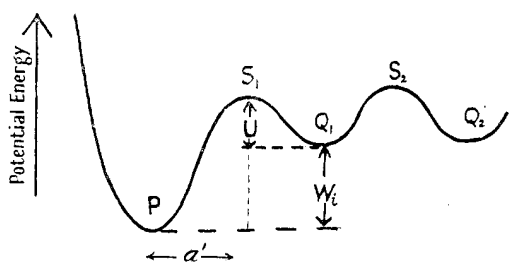

Figure 12. Potential energy of an interstitial ion in the neighbourhood of the metal–oxide interface.

Since $n_i = a^{-3} \exp(-W_i/\boldsymbol{k}T)$, $D_i = \nu a^2 \exp(-U/\boldsymbol{k}T)$, the two formulae could be comprised in the general formula

$$\frac{dX}{dt} = a\nu \exp(-W/\boldsymbol{k}T) \sinh\frac{qa'F}{\boldsymbol{k}T}, \qquad \ldots\ldots(18)$$

but for the fact that N' may be much less than $1/a^2$. A proper estimate of N' has not been made, since it depends on the number of "kinks" (Figure 2) present on the surface (Burton and Cabrera 1949); it is hoped to publish an estimate soon (Cabrera 1949 b).

Formula (17), for the growth rate in oxygen, can be used to describe two different phenomena:

(*a*) The growth of films in oxygen, where F is V/X, V being the contact potential difference between the metal and the adsorbed oxygen layer. This is the phenomenon discussed hitherto.

(*b*) The anodic formation of oxide films in an electrolyte containing oxide ions. V is then the voltage across the film.

In either case the equation may be written

$$dX/dt = u \exp(X_1/X), \qquad \ldots\ldots(19)$$

where $X_1 = qa'V/\boldsymbol{k}T$, $u = u_0 \exp(-W/\boldsymbol{k}T)$, $u_0 = N'\Omega\nu$.

X_1 is of order $10^{-6} - 10^{-5}$ cm., $u_0 \sim 10^4$ cm/sec. (or less). The formula (19) is valid only for $X \ll X_1$; it shows that the growth rate is very large for small X.

A particular and important consequence of formula (19) is that for constant V growth up to a certain limiting thickness occurs even at low temperatures where u is negligibly small; this will be the case when the solubility of metal ions in the oxide is negligible. This may be shown as follows. Suppose we say that growth has virtually stopped when one layer of atoms is added in 10^5 seconds, so that $dX/dt = 10^{-13}$. This occurs at a thickness X_L for which $\exp(X_L/X_1 - W/\boldsymbol{k}T) = 10^{-17}$. Substituting for X_1, this gives, since $17 \ln 10 = 39$,

$$X_L = Va'q/(W - 39\boldsymbol{k}T). \qquad \ldots\ldots(20)$$

Thus there exists a critical temperature $W/39\boldsymbol{k}$; for temperatures below this critical temperature the film grows rapidly up to some critical thickness and then stops, while for higher temperatures there is no limiting thickness, the initial rapid growth rate going over into the parabolic type of growth.

For $X \ll X_1$ an approximate integration of equation (19) can be given. Since

$$t = \frac{1}{u}\int_0^X \exp(-X_1/x)\,dx,$$

an integration by parts and neglect of higher terms in X/X_1 gives

$$ut = (X^2/X_1)\exp(-X_1/X).$$

For $X \ll X_1$ we may thus set

$$X_1/X = \ln(X_1 ut/X_L^2), \qquad \ldots\ldots(21)$$

giving a logarithmic type of growth law of the type $X_1/X = A - \ln t$. X_1 has values between 10^{-6} and 10^{-5} cm.

4.1. *Numerical values for an oxide which forms an excess semiconductor (aluminium).* For aluminium it is possible to deduce the unknown parameters W, a' in the theory from experimental work on the formation of anodic films on oxides. Following Verwey (1935) and Mott (1947 a), we make use of experimental work by Gunterschultze and Betz (1934). These authors find that the current J through an oxide film during anodic formation depends on the field F through the formula

$$J = \alpha e^{\beta F}, \qquad \ldots\ldots(22)$$

where at room temperature $1/\alpha = 2{\cdot}75 \times 10^{16}$ μa/cm^2, or 0·92 E.S.U. If F is in volts, $\beta = 4{\cdot}2 \times 10^{-6}$. For small fields ($\beta F \sim 1$) the current is negligible. The formula is obviously to be compared with (17). We set

$$qa'/\boldsymbol{k}T = \beta, \qquad W = \boldsymbol{k}T \ln(N'q\nu/\alpha).$$

Taking $N' \sim 10^{15}$ cm^{-2}, $q = 3\boldsymbol{e}$, $\nu = 10^{12}$ sec^{-1} and $\boldsymbol{k}T = 0{\cdot}025$ ev., we find $W = 1{\cdot}8$ ev., $a = 3{\cdot}5 \times 10^{-8}$ cm. These values seem reasonable.

Inserting these values into formula (20) for the limiting thickness, we find for aluminium

$$X_L = 6 \times 10^{-8} V/(1 - T/530) \text{ cm.},$$

where V is measured in volts. At room temperature this gives, in cm., $10^{-7}V$.

At room temperature the thickness found by Cabrera and Hamon (1947) is about 20 A. (Figure 9), giving $V \sim 2$ volts. The same authors have been able to verify roughly the temperature dependence of the limiting thickness X_L given by the theory. They find that the limiting thickness increases slowly with temperature, while above 300° C. (573° K.) the growth is rapid and seems to continue without limit. This agrees well with the predicted value.

Cabrera, Terrien and Hamon (1947) have also found that an increase in the thickness of the order 50% could be produced by ultra-violet illumination (Figure 9). This has been explained by Cabrera (1949 a) as due to the ejection of electrons from the metal to the adsorbed oxygen, thereby increasing the field in the layer. This is only possible when the thickness of oxide is bigger than 10 A., otherwise the current of electrons going from the absorbed oxygen back to the metal by tunnel effect will compensate the increase in the electrons going in the reverse direction produced by photoelectric effect. This is the behaviour actually observed (Figure 9).

4.2. *Oxides which absorb oxygen; the case of copper.* In the case of Cu_2O forming on copper the difference of potential set up across the oxide film must be 0·7 volts. The energy levels of Cu_2O are as shown in Figure 13. In the first place the interval from the full band of Cu_2O to the top of the Fermi distribution in the metal is known to be 0·7 ev., this being the height of the Schottky barrier in a $Cu-Cu_2O$ rectifier (Mott and Gurney 1948, p. 189). In the second place the full band is believed to be due to the Cu^+ 3d shells, and will probably be *higher* than the empty levels due to the adsorbed oxygen. Thus in equilibrium charge will distribute itself as in Figure 13 (b).

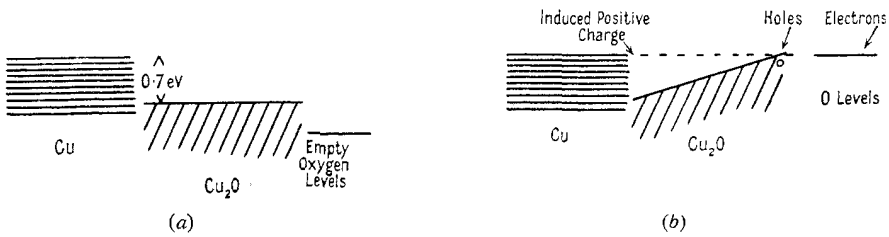

Figure 13. Electronic levels in Cu, Cu_2O and oxygen: (*a*) before equilibrium is reached, (*b*) afterwards.

The critical process which is so much accelerated by the field must now be the formation of a vacant cation site at the oxide–air interface. Though the mechanism must be very similar to that described for aluminium, the details have not yet been worked out.

The fact that the thickness of oxide formed at room temperature (130 A.) is much bigger than that formed on aluminium, in spite of the fact that V is smaller, could be explained by the fact that the critical temperature $W/39\boldsymbol{k}$ at which the logarithmic law goes over into a cubic law is now just above room temperature, if we take for $W = W_i + U$ the value 1·1 ev. suggested by the measurements of Campbell and Thomas. At liquid air temperature we should expect a thinner layer on Cu than Al, but this does not seem to be the case according to new measurements now in progress at this Laboratory by Aitchison and Allen.

§5. ADHESION AND CRYSTAL FORM OF AN OXIDE FILM

We do not know of any detailed theoretical discussion of the cohesive forces between an oxide layer and a metal substrate, or any experimental measurement of the surface energy of the interface. However, all oxides are at least partly polar; and the charges on the metal and oxygen ions must be strongly attracted to the substrate metal. Thus strong cohesive forces between metal and oxide must exist, whether or not the lattice parameters of the metal and of the oxide are equal or nearly equal.

Nevertheless, the influence of the lattice parameter of the substrate metal on the structure of the oxide is of great importance. In some cases (ZnO on the base planes of Zn) a pseudomorphic structure grows up to a considerable thickness (Finch and Quarrell 1934, 1939), the normal oxide structure being squashed into congruence with that of the zinc underneath. In other cases an oriented overgrowth is observed (Cu_2O, FeO); in others (e.g. Al_2O_3 on Al) no orientation is apparent.

A theoretical discussion of oriented overgrowths has recently been given by Frank and van der Merwe (1949, see also van der Merwe 1949) which promises to be of great importance for the theory of oxidation. These authors consider what will happen when the first monolayer of a film to be deposited on a metal is put down. Their theory is applicable first of all to one solid put down by evaporation or electro-plating on another, but their ideas are useful also for a metal exposed to oxygen. In this case, as soon as a monolayer of adsorbed oxygen is formed, atoms from the metal will start to pass through it by the mechanism which has already been described. By a monolayer of oxide, then, we mean a monolayer of oxygen through which one layer of metal atoms has passed.

Frank and van der Merwe denote by a the lattice spacing of the substrate metal and by b the "natural" spacing of the oxide layer, by which is meant the spacing that it would have if it were not attached to the metal. This is assumed to be that of the oxide in bulk. They then represent the monolayer of oxide (in a preliminary one-dimensional model) by a row of balls connected by springs of natural length b and force constant μ; that is to say, the restoring force for a displacement δx is $\mu\delta x$. The row of balls is acted on also by a force due to the substrate, the potential energy of each ball being represented, as a function of its coordinate x measured along the substrate, by

$$\tfrac{1}{2}W\cos(2\pi x/a). \qquad \ldots\ldots(23)$$

The "misfit" M between the substrate and the monolayer is defined by $M=(b/a)-1$. In practical cases b is greater than a and M is positive. The fit or misfit of the monolayer and substrate is naturally described in terms of dislocations. If, for instance, 99 or 101 atoms (balls) lie over 100 of the troughs in the potential (23), then in equilibrium the majority of the atoms lie nearly at the bottoms of their troughs, while there is a small region where the atoms ride over the crests, to miss a trough or squeeze an extra atom in. This region of misfit is called a surface dislocation; if a crystal is built above it, it will develop into a dislocation of the type used in the theory of plastic flow (Taylor 1934; for a review, see Bristol Conferences on Solids, 1940 and 1947, published by the Physical Society).

The mathematical investigation shows that if a line of balls (atoms) of finite length is put down on the substrate, then *in its state of lowest energy* each ball will lie at the bottom of a trough, except just near the ends, so long as the misfit M is less than a critical misfit M_0 given by

$$M_0=\frac{2}{\pi}\left(\frac{\mu a^2}{2W}\right)^{-\frac{1}{2}}.$$

If M exceeds M_0 by more than a very small proportion, however, and the chain is in its state of lowest energy, the spacing that the chain will take up is very nearly its equilibrium value b. However, even if the misfit is greater than M_0, then, if a line of balls is put down with each ball at the bottom of a trough, they

will remain there in metastable equilibrium unless M is greater than $\frac{1}{2}\pi M_0$—some 40% greater. Only if M is greater than $\frac{1}{2}\pi M_0$ will dislocations be generated spontaneously at the edge of the chain, so that a chain put down in a compressed state (as will happen if the balls are put down one by one) can expand to its natural length.

The application of this model to oxidation is as follows: an estimate of the interatomic forces shows that M_0 may be of the order 0·09 in an average case for a monolayer of oxide, though there may be wide variations from one metal to another. Thus, if the misfit is less than 9%, the first monolayer of oxide should have the lattice parameter of the substrate. If the temperature of deposition is low, the same will be true up to a misfit of 14%; but at high temperatures dislocations may be generated at the edge of the layer, so the value of the misfit, below which the oxide layer will in fact take up the parameter of the substrate, is smaller. If the layer does *not* take up the parameter of the substrate, each island of oxide would rotate very easily about a line perpendicular to the surface; we should not in this case expect any orientation, either in the first monolayer or in subsequent growth, except perhaps for a common crystal axis.

Suppose then that the degree of misfit is less than 9 or 14%, or whatever the figure may be, and that the first monolayer of oxide grows with the lattice parameter of the substrate and covers the whole available surface. By that time the second and third layers will have begun their growth, and will soon cover the whole surface too. The film, compressed as it is to fit the lattice parameter of the substrate, is no longer in its state of lowest energy; in terms of the ball and spring model, μ has become two or three times as big without any great change in W, it being assumed that W is mainly due to interaction between nearest neighbours. But none the less the film is in metastable equilibrium; it cannot expand by forming dislocations at the edges, because if the film covers the surface there are no free edges.

We believe that films such as that of ZnO on zinc are formed in this way. The first monolayer of oxide is formed with the parameter of the substrate, and the film continues to grow with this parameter. In the case of aluminium, on the other hand, the initial misfit is too great for this to happen, and a polycrystalline or amorphous film results.

It seems *a priori* highly probable that the thin films (*c.* 100 A.) formed at moderately low temperatures by the mechanism described in § 4 are compressed to fit the substrate in the way described here, and remain in that state. The compressive strains, of the order 10%, are, of course, much greater than the bulk material can support; in zinc the misfit is actually 20%; but it is a fairly obvious consequence of the modern theory of strength of solids (see, for instance, Mott 1949 b) that very thin films should show a much higher compressive strength than the bulk material. At some period in the growth, however, the film must break away and achieve its equilibrium lattice parameter; this will certainly have occurred for thick films (*c.* 10^{-4} cm.) growing according to the mechanism of § 2. Two mechanisms are possible by which the film may break away: slip or recrystallization. One or other of those processes is probably responsible for the kink in the oxidation curve shown for copper in Mrs. Garforth's work illustrated in Figure 1.

Some of the consequences of any mechanism by which the film continually breaks and heals have been explored by Evans, who in particular has shown that a logarithmic growth law is to be expected in cases of this sort; and when growth to a thickness of several hundred Ångströms is observed to follow a logarithmic law, it seems very probable that a mechanism such as this is valid. In general we may say that this intermediate region between the very thin, probably pseudomorphic films of 100 A. or less in thickness, described in § 4, and the thick films growing according to the parabolic law is imperfectly understood.

In conclusion, we would like to express our thanks to Dr. J. W. Mitchell and the group working under his direction on the experimental side of this subject for many discussions and permission to reproduce some of their results prior to publication.

REFERENCES

BARDEEN, J., 1947, *Phys. Rev.*, **71**, 374.
BARDEEN, J., BRATTAIN, W. H., and SHOCKLEY, W., 1946, *J. Chem. Phys.*, **14**, 714.
BATES, D. R., and MASSEY, H. S. W., 1943, *Phil. Trans.*, **239**, 269.
BÉNARD, J., and COQUELLE, O., 1946, *C.R. Acad. Sci., Paris.*, **222**, 796.
BÉNARD, J., and TALBOT, J., 1948, *C.R. Acad. Sci., Paris*, **225**, 411.
BURTON, W. K., CABRERA, N., and FRANK, F. C., 1949, *Nature, Lond.*, **163**, 398.
BURTON, W. K., and CABRERA, N., 1949, *Trans. Faraday Soc.*, in press.
CABRERA, N., 1949 a, *Phil. Mag.*, **40**, 175; 1949 b, to be published.
CABRERA, N., and HAMON, J., 1947, *C.R. Acad. Sci., Paris*, **224**, 1713.
CABRERA, N., TERRIEN, J., and HAMON, J., 1947, *C.R. Acad. Sci., Paris*, **224**, 1558.
CAMPBELL, W. E., and THOMAS, U. B., 1947, *Trans. Electrochem. Soc.*, **91**, 345.
EVANS, U. R., 1946, *Nature, Lond.*, **157**, 732; 1948, *Metallic Corrosion*, 2nd ed. (London. Edward Arnold).
FINCH, G. I., and QUARRELL, A. G., 1933, *Proc. Roy. Soc.* A, **141**, 398; 1934, *Proc. Phys. Soc.*, **46**, 148.
FRANK, F. C., 1949, *Trans. Faraday Soc.*, in press.
FRANK, F. C., and VAN DER MERWE, J., 1949 a, *Nature, Lond.*, in press; 1949 b, *Proc. Roy. Soc.* A, in press.
GARFORTH, F., 1949, to be published.
GULBRANSEN, E. A., and WYSONG, W. S., 1947, *J. Phys. Colloid. Chem.*, **51**, 1087.
GUNTERSCHULTZE, A., and BETZ, H., 1934, *Z. Phys.*, **92**, 367.
GWATHMEY, A. T., and BENTON, A. F., 1940, *J. Chem. Phys.*, **8**, 431; 1942, *J. Phys. Chem.*, **46**, 969.
KRUPKOWSKI, A., and BALICKI, S., 1937, *Métaux et Corrosion*, **12**, 89.
LENNARD-JONES, J. E., and DENT, B., 1928, *Trans. Faraday Soc.*, **24**, 92.
VAN DER MERWE, J., 1949, *Trans. Faraday Soc.*, in press.
MOTT, N. F., 1940, *Trans. Faraday Soc.*, **39**, 472; 1947 a, *Ibid.*, **43**, 429; 1947 b, *J. Chim. Phys.*, **44**, 172; 1949 a, *J. Instn. Elect. Engrs.*, in press; 1949 b, *Research*, **2**, 162.
MOTT, N. F., and GURNEY, R. W., 1948, *Electronic Processes in Ionic Crystals*, 2nd ed. (Oxford: University Press).
STEINHEIL, A., 1934, *Ann. Phys., Lpz.*, **19**, 465.
TAYLOR, G. I., 1934, *Proc. Roy. Soc.* A, **145**, 362.
VERWEY, E. J. W., 1935, *Physica*, **2**, 1059.
WAGNER, C., and GRÜNEWALD, K., 1938, *Z. Phys. Chem.* (B), **40**, 455.

3

BURTON W.K., CABRERA N., FRANK F.C.
THE GROWTH OF CRYSTALS AND THE EQUILIBRIUM STRUCTURES
OF THEIR SURFACES.
PHIL. TRANS. ROYAL SOC., LONDON 243, 299 (1951).

THE GROWTH OF CRYSTALS AND THE EQUILIBRIUM STRUCTURE OF THEIR SURFACES

By W. K. BURTON*, N. CABRERA and F. C. FRANK
H. H. Wills Physical Laboratory, University of Bristol

(*Communicated by N. F. Mott, F.R.S.—Received* 15 *March* 1950—
Revised 25 *July* 1950—*Read* 2 *November* 1950)

CONTENTS

* Seconded from Imperial Chemical Industries Ltd., Butterwick Research Laboratories, The Frythe, Welwyn, Herts.

Vol. 243. A. 866. (Price 14*s*.) 40 [Published 12 June 1951

Parts I and II deal with the theory of crystal growth, parts III and IV with the form (on the atomic scale) of a crystal surface in equilibrium with the vapour. In part I we calculate the rate of advance of monomolecular *steps* (i.e. the edges of incomplete monomolecular layers of the crystal) as a function of supersaturation in the vapour and the mean concentration of *kinks* in the steps. We show that in most cases of growth from the vapour the rate of advance of steps will be independent of their crystallographic orientation, so that a growing closed step will be circular. We also find the rate of advance for parallel sequences of steps, and the dependence of rate of advance upon the curvature of the step.

In part II we find the resulting rate of growth and the steepness of the growth cones or growth pyramids when the persistence of steps is due to the presence of dislocations. The cases in which several or many dislocations are involved are analysed in some detail; it is shown that they will commonly differ little from the case of a single dislocation. The rate of growth of a surface containing dislocations is shown to be proportional to the square of the supersaturation for low values and to the first power for high values of the latter. Volmer & Schultze's (1931) observations on the rate of growth of iodine crystals from the vapour can be explained in this way. The application of the same ideas to growth of crystals from solution is briefly discussed.

Part III deals with the equilibrium structure of steps, especially the statistics of kinks in steps, as dependent on temperature, binding energy parameters, and crystallographic orientation. The shape and size of a two-dimensional nucleus (i.e. an 'island' of new monolayer of crystal on a completed layer) in unstable equilibrium with a given supersaturation at a given temperature is obtained, whence a corrected activation energy for two-dimensional nucleation is evaluated. At moderately low supersaturations this is so large that a *perfect* crystal would have no observable growth rate. For a crystal face containing two screw dislocations of opposite sense, joined by a step, the activation energy is still very large when their distance apart is less than the diameter of the corresponding critical nucleus; but for any greater separation it is zero.

Part IV treats as a 'co-operative phenomenon' the temperature dependence of the structure of the surface of a perfect crystal, free from steps at absolute zero. It is shown that such a surface remains practically flat (save for single adsorbed molecules and vacant surface sites) until a transition temperature is reached, at which the roughness of the surface increases very rapidly ('*surface melting*'). Assuming that the molecules in the surface are all in one or other of two levels, the results of Onsager (1944) for two-dimensional ferromagnets can be applied with little change. The transition temperature is of the order of, or higher than, the melting-point for crystal faces with nearest neighbour interactions in both directions (e.g. (100) faces of simple cubic or (111) or (100) faces of face-centred cubic crystals). When the interactions are of second nearest neighbour type in one direction (e.g. (110) faces of s.c. or f.c.c. crystals), the transition temperature is lower and corresponds to a surface melting of second nearest neighbour bonds. The error introduced by the assumed restriction to two available levels is investigated by a generalization of Bethe's method (1935) to larger numbers of levels. This method gives an anomalous result for the two-level problem. The calculated transition temperature decreases substantially on going from two to three levels, but remains practically the same for larger numbers.

Note on authorship. Although at all times a constant interchange of ideas took place between all three authors, the principal contributions of one of us (F.C.F.) are to part II of this paper. Part IV, and all the calculations in parts I and III, are due exclusively to W.K.B. and N.C.

A THEORY OF GROWTH OF REAL CRYSTALS

PART I. MOVEMENT OF STEPS ON A CRYSTAL SURFACE

1. *Introduction*

The theory of growth of perfect crystals has been developed extensively during the past thirty years, especially by the work of Volmer (1939), Stranski (1928, 1934), and Becker & Döring (1935). The essential ideas were put forward earlier by Gibbs (1878).

According to this theory, when all surfaces of high index (stepped surfaces) have disappeared, the crystal will continue to grow by two-dimensional nucleation of new molecular layers on the surfaces of low index (saturated surfaces). As in all nucleation processes, the probability for the formation of these two-dimensional nuclei is a very sensitive function of the supersaturation. This probability is quite negligible below a certain critical supersaturation and increases very rapidly above it. Assuming reasonable values for the edge energy of the two-dimensional nuclei, one recognizes that this critical supersaturation should be of the order of 50 %. At the supersaturations at which real crystals grow (1 % and even lower) the probability of formation of nuclei should be, according to this theory, absolutely negligible (Burton, Cabrera & Frank 1949; Burton & Cabrera 1949, cf. also part III).

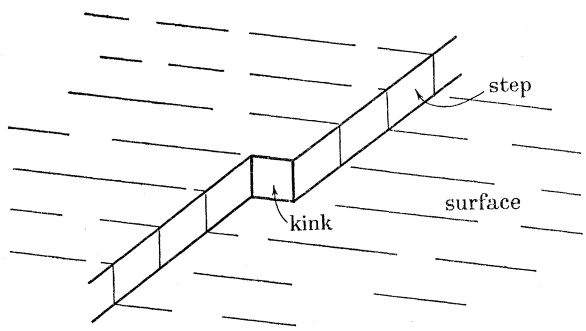

FIGURE 1. The presence of a kink in a step on a crystal surface.

Recently, Frenkel (1945) pointed out that the structure of a perfect crystal surface above the absolute zero of temperature would have a certain roughness produced by thermal fluctuations. He discussed the structure of a monomolecular *step* and proved that it will contain a high concentration of *kinks*, illustrated in figure 1, and introduced before by Kossel (1927) and Stranski (1928). Burton & Cabrera (1949, cf. also part III) have shown that the concentration of *kinks* is even larger than was supposed by Frenkel; this result is very important from the point of view of the rate of advance of the steps, which will be developed in part I of this paper. On the other hand, Frenkel generalized this idea to the formation of steps in a perfect crystal surface, but Burton & Cabrera (1949, cf. also part IV) have shown that steps will not be created by thermodynamical fluctuations in a low-index crystal surface, unless, perhaps, close to the melting-point; therefore the steps required for growth can only be produced, on a perfect crystal surface, under a highly supersaturated environment.

We conclude that the growth of crystals under low supersaturations can only be explained by recognizing that the crystals which grow are *not* perfect, and that their imperfections (in particular, dislocations terminating in the surface with a screw component) will provide the steps required for growth, making two-dimensional nucleation unnecessary. This idea, introduced by Frank (Burton *et al.* 1949; Frank 1949) will be developed in this paper, and we shall see that it explains most of the features of crystal growth at low supersaturations.

This theory of growth of real crystals assumes the existence of dislocations in them, but does not depend critically on their concentration. The study of crystal growth should perhaps also explain the formation of dislocations which, as in the case of steps in a crystal surface, cannot be due to thermodynamical fluctuations. Several mechanisms can be visualized for

the formation of new dislocations during growth (Frank 1949), but no detailed theory has yet been formulated.

2. *Mobility of adsorbed molecules on a crystal surface*

We know that in general a crystal surface in contact with its vapour will contain a certain concentration n_s per cm.^{2} of adsorbed, essentially mobile molecules. Under equilibrium conditions, the concentration n_{s0} of adsorbed molecules will be given by a formula of the type

$$n_{s0} = n_0 \exp(-W_s/kT), \tag{1}$$

where W_s is the energy of evaporation from the kinks on to the surface; n_0 contains entropy factors, but in simple cases will be of the order of the number per cm.^{2} of molecular positions on the surface.

The process of growth of a crystal surface *with* steps will be the result of three separate processes: (i) exchange of molecules between adsorbed layer and vapour, (ii) diffusion of adsorbed molecules towards the steps and exchange with them, and (iii) perhaps also diffusion of adsorbed molecules in the edge of the steps toward the kinks and exchange with them.

In order to discuss the role of the diffusion on the surface we must introduce the *mean displacement x_s of adsorbed molecules*. This can be defined in quite general terms by Einstein's formula:

$$x_s^2 = D_s \tau_s, \tag{2}$$

where D_s is the diffusion coefficient and τ_s the mean life of an adsorbed molecule before being evaporated again into the vapour. For simple molecules we can write

$$D_s = a^2 \nu' \exp(-U_s/kT), \tag{3}$$

and

$$1/\tau_s = \nu \exp(-W_s'/kT), \tag{4}$$

where U_s is the activation energy between two neighbouring equilibrium positions on the surface, distant a from each other, and W_s' the evaporation energy from the surface to the vapour. The frequency factors ν' and ν would both be of the order of the atomic frequency of vibration ($\nu \sim 10^{13}$ sec.$^{-1}$) in the case of monatomic substances, but they will be different in the case of more complicated molecules. Using (3) and (4), (2) becomes

$$x_s = a \exp\{(W_s' - U_s)/2kT\}, \tag{5}$$

assuming $\nu' \sim \nu$. The condition for the diffusion on the surface to play an important role is that $x_s > a$, and therefore from (5), $W_s' > U_s$. This is probably always the case; then x_s can be much larger than a and increases rapidly as the temperature decreases.

In order to have an idea of the values that we can expect for x_s, let us consider, for instance, a (1, 1, 1) close-packed surface of a face-centred cubic crystal. By simple considerations regarding the interaction ϕ between nearest neighbours only, $W_s' = 3\phi$, i.e. half the total evaporation energy $W = W_s + W_s'$; while $U_s \sim \phi = \frac{1}{6}W$. However, fuller calculations carried out by Mackenzie (1950) using Lennard-Jones forces show that U_s is considerably smaller, about $\frac{1}{20}W$. Hence, in this case, (5) becomes

$$x_s \sim a \exp(3\phi/2kT) \sim 4 \times 10^2 a \tag{6}$$

for the typical value $\phi/kT \sim 4$.

It is interesting to notice that x_s will be a function of the crystal face considered, both W_s' and U_s being different for different faces. In general, x_s will be smallest for the closest packed surface, because W_s' increases more rapidly than U_s. For instance, for a (1, 0, 0) surface in a face-centred cubic (f.c.c.) crystal assuming nearest neighbour forces, $W_s' = 4\phi$ and U_s is probably still very small. Then

$$x_s \sim a \exp(2\phi/kT) \sim 3 \times 10^3 a.$$

3. *Concentration of kinks in a step*

Frenkel (1945) and Burton & Cabrera (1949, cf. also part III) have shown that these steps must always contain a large concentration of kinks. In the case of short-range intermolecular forces, we can briefly summarize in the following manner the results of the theory which have an important bearing on growth.

Let a close-packed crystallographic direction be taken as the x-axis, and consider a step which follows this axis in the mean, so that the surface is one molecule higher in the region $y \ll 0$ than in the region $y \gg 0$. Following the step along the direction of increasing x, points where y increases or decreases by a unit spacing a are called positive or negative kinks respectively. For this orientation, the step contains equal numbers of positive and negative kinks, and their total number is less than for any other orientation. Let $2n$ and q be the probabilities for having a kink or no kink, respectively, at a given site in the step. Then we must have

$$n/q = \exp(-w/kT), \quad 2n+q = 1,$$

where w is the energy necessary to form a kink. Hence the mean distance $x_0 = a/2n$ between kinks is

$$x_0 = \tfrac{1}{2}a\{\exp(w/kT)+2\} \sim \tfrac{1}{2}a \exp(w/kT), \tag{7}$$

where a is the intermolecular distance in the direction of the step.

As the inclination θ of the step relative to a close-packed direction increases, the number of kinks increases. Let n_+ and n_- be the probabilities for having a positive or negative kink respectively.

As an approximation, we neglect the difference between q and unity. Then

$$2n = n_+ + n_-, \quad \theta = n_+ - n_-,$$

where n is the probability for having a kink of any kind and θ is assumed to be small. For any inclination, and from thermodynamical considerations,

$$n_+ n_- = \exp(-2w/kT).$$

Thus the mean distance $x_0(\theta)$ between kinks will now be

$$x_0(\theta) = x_0\{1 - \tfrac{1}{2}(x_0/a)^2 \theta^2\}, \tag{8}$$

assuming $\theta < a/x_0$ and x_0 is given by (7).

No detailed calculation of w has yet been made, but simple considerations suggest that w must be a small fraction of the evaporation energy. For instance, in a close-packed step in a (1, 1, 1) face of a f.c.c. crystal, with nearest neighbour interactions ϕ, it is easy to see that w is equal to a quarter of the energy necessary to move one molecule from a position in the

straight step to an adsorption position against the straight step, equal to 2ϕ; hence $w = \frac{1}{2}\phi$ or $\frac{1}{12}W$, and the mean distance between kinks is, from (7),

$$x_0 = \tfrac{1}{2}a \exp(\phi/2kT) \sim 4a, \tag{9}$$

for the typical value $\phi/kT \sim 4$.

The concentration of kinks in the steps will remain practically unchanged even if the vapour is supersaturated. Hence the problem of the rate of advance of a step is reduced to a classical diffusion problem on the surface. The important ratio in this calculation is x_s/x_0. From (5) and (7) this is approximately $2\exp\{(\frac{1}{2}W_s' - \frac{1}{2}U_s - w)/kT\}$. With the estimates of W_s', U_s and w which we have made above on the basis of the simple model of a close-packed homopolar crystal, this is about 10^2. Thus it appears that we may generally assume $x_s \gg x_0$, in which case we can perform the diffusion calculation regarding the step as a continuous-line sink. It is an interesting corollary of this case that the rate of advance of a step is then independent of its crystallographic orientation. However, the estimate is uncertain for various reasons, such as the neglect of entropy factors, and we shall also examine the cases in which x_0 is comparable with or larger than x_s.

4. *Rate of advance of a step*

The supersaturation σ in the vapour is defined as

$$\sigma = \alpha - 1, \quad \alpha = p/p_0, \tag{10}$$

where p is the actual vapour pressure, p_0 the saturation value, and α will be called the saturation ratio. We assume σ to be constant above the surface. There will also be a supersaturation σ_s of adsorbed molecules on the surface (in general, dependent on position) defined by

$$\sigma_s = \alpha_s - 1, \quad \alpha_s = n_s/n_{s0}, \tag{11}$$

where n_s and n_{s0} are the actual and equilibrium concentration of adsorbed molecules respectively.

The equations governing the diffusion of adsorbed molecules towards the step are easily written down. The current on the surface will be

$$j_s = -D_s \operatorname{grad} n_s = D_s n_{s0} \operatorname{grad} \psi, \quad \psi = \sigma - \sigma_s, \tag{12}$$

where D_s is the diffusion coefficient of adsorbed molecules. There will also be a current j_v going *from* the vapour *to* the surface, which is easily seen to be

$$j_v = (\alpha - \alpha_s)\, n_{s0}/\tau_s = n_{s0}\psi/\tau_s, \tag{13}$$

where τ_s is the *mean life* of an adsorbed molecule on the surface, defined in § 2.

Let us make the assumption (to be justified *a posteriori*) that the movement of the step can be neglected in the diffusion problem, so that the adsorbed molecules have a steady distribution on either side of the step which is practically the same as though the step were absorbing molecules without moving. Under these conditions ψ must satisfy the continuity equation

$$\operatorname{div} j_s = j_v,$$

or using (6) and (7) and assuming D_s independent of direction in the surface

$$x_s^2 \nabla^2 \psi = \psi, \tag{14}$$

where x_s is the *mean displacement* of adsorbed molecules, defined in § 2.

Now if we compare the typical values for x_s and x_0 estimated in (6) and (9) respectively, we see that in most cases, certainly for monatomic substances, $x_s \gg x_0$. Under these conditions, each molecule deposited from the vapour on the surface near the step will have a high probability to reach a kink in the step before being evaporated again into the vapour. Therefore the concentration of adsorbed molecules near the step will be controlled by evaporation from and condensation into the kinks. Then, provided this exchange is very rapid, the concentration near the step should be maintained equal to the equilibrium value, independently of the supersaturation existing in the vapour.

Thus, if we assume that $\sigma_s = 0$ near the step, and $\sigma_s = \sigma$ far from it, equation (14) has the simple solution

$$\psi = \sigma \exp(\mp y/x_s), \tag{15}$$

where y is the distance to the step, the minus sign being used for $y>0$ and the plus sign for $y<0$. Now the current j going into the step per cm. per sec. will be obtained from (12) using (15) and putting $y = 0$. The velocity of the step is then $v_\infty = j/n_0$, where $1/n_0$ is the area per molecular position; therefore

$$v_\infty = 2\sigma x_s \nu \exp(-W/kT), \tag{16}$$

where expressions (1) and (4) for n_{s0} and τ_s have been used, and $W = W_s + W_s'$ is the total evaporation energy. The factor 2 comes about because of the contribution from $y>0$ and $y<0$. The advance of the step is therefore owing to the molecules condensing from the vapour on a strip of width x_s at both sides of the step. This expression represents the maximum velocity of a step in a given direction, and if D_s and therefore x_s were independent of direction, then the velocity of the step would be independent of its orientation.

We can now justify our neglect of the motion of the step when treating the diffusion problem. This is permissible if the characteristic distance (D_s/v_∞) is great compared with the characteristic distance x_s. Now, from (3), (5) and (16),

$$v_\infty x_s/D_s = 2\sigma \exp(-W_s/kT) \sim 2\sigma \exp(-12) \ll 1.$$

We believe that (16) is correct, at least in the case of monatomic substances. In the case of molecular substances we must introduce two possible complications: (i) as Wyllie (1949) has pointed out the exchange between the kinks and the adsorbed layer might not be rapid enough to maintain $\sigma_s = 0$ near the kinks; (ii) the condition $x_s \gg x_0$ is perhaps not satisfied.

It is easy to see that (i) introduces a supplementary factor $\beta<1$ in formula (16) given by

$$\beta = (1 + x_s\tau/a\tau_s)^{-1}, \tag{17}$$

where τ is the time of relaxation necessary to re-establish equilibrium near the step. The supersaturation near the step will then be $\sigma_s(0) = (1-\beta)\sigma$; β will be smaller than 1, for instance, when the rotational entropy of the adsorbed molecules is much larger than that of the molecules in the solid. If condition $x_s \gg x_0$ is nevertheless satisfied, then v_∞ should still be independent of the orientation of the step.

On the other hand, if $x_s \gg x_0$ is not satisfied, the supersaturation near the step will not be constant, and will be a function of x_0. The other extreme case, when $x_0 \gg x_s$, is easy to consider. It is then necessary to discuss the influence of the diffusion of adsorbed molecules in the edge of the step. If the contribution of the current via the edge is important, then this will help

to keep the supersaturation constant near the step, even if $x_0 \gg x_s$. The most unfavourable case would be when the current via the edge can be neglected altogether. Then, assuming D_s to be independent of direction, the required solution of (14), around an isolated kink on the step, is

$$\psi(r) = \beta\sigma \frac{K_0(r/x_s)}{K_0(a/x_s)},$$

where K_0 is the Bessel function of second kind with imaginary argument and order zero, and we assume that the supersaturation of adsorbed molecules is maintained equal to $(1-\beta)\,\sigma$ at a distance $r = a$ from the kink. The current going into every step is then easily calculated and the velocity of advance of the step is given by

$$v_\infty = \{2\sigma\beta x_s \nu \exp(-W/kT)\}\,\pi x_s/x_0 \ln(2x_s/\gamma a),$$

where we assume always $x_s > a$ and we use the approximate formulae

$$K_0(a/x_s) = \ln(2x_s/\gamma a), \quad K_1(a/x_s) = -x_s/a,$$

$\gamma = 1{\cdot}78$ being Euler's constant. We may verify once again that, at least for sufficiently small supersaturations, we may neglect the motion of the kink in treating the corresponding diffusion problem. The criterion this time is $(v_{\text{kink}}\, x_s/D_s) \ll 1$, where $v_{\text{kink}} = v_\infty x_0/a$. Now by use of (3) and (5)

$$v_{\text{kink}}\, x_s/D_s = [2\pi\beta\sigma \exp\{-(W+\tfrac{1}{2}U_s-\tfrac{3}{2}W_s')/kT\}]/\{\ln(2/\gamma)+(W_s'-U_s)/kT\}.$$

The exponential factor here remains considerably less than unity for any reasonable estimate of the energies, especially as the condition $x_0 > x_s$ is only likely to arise when U_s is unusually large or W_s' unusually small, though U_s can scarcely exceed W_s' so as to make the denominator small.

We see that apart from the factor β, the maximum velocity (16) is multiplied by another factor $c_0 < 1$, given by

$$c_0 = \pi x_s/x_0 \ln(2x_s/\gamma a). \tag{18}$$

In the general case, the velocity of advance of the step can also be represented by the general formula

$$v_\infty = 2\sigma x_s \nu \exp(-W/kT)\,\beta c_0, \tag{19}$$

where c_0 is between 1 and the value given by equation (18).

The calculation of c_0 in the general case is a difficult problem. The easiest way to solve it is to assume that *there is* a diffusion in the edge of the step and that it is important enough for the current going directly from the surface to the kinks to be neglected. In appendix A we treat along these lines the problem of a single step with equally spaced kinks.

The relative importance of the current diffusing in the edge of the step and that diffusing on the surface will be represented by the non-dimensional factor

$$D_e n_{e0}/D_s n_{s0} a,$$

where D_e and n_{e0} are the diffusion coefficient and the equilibrium concentration respectively of adsorbed molecules in the edge. This factor is equal to $(x_e/a)^2$, where x_e is the mean displacement of adsorbed molecules in the edge. Actually $x_e^2 = D_e \tau_e$, and by definition

$$\tau_e = n_{e0} a/D_s n_{s0} = (1/\nu) \exp\{(W_e'+U_s)/kT\};$$

therefore

$$x_e^2 = D_e n_{e0} a/D_s n_{s0} \sim a^2 \exp\{(W_e'+U_s-U_e)/kT\}, \tag{20}$$

where W'_e is the energy necessary to take an adsorbed molecule from the edge to the surface and U_e is the activation energy for diffusion in the edge.

It is clear that $D_s > D_e$; on the other hand, $n_{s0}a < n_{e0}$. If $x_e > a$, the current going into the kinks goes essentially via the edge and the point of view adopted above is justified. If, on the contrary, $x_e < a$, the important contribution is that due to direct condensation from the surface into the kinks. The case $x_e \sim a$ can also be interpreted as if the edge did not exist at all, since this would correspond to $W'_e = 0$, $U_e = U_s$, which implies also $x_e = a$. Hence the method of calculation suggested above should give for $x_e \sim a$ the same result as if the influence of diffusion in the edge were neglected altogether.

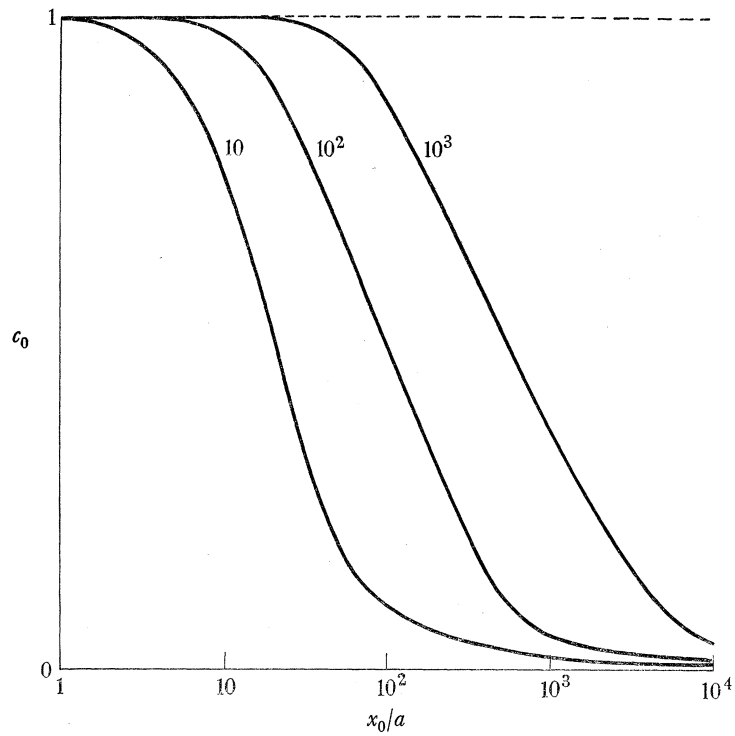

FIGURE 2. The factor c_0 as a function of x_0/a for the values of x_s/a indicated on the curves.

It is difficult in general to estimate x_e. In the particular case of a close-packed step in a (1, 1, 1) face of a f.c.c. crystal, with nearest neighbour interactions ϕ, we can estimate $W'_e = 2\phi$, $U_s \sim 0$, $U_e \sim 2\phi$, hence $x_e \sim a$. Assuming this to be the case, the general formula given in appendix A reduces to

$$1/c_0 = 1 + 2b \ln \{(4bx_s/a)/(1 + (1 + b^2)^{\frac{1}{2}})\}, \quad b = x_0/2\pi x_s, \tag{21}$$

which is represented in figure 2 as a function of x_0/a for several values of x_s/a. It is interesting to notice that if x_0 increases indefinitely in (21), then

$$c_0 = \pi x_s/x_0 \ln (4x_s/a),$$

which practically coincides with (18) as we should expect. We notice that c_0 differs appreciably from unity for $x_0 \geqslant x_s$.

In conclusion to this paragraph, and from the estimates of x_s and x_0 made in §§ 2 and 3, we deduce that in most cases of growth from the vapour *the rate of advance of the step must be practically independent of its orientation.* In some cases, perhaps, the factor c_0 in (19) could be smaller than 1 for the close-packed slowest steps, containing a minimum number of kinks. As the orientation of the step deviates from that of closest packing, c_0 will become rapidly equal to 1.

5. *Parallel sequence of steps*

Another interesting problem is that of the movement of a parallel sequence of steps separated by equal distances y_0.

If we assume that the distance x_0 between kinks in every step satisfies the condition $x_0 \ll x_s$, and that near every step $\sigma_s = 0$, the solution of equation (14) is easily seen to be

$$\psi = \sigma \frac{\cosh(y/x_s)}{\cosh(y_0/2x_s)} \tag{22}$$

between two steps, where y is the distance from the mid-point between two steps. The current going into every step is again calculated from (12), using (22) and putting $y = \frac{1}{2}y_0$; the velocity of every step is then

$$v_\infty = 2\sigma x_s \nu \exp(-W/kT) \tanh(y_0/2x_s), \tag{23}$$

which reduces to (16) if $y_0 \to \infty$.

In the general case where (i) the interchange with the kinks is not rapid enough to maintain $\sigma_s = 0$ near the step and (ii) the condition $x_0 \ll x_s$ is not satisfied, we obtain again a general formula of the type

$$v_\infty = 2\sigma x_s \nu \exp(-W/kT) \tanh(y_0/2x_s)\, \beta c_0, \tag{24}$$

where $c_0 \leqslant 1$ is a function of x_0 and y_0. The calculation of c_0 is now rather complicated.

In the particular case when $x_e \sim a$ in the edge of the steps, one can give for c_0 the approximated expression

$$1/c_0 = 1 + 2b \tanh(y_0/x_s)\,[\ln\{(4bx_s/a)/(1+(1+b^2)^{\frac{1}{2}})\} + (2x_s/y_0)\tan^{-1} b], \tag{25}$$
$$b = x_0/2\pi x_s.$$

For $y_0 \to \infty$ this expression reduces of course to (21). As y_0 decreases, c_0 in general will be nearer 1 than (21) is, as we should expect, but this does not mean that for a sufficiently small value of y_0 we shall get $c_0 = 1$, because of the second term in the parentheses in (25).

6. *The rate of advance of small closed step-lines*

We know that, given a certain supersaturation in the vapour, there will be a certain two-dimensional nucleus which is in unstable equilibrium with it. The shape and size of this *critical* nucleus are perfectly defined; its shape has been studied in detail in one special case, Burton *et al.* 1949; cf. also part III. It is interesting to notice at this point that the number of kinks per unit length in every position of the edge of the critical nucleus is the same as that in an infinite step having the same orientation.

If the nucleus is larger than the critical one it will grow. Then its shape will be determined essentially by the differences in velocity for the different orientations and *not* by thermo-

dynamical considerations. In particular, if the velocity is the same for all orientations, it will become circular. The study of the shape of a growing nucleus of large dimensions will be considered in detail by one of us (F. C. F.) in a later paper; here we are concerned with the absolute value of the velocity when the dimensions are not very different from those of the critical nucleus.

Let us consider first the case of independence of velocity on orientation, when the nucleus is circular. We shall consider afterwards what changes can be expected when the velocity depends on the orientation.

The mean evaporation from the nucleus to the surface will be a function of its dimensions. If its radius is ρ, and we define an edge energy of the nucleus equal to γ per molecule, the mean energy of evaporation will be

$$W_s(\rho) = W_s - (\gamma a/\rho),$$

where a is as usual the intermolecular distance.

Let σ be the supersaturation in the vapour; the nucleus will grow, but at every moment a steady distribution of adsorbed molecules will be formed provided the nucleus is not too small. The influence of the movement of the boundary on the diffusion problem can be neglected for the low supersaturations considered. The steady supersaturation in the surface will satisfy the continuity equation (14) which now becomes

$$x_s^2 \nabla^2 \psi(r) = \psi(r), \quad \psi(r) = \sigma - \sigma_s(r). \tag{26}$$

The solution of this equation is

$$\psi(r) = \psi(\rho) \frac{I_0(r/x_s)}{I_0(\rho/x_s)} \quad (r<\rho),$$

$$\psi(r) = \psi(\rho) \frac{K_0(r/x_s)}{K_0(\rho/x_s)} \quad (r>\rho), \tag{27}$$

where I_0 and K_0 are the Bessel functions of first and second kind with imaginary argument. $\psi(\rho)$ is the value of ψ near the edge of the nucleus. If the interchange of molecules between the nucleus and the surface is rapid enough, the supersaturation $\sigma_s(\rho)$ near the edge of the nucleus will be maintained equal to that which would be in equilibrium with it. This supersaturation $\sigma_s(\rho)$ is given by

$$\sigma_s(\rho) = \frac{\exp[-W_s(\rho)/kT]}{\exp[-W_s/kT]} - 1 = \exp(\gamma a/\rho kT) - 1;$$

therefore

$$\psi(\rho) = \sigma - \sigma_s(\rho) = \sigma - [\exp(\gamma a/\rho kT) - 1]. \tag{28}$$

The current going into the nucleus is now

$$j = 2\pi\rho D_s n_{s0} (\partial\psi/\partial r)_{r=\rho} = 2\pi D_s n_{s0} \psi(\rho)/I_0(\rho/x_s)\, K_0(\rho/x_s),$$

where the formulae

$$I_0'(z) = I_1(z), \quad K_0'(z) = -K_1(z), \quad I_0(z)\, K_1(z) + I_1(z)\, K_0(z) = 1/z$$

have been used. The radial velocity, $v(\rho) = j(\rho)/2\pi\rho n_0$, is therefore

$$v(\rho) = x_s^2 \nu \exp(-W/kT)\, \psi(\rho)/\rho I_0(\rho/x_s)\, K_0(\rho/x_s), \tag{29}$$

where we have used the expressions for x_s, τ_s and n_{s0}, given by (2), (4) and (1). Current and velocity change sign when $\sigma_s(\rho_c) = \sigma$, which defines the critical nucleus to have a radius ρ_c given by

$$\rho_c = \gamma a/kT \ln \alpha, \quad \alpha = 1+\sigma. \tag{30}$$

When $\rho > x_s$ we can use the approximation

$$I_0(\rho/x_s)\, K_0(\rho/x_s) = x_s/2\rho,$$

so that (29) becomes

$$v(\rho) = v_\infty(\alpha - \alpha^{\rho_c/\rho})/\sigma, \quad \alpha = 1+\sigma, \tag{31}$$

or if σ is small,

$$v(\rho) = v_\infty(1-\rho_c/\rho), \tag{32}$$

where v_∞ is the maximum velocity (16) of a straight step of any orientation, calculated in § 4. This formula will be valid down to $\rho = \rho_c$, provided the supersaturation is low enough for ρ_c to be larger than x_s, and $\ln\alpha \sim \sigma$. As σ increases and ρ_c decreases, $v(\rho)$ will be a more complicated function for $\rho \sim \rho_c$.

It is also interesting to consider the rate of advance of a sequence of concentric circles, distant y_0 from each other. The diffusion problem can also be solved in a similar way. The radial velocity of the circle of radius ρ turns out to be

$$v(\rho) = 2\sigma x_s \nu \exp(-W/kT) \tanh(y_0/2x_s)\,(1-\rho_c/\rho), \tag{33}$$

when $\rho > x_s$, $y_0 \ll \rho$ and $\ln\alpha \sim \sigma$. We see that $v(\rho)$ is again of the general form (32), if v_∞ means now the velocity (23) corresponding to a sequence of parallel steps. We see therefore that the only change in the rate of advance of a large closed step of radius ρ, with respect to that of an infinite step is the factor $(1-\rho_c/\rho)$. This is just what we should expect because the mean supersaturation near the edge of the nucleus is not zero, as in the case of the straight step, but $\sigma\rho_c/\rho$.

The same general formula (32) will apply also when (i) the interchange of molecules between nucleus and surface is not rapid, and (ii) the velocity depends on the orientation of the edge. Then the nucleus will not be a circle, but the close-packed slowest orientations of the edge will move according to (32) where v_∞ is now given by the general formula (24); ρ will be the normal distance from the edge to the centre of the nucleus and ρ_c that corresponding to the critical nucleus.

Part II. Rates of growth of a crystal surface

7. *Introduction*

In part I we have studied the movement of steps on a perfect crystal surface, without considering their origin. This information is sufficient to calculate the rates of growth of stepped surfaces (those of high index) where the steps exist because of the geometry of the surface; nevertheless, it is clear that these steps will disappear in any finite crystal, after a finite amount of growth which completes the body bounded by close-packed, unstepped surfaces circumscribed to the initial crystal.

Frank (1949) has shown that further growth of these surfaces must be attributed to the presence of steps associated with crystal defects, in particular dislocations having a component of displacement vector normal to the crystal face at which they emerge, 'screw dislocations'

for short, though they are not necessarily 'pure screw' dislocations. He has also shown that when the crystal is growing under a supersaturated environment, the step due to a dislocation winds itself in a spiral in such a way that a single screw dislocation sends out successive turns of steps (figure 3). If the step is due to a right- and left-handed pair of dislocations, they will send out closed loops (figure 4) provided their distance apart is greater than the diameter of a critical nucleus. In both cases the dislocations will form pyramids and the concentration of step lines thereon will be large and practically independent of the number of dislocations. This provides an interpretation of the pyramids of vicinal faces long recognized as a normal

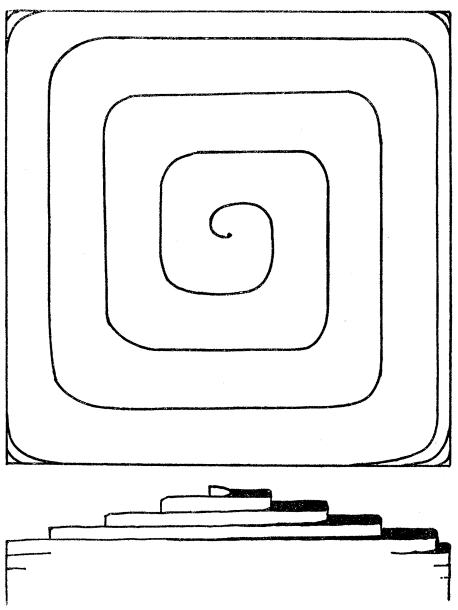

FIGURE 3. Growth pyramid due to a single screw dislocation.

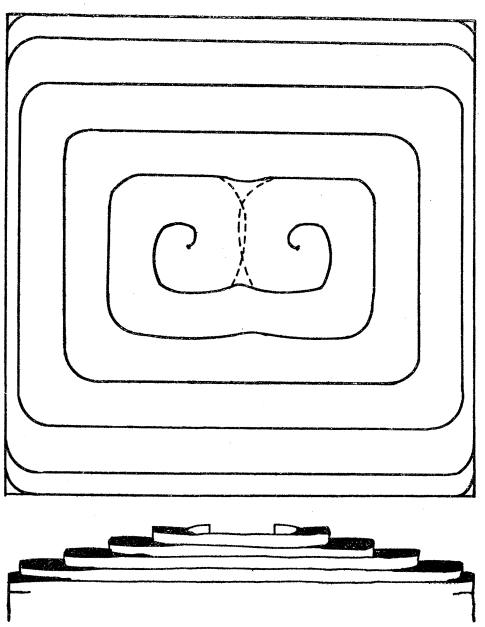

FIGURE 4. Growth pyramid due to a pair of dislocations.

feature of slow crystal growth (Miers 1903, 1904). In this part we shall study in more detail the mathematics of these pyramids (§§ 8, 9); once the rate at which these pyramids grow is known we shall apply the results to growth from the vapour using the formulae for rate of advance of steps deduced in I (§§ 10, 11). The application of the same ideas to growth from solution will also be considered briefly in § 12. The resulting topography of the crystal surface will be discussed by one of us in a later paper.

8. *The growth pyramid due to a single dislocation*

Let us first consider the spiral due to a single dislocation ending on an otherwise perfect crystal surface. We may suppose that, as new layers are added, the direction of the dislocation remains perpendicular to the surface, since this will usually minimize the elastic energy. If the rate of advance of a step is independent of its orientation (probably the case during growth from the vapour, see I) the growing spiral will form a low cone, but it will tend to form a pyramid when the rate of advance depends on the orientation (as is illustrated in figures 3 and 4). We consider first the case of a growing cone.

Following any increase in supersaturation, the step due to the dislocation will rapidly wind itself up into a spiral centred on the dislocation, until the curvature at the centre reaches the critical value $1/\rho_c$, at which curvature the rate of advance falls to zero; the whole spiral will then rotate steadily with stationary shape.

We know (I, formula (32)) that the normal rate of advance of a portion of spiral with radius of curvature ρ is given by

$$v(\rho) = v_\infty(1-\rho_c/\rho), \tag{34}$$

provided the supersaturation is not too high. Now let $\theta(r)$ represent the rotating spiral, in (rotating) polar co-ordinates (r, θ). The radius of curvature at a point r will be

$$\rho = (1+r^2\theta'^2)^{\frac{3}{2}}/(2\theta'+r^2\theta'^3+r\theta''), \tag{35}$$

θ' and θ'' being the derivatives of $\theta(r)$. If the angular velocity of the whole spiral is ω, the normal velocity at the point r is

$$v(r) = \omega r(1+r^2\theta'^2)^{-\frac{1}{2}}. \tag{36}$$

We must now find $\theta(r)$ and ω from these three equations.

A good approximation is obtained by taking an Archimedean spiral

$$r = 2\rho_c\theta > 0, \tag{37}$$

which has the proper central curvature. ω is then given by

$$\omega = v_\infty/2\rho_c. \tag{38}$$

This approximation does not satisfy (34), especially for small r, but nevertheless gives a good approximation to ω.

A better approximation can be obtained in the following way: one obtains the solutions for small r (neglecting r^2) and for large r (neglecting $1/r^2$):

$$r \to 0: \quad \theta' = 1/2\rho_c - \omega r/3v_\infty\rho_c, \tag{39}$$

$$r \to \infty: \quad \theta' = (\omega/v_\infty)\,(1+\rho_c/r). \tag{40}$$

Then, choosing a general expression of the form

$$\theta' = a+b/(1+cr), \tag{41}$$

one determines, a, b, c and ω in such a way that (41) reduces to (39) and (40) for the proper ranges of r. We obtain in this way

$$\left.\begin{aligned} \theta &= \frac{3^{\frac{1}{2}}}{2(1+3^{\frac{1}{2}})}\,[r/\rho_c+\ln(1+r/3^{\frac{1}{2}}\rho_c)], \\ \omega &= 3^{\frac{1}{2}}v_\infty/2\rho_c(1+3^{\frac{1}{2}}) = 0{\cdot}63v_\infty/2\rho_c. \end{aligned}\right\} \tag{42}$$

This solution satisfies (34) within a few units per cent of v_∞ for all values of ρ. The interesting point is that the value of ω obtained differs from (38) only by a factor close to 1, showing that ω is insensitive to the actual law of dependence of v on ρ in the range in which $\rho \sim \rho_c$. Even the crudest approximation to (34),

$$\rho = \rho_c: \quad v = 0; \qquad \rho > \rho_c: \quad v = v_\infty,$$

(Frank 1949) gives an angular velocity only twice as large as (38), i.e. just over three times the best approximation (42).

In the rest of this part, the number of turns of the spiral per second, $\omega/2\pi$, will be called the *activity*. The actual rate of vertical growth R of the pyramid and therefore of the crystal will clearly be

$$R = \omega a/2\pi = n_0 \Omega v_\infty / 4\pi\rho_c, \tag{43}$$

where $a = n_0\,\Omega$ is the height of a step (n_0 the number of molecular positions per cm.^{2} in the surface, Ω the volume of a molecule), and we have used the approximation (38) for ω.

The distance y_0 between successive turns of the spiral for large r is given by

$$y_0 = 2\pi/\theta' = 4\pi\rho_c. \tag{44}$$

These formulae will also be approximately valid when there is an influence of the crystallographic orientation on the rate of advance of the steps. v_∞ is then the value corresponding to the slowest advancing orientation, and ρ_c half the dimension of the critical two-dimensional nucleus.

9. *The growth pyramids due to groups of dislocations*

9·1. *Topological considerations*

We now consider the interactions between the growth spirals centred on different dislocations. We have already considered the case of a pair of opposite sign, and seen that if they are closer together than a critical distance ($2\rho_c$ in the simple case) no growth occurs, while if they are further apart than this they send out successive closed loops of steps. It is obvious that if there are *two such pairs* these loops unite on meeting, and the number of steps passing any distant point in a given time is the same as if only one pair existed. The whole area may be formally divided into two areas by a locus of intersections of the two families, and one area may be considered to receive steps from the one centre, the other from the other centre.

Hence two similar pairs of dislocations of opposite sign, separated by a distance large compared with the separation in the pairs, have the same activity as one pair alone. Unless the separation between pairs is a visible distance, there will be no macroscopic distinction from the case of one pair.

If the two families of loops are circles growing at the same rate the locus of intersections is a hyperbola in the general case, and in the symmetrical case a straight line bisecting the line of centres. Consideration of the locus of intersections, though trivial in the present case, is useful for the treatment of more complex cases later. The conclusion remains valid if the loops are not circles, but, on account of dependence of growth rate on crystallographic orientation, are deformed into polygons. The same point applies in cases treated later.

We chose to start with the case of two opposed pairs as the simplest, since it can be topologically analyzed in terms of the locus of intersections of growing circles. When we consider *two simple dislocations*, instead of pairs, we have to consider the locus of intersections of spirals. If they are *of opposite sign*, a locus of intersections still divides the area into two parts which may be said to be fed with steps from each centre respectively. Of the possible loci of intersections, depending on the relative phase of rotation of the two spirals, the most important one is that which is symmetrical—the bisector of the line of centres. For in this case there is a possibility for an influence to be transmitted along each step from the point where turns of the two spirals meet, in to the respective centres, and there modify the rate of rotation. If

they meet nearer to the centre of one than the other, there is a tendency for the rate of rotation of the former to be increased. So, in time, the two become synchronized in phase and the locus of intersections is the symmetrical one. As shown in appendix B, the increase in rate of advance of the steps which is transmitted along the spirals from their meeting point to the neighbourhood of their dislocation centres produces a small increase in the rate of rotation of the spirals amounting probably at most to a few units per cent when the distance between dislocations is of the order of $3\rho_c$ and decreasing exponentially for larger distances. Then the activity of the pair is indistinguishable from the activity of one; at the same time there is no important topological difference from the case of growing circles.

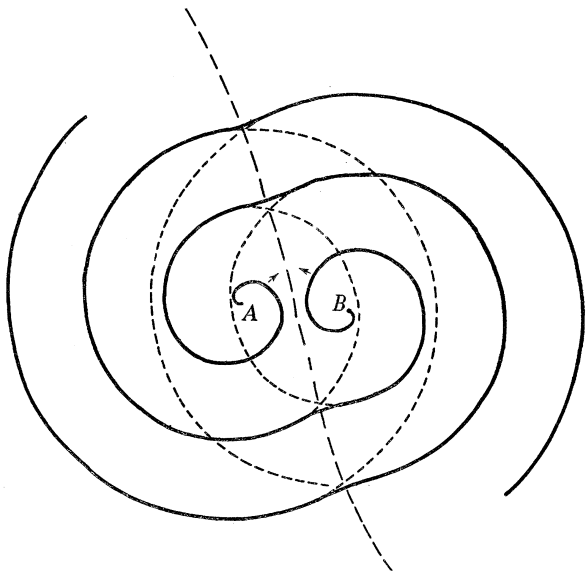

FIGURE 5. A pair of dislocations of like sign, separated by a distance $l = AB > 2\pi\rho_c$.

A pair of dislocations of like sign gives a more complex situation. If they are *far apart*, a locus of intersections still divides the area into two parts, which may be said to be fed with steps from each centre respectively. As before, there will be a tendency for the symmetrical case to establish itself. The locus of intersections is then no longer a straight line, but an S-shaped curve. If the spirals are represented by equation (37) and their centres are a distance l apart, the locus crosses the line of centres at an angle $\tan^{-1}(l/4\rho_c)$ and passes to infinity on asymptotes which make an angle $\cos^{-1}(2\pi\rho_c/l)$ with the line of centres (figure 5). The activity is still indistinguishable from that of one dislocation.

However, if the centres are *closer together* than half the radial separation between successive turns, i.e. than $2\pi\rho_c$, the spirals have no intersections except near the origin. The locus of intersections is now an S-shaped curve running from one centre to the other, and no longer divides the area into two (figure 6). In this case the turns of both spirals reach the whole of the area. In the limiting case in which the distance between dislocations l is much less than ρ_c we have effectively the complete Archimedean spiral $r = 2\rho_c\theta$, with the branches for both negative and positive r. Actually it still consists of a pair of spirals, which exchange centres on meeting, at every half-turn. If $l \ll \rho_c$ this shift of centres should scarcely affect the

rotation of the spirals, so that the activity of the pair should be *twice* the activity of a single dislocation. For small non-negligible values of l/ρ_c we may crudely estimate that the shift of centres imposes a delay corresponding to the time required for an unperturbed spiral to turn through an angle of the order of magnitude l/ρ_c, but we make no quantitative estimate

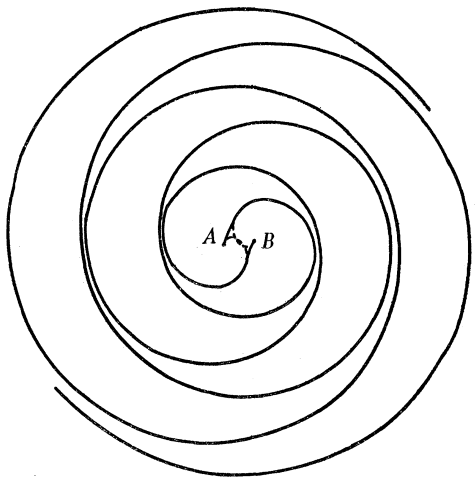

FIGURE 6. Pair of dislocations of like sign, at a distance $d < 2\pi\rho_c$.

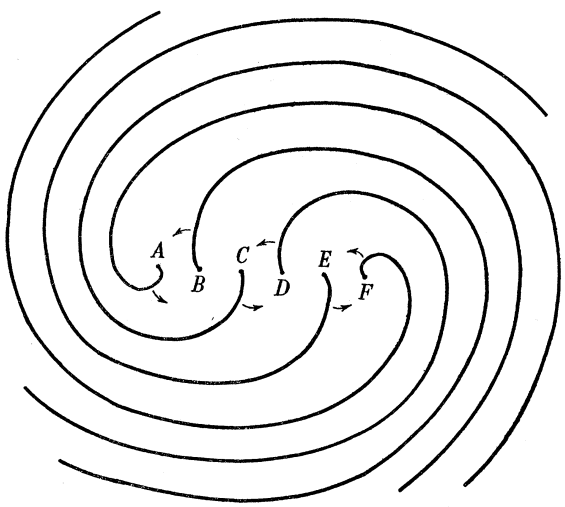

FIGURE 7. A group of dislocations of the same sign.

beyond saying that the activity of the pair now lies between 1 and 2 times the activity of a single dislocation.

A group of s dislocations of the same sign, each a distance smaller than $2\pi\rho_c$ from its next neighbour, will generate a spiral system of s branches. Supposing they are arranged in a line (the most likely arrangement, since groups of dislocations usually belong to 'mosaic', 'subgrain' or 'lineage' boundaries), and the length of the line is L, it is easy to see that each branch will take a time of the order of $2(L+2\pi\rho_c)/v_\infty$ to execute a circuit round the group so that the resultant activity of the group is $s/(1+L/2\pi\rho_c)$ times that of a single dislocation (figure 7).

If L is small compared with ρ_c, the activity of the group is s times that of a single dislocation; if L is large, and the average distance between dislocations is $\bar{l} = L/S$, the activity is $2\pi\rho_c/\bar{l}$ times that of a single dislocation.

In the more general case of a group of like dislocations not in a straight line, we may replace L in the above formula by $\frac{1}{2}P$, where P is the perimeter of the group. But in this case it may happen that the growth fronts have difficulty in penetrating into the group itself. The dislocation group will still promote growth outside it, but may develop a pit in the surface of the crystal.

In concluding this subsection we can say that the activity of a group of dislocations is in general greater than that of a dislocation alone by a factor ϵ, which in the case of a group of dislocations of the same sign can be as great as the number of dislocations contained in it.

In any case, the distance y_0 between steps produced by the group, far from it, will be given by their rate of advance v_∞, divided by the number of steps passing a given point per sec.: $\epsilon\omega/2\pi$. Therefore, using (38),

$$y_0 = 4\pi\rho_c/\epsilon. \tag{45}$$

We shall see in § 10 that in spite of the fact that the activity of a group can be several times greater than that of a single dislocation, the absolute value of the activity cannot surpass a certain maximum, the reason being that the rate of advance decreases when the distance between steps decreases.

9·2. *General case*

Suppose now we have *any distribution* whatever of dislocations in a crystal face, and a fixed degree of supersaturation σ, and consequently a fixed value of ρ_c (where σ and ρ_c may be slowly varying functions of position on the face). We now make a formal grouping of the dislocations. The first group consists of *inactive pairs*, all pairs of dislocations of opposite sign, closer together than $2\rho_c$. These have no activity by themselves, and their only effect, save in exceptional cases when they may possibly fence off a region of the crystal face, and inhibit growth there, is to impose a small delay on the passage of steps originating elsewhere, which to a first approximation may be disregarded. When a particular dislocation has two neighbours closer than $2\rho_c$, the pairing may be made arbitrarily, but in such a way that as many close pairs as possible are assigned to this class. We now take $2\pi\rho_c$ as the effective distance within which dislocations influence each other's activity, and by drawing imaginary lines connecting all dislocations closer together than this, divide all the remaining dislocations into groups, whose members influence each other's activity, but in which the groups are without influence upon each other. The number of these groups will increase with the supersaturation. Each group can be assigned a *strength* $s = 0, \pm 1, \pm 2, \ldots$, according to the excess of right-handed over left-handed screws in the group. A group of strength 0 has an activity ϵ times that of a single dislocation, where ϵ is now approximately 1 and generally slightly greater (the inactive groups of this strength have already been put into a separate class). If the supersaturation is increased, so that ρ_c decreases, ϵ tends rapidly to 1. When it reaches 1 the group can be subdivided into two, of strengths s_1, s_2, where $s_1 + s_2 = 0$. If the dislocations are in random arrangement, $|s_1|$ will seldom exceed 1 or 2, but it must be borne in mind that dislocations are likely to be in regular arrangements, as in mosaic or subgrain boundaries, in which case this conclusion does not necessarily follow.

Reduction of ρ_c will also transform some of the inactive pairs into active groups of strength 0.

Groups of strength $s \neq 0$ may have an activity up to $\epsilon = |s|$ times that of a single dislocation.

With increase of supersaturation, diminishing ρ_c, the groups of strength s subdivide into groups of strength s_1, s_2, where $s_1 + s_2 = s$. Since s_1 and s_2 can be of opposite signs $|s_1|$ may be larger than s. But with increasing supersaturation the groups are ultimately all subdivided into single dislocations behaving independently.

At every stage prior to this, there is in general some group more active than the rest.

The resultant activity is always that of the most active independent group.

10. *Rate of growth from the vapour*

Let us first consider the simplest case of one screw dislocation in an otherwise perfect crystal surface. The rate of growth will then be given by (43), where v_∞ is the rate of advance of the steps, far from the centre of the spiral.

The value of v_∞ has been calculated in I, formula (24), that is to say,

$$v_\infty = 2\sigma x_s \nu \exp(-W/kT) \tanh(y_0/2x_s)\, \beta c_0(x_0, y_0), \tag{46}$$

where σ is the supersaturation, x_s the mean displacement of adsorbed molecules, ν a frequency factor, W the evaporation energy, y_0 the distance between successive turns of the spiral, β a factor taking account of the fact that perhaps the exchange of molecules between the step and the adsorbed layer is not rapid enough to maintain around them the equilibrium concentration of adsorbed molecules, and c_0 another factor, which is a function both of y_0 and of the distance x_0 between kinks in the steps, and given in general by formula (25), I. According to the estimates made in I for x_s and x_0 we expect the condition $x_s \gg x_0$ to be satisfied in most cases; then the factor c_0 is of the order of 1, and the rate of advance of the steps is independent of their orientation. In this case, using (46) and (44) for the distance y_0 between successive turns of the spiral, (43) becomes

$$R = \beta\Omega n_0 \nu \exp(-W/kT)\, (\sigma^2/\sigma_1) \tanh(\sigma_1/\sigma), \tag{47}$$

where

$$\sigma_1 = (2\pi\rho_c/x_s)\, \sigma = 2\pi\gamma a/kTx_s \tag{48}$$

(cf. I, equation (30)). *For low supersaturations* ($\sigma \ll \sigma_1$) we obtain the *parabolic law*

$$R = \beta\Omega n_0 \nu \exp(-W/kT)\, \sigma^2/\sigma_1. \tag{49}$$

For *high supersaturations* ($\sigma \gg \sigma_1$) (47) becomes the *linear law*

$$R_1 = \beta\Omega n_0 \sigma \nu \exp(-W/kT), \tag{50}$$

which corresponds to the case when x_s is larger than the distance between successive turns of the spiral. We see that there is a critical supersaturation σ_1, given by (48), below which the rate of growth is essentially parabolic, and above which it is essentially linear. For the typical values $\gamma/kT \sim 4$, $x_s \sim 4 \times 10^2 a$ we obtain $\sigma_1 \sim 10^{-1}$. In figure 8 we plot the factor

$$R/R_1 = (\sigma/\sigma_1) \tanh(\sigma_1/\sigma)$$

as a function of σ/σ_1 (continuous curve).

In the case (an unusual one, we believe) when the condition $x_s \gg x_0$ is not satisfied, expression (47) has to be multiplied by the factor $c_0(\sigma/\sigma_1, b)$ given by (cf. I, formula 25)

$$c_0(\sigma/\sigma_1, b) = \{1+2b(A+B\sigma/\sigma_1)\tanh(\sigma_1/\sigma)\}^{-1},$$

where $$b = x_0/2\pi x_s, \quad A = \ln[4bx_s/a(1+(1+b^2)^{\frac{1}{2}})], \quad B = \tan^{-1} b.$$

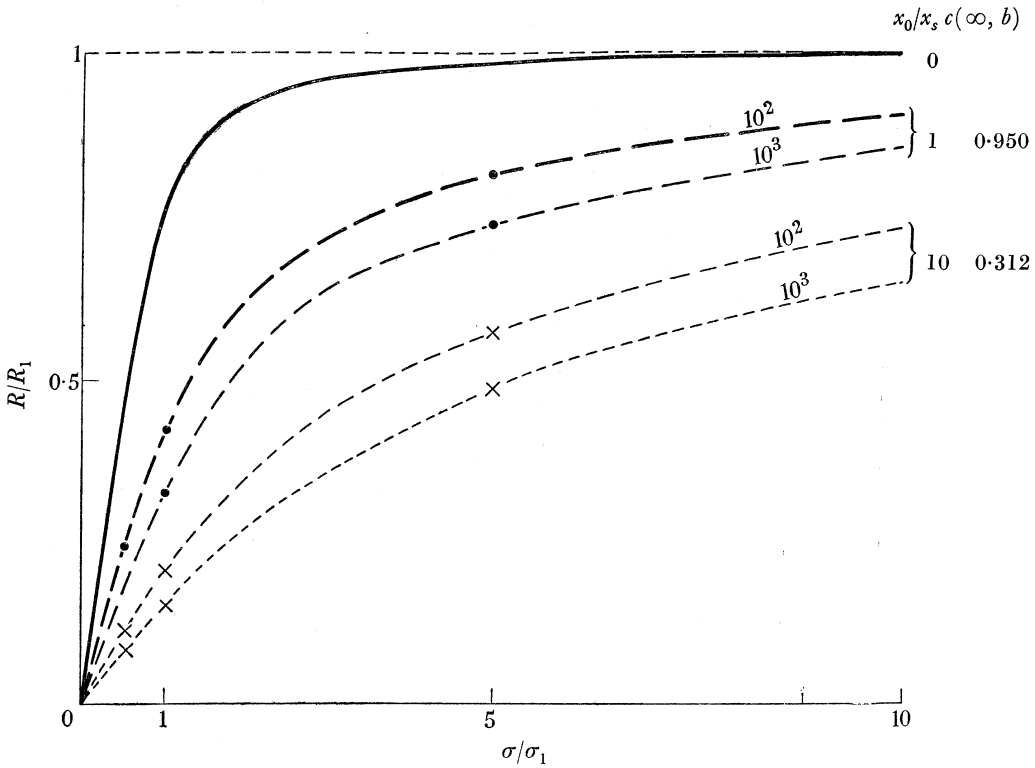

FIGURE 8. Correcting factor R/R_1 to the linear rate of growth as a function of σ/σ_1. The numbers on the curves indicate the values of x_s/a.

For low supersaturations ($\sigma \ll \sigma_1$) the parabolic law (49) will be multiplied by the factor

$$c_0(0, b) = (1+2bA)^{-1};$$

for high supersaturations ($\sigma \gg \sigma_1$), the linear law (50) will be multiplied by

$$c_0(\infty, b) = (1+2Bb)^{-1},$$

which can be included in the unknown constant β. The factor $c_0(0, b)$ is always smaller than $c_0(\infty, b)$. The correcting factor $\{(\sigma/\sigma_1)\tanh(\sigma_1/\sigma)\}c_0(\sigma/\sigma_1, b)/c_0(\infty, b)$ is also represented in figure 8; for a given value of b, A is also a slowly varying function of x_s/a. We see that the influence of the factor c_0 is important for $x_0/x_s \geqslant 1$, which we do not think will usually occur. As x_0/x_s increases, the linear law is reached for higher values of σ/σ_1.

Similar considerations apply to the rate of growth produced by a group of dislocations. If the group is a balanced one (equal number of right- and left-handed dislocations, strength $s = 0$) then there must be another critical supersaturation σ_2 below which no growth occurs

at all. σ_2 will be defined by the condition $2\rho_c = l$, where l is the maximum distance between pairs of dislocations actually coupled by a step; therefore

$$\sigma_2 = 2\gamma a/kTl. \tag{51}$$

For an unbalanced group (strength $s \neq 0$), or a balanced group above σ_2, the rate of growth will be given by

$$R = \Omega n_0 \epsilon(\sigma)\, v_\infty / 4\pi\rho_c, \tag{52}$$

where the factor $\epsilon(\sigma)$ is of the order of magnitude 1 for a balanced group, but can be larger for an unbalanced group; in both cases $\epsilon(\sigma)$ tends ultimately to 1 when σ increases. Using (46) (assuming $c_0 = 1$) and (12) for the distance y_0 between steps, (52) becomes

$$R = \beta\Omega n_0 \nu \exp(-W/kT)\, \epsilon(\sigma)\, (\sigma^2/\sigma_1) \tanh[\sigma_1/\epsilon(\sigma)\, \sigma]. \tag{53}$$

We see from this expression that, however large $\epsilon(\sigma)$ is, R cannot surpass the linear law (50). On the other hand, R cannot be smaller than (47) for an unbalanced group, but it could become zero for a balanced group below the critical supersaturation σ_2.

In the general case of an arbitrary distribution of dislocations in the crystal face we expect to have values for the rate of growth between that for a single dislocation (47) and the linear law (50), according to the distribution occurring in the particular crystal considered. A critical supersaturation σ_2 of the type (51) could occur in some random distributions of dislocations or a grouping of dislocations in balanced groups only; nevertheless, there is evidence showing that the dislocations are distributed in a very irregular way, and groups of dislocations of the same sign occur in mosaic or subgrain boundaries, in which case we do not expect critical supersaturations of the type (51) to occur.

11. *Comparison with experiment*

There are few quantitative measurements of the rate of growth of crystals from the vapour. The most interesting from our point of view are those of Volmer & Schultze (1931). These authors studied very carefully the growth from the vapour of naphthalene, white phosphorus and iodine crystals just below 0° C, under different supersaturations σ (from 10^{-3} to 10^{-1}). For all three substances they found a rate of growth proportional to the supersaturation. This linear law was valid for $C_{10}H_8$ and P_4 down to the lowest supersaturation used ($\sim 10^{-3}$), but for iodine the rate of growth becomes smaller than that given by the linear law when $\sigma < 10^{-2}$.

Let us first compare their linear law with (50) calculated in the preceding section for high supersaturations. This formula is actually the same as that used by Hertz (1882) and other authors (Volmer 1939; Wyllie 1949) for the growth of liquids and crystals from the vapour; it can be written also in the equivalent form

$$R = \beta\Omega p_0 (2\pi mkT)^{-\frac{1}{2}} \sigma, \tag{54}$$

as follows from the equality

$$n_0 \nu \exp(-W/kT) = p_0 (2\pi mkT)^{-\frac{1}{2}} \tag{55}$$

representing the balance between the current of evaporation and that of condensation at equilibrium. β in (54) is usually called the *condensation coefficient*, p_0 is the saturation pressure and m the mass of a molecule.

In table 1 we compare the experimental linear laws obtained by Volmer & Schultze (1931) with (54). The first column gives the average experimental value for R/σ. The supersaturation σ was obtained by maintaining a reservoir at 0° C and cooling the crystal under examination to a temperature $-\Delta T$° C. Assuming that the vapour pressure between the two crystals is uniform, the supersaturation at the growing crystal is $\sigma = W\Delta T/kT^2$. The second column gives the theoretical values for $R/\beta\sigma$ from (54), taking for p_0 the values measured by Gillespie & Fraser (1936) for I_2, by Centnerszwer (1913) for P_4 and by Andrews (1927) for $C_{10}H_8$. The first row gives the Volmer-Schultze results for liquid Hg, for which careful measurement by Knudsen (1915) showed that $\beta = 1$. For all the three molecular crystals, $\beta < 1$.

TABLE 1. LINEAR RATES OF GROWTH R FROM THE VAPOUR AT 0° C, AS FUNCTIONS OF SUPERSATURATION

	R/σ (exp.) (cm./sec.)	$R/\beta\sigma$ (theor.) (cm./sec.)	β	W (eV)	ν (sec.$^{-1}$)
Hg (liquid)	$0{\cdot}66\times10^{-6}$	$0{\cdot}6\times10^{-6}$	1·1	0·66	10^{13}
I_2	$0{\cdot}9\times10^{-4}$	3×10^{-4}	0·3	0·70	5×10^{16}
P_4	$0{\cdot}9\times10^{-5}$	$0{\cdot}8\times10^{-4}$	0·1	0·63	10^{15}
$C_{10}H_8$	$0{\cdot}8\times10^{-4}$	$1{\cdot}5\times10^{-4}$	0·5	0·79	10^{18}

The last two columns in table 1 give the values of W and ν deduced from (22). For Hg the frequency factor is of the order of the frequency of atomic vibrations, as we should expect; in the other cases ν is larger, due to the difference in rotational entropy between the crystal and the vapour.

Coming back to the deviations from the linear law, we notice first that P_4 and $C_{10}H_8$ follow the linear law to the lowest supersaturations observed. That means that σ_1 is smaller than 10^{-3}, and therefore, from (48), that $x_s > 10^4 a$. This is not surprising; in fact, the estimate of x_s/a made in I, equation (6), is valid for spherical molecules, for which the energy of evaporation W_s' of an adsorbed molecule was assumed to be of the order of $\frac{1}{2}W$; in the case of a flat molecule like $C_{10}H_8$, we expect W_s' to be larger, and therefore x_s/a will also be larger.

Figure 9 gives the results (logarithmic scale for both axes) obtained by Volmer & Schultze on several I_2 crystals. The experimental rates of growth are not reproducible even for the same face of the same crystal; this is not unexpected on the basis of the present theory.

Assuming that the rate of advance of steps is independent of orientation ($x_s \gg x_0$), one can choose a value for $\sigma_1 \sim 0{\cdot}2$ such that most of the experimental results are contained between the rate of growth (47) of a single dislocation (continuous line in figure 9) and the linear law (50) (broken line in figure 9). Taking $\sigma_1 \sim 0{\cdot}2$ and $\gamma/kT \sim 4$, we deduce from (48), $x_s \sim 10^2 a$ for I_2 at 0° C, which is in reasonable agreement with what we should expect (cf. I, equation (6)).

Nevertheless, one notices that the experimental rates of growth for the lowest supersaturations are below the theoretical curve (47); in particular, the rate of growth at

$$\sigma = 3{\cdot}8\times10^{-3} (\Delta T = 0°{\cdot}037)$$

is $< 10^{-3}$ times the rate of growth given by the linear law. The reduction given by formula (47) is only a factor $\sigma/\sigma_1 \sim 5\times10^{-2}$ with respect to the linear law. This fact could be explained in a number of ways:

(i) It is an obvious corollary to our view of crystal growth that it is susceptible to poisoning by traces of impurity, particularly at low supersaturations at which the number of

dislocations producing growth is smallest. From this point of view new measurements of the rate of growth would be very welcome.

(ii) There may be a critical supersaturation of the type (51) of the order of $\sigma_2 \sim 10^{-2}$, and therefore the dislocations are about 10^{-3} cm. apart; nevertheless, we are loath to draw this conclusion from such slight evidence.

(iii) Of course, it would be possible to choose a larger value for σ_1, in order to explain the small rates of growth at the lowest supersaturations, but the corresponding value for $x_s \sim 6a$

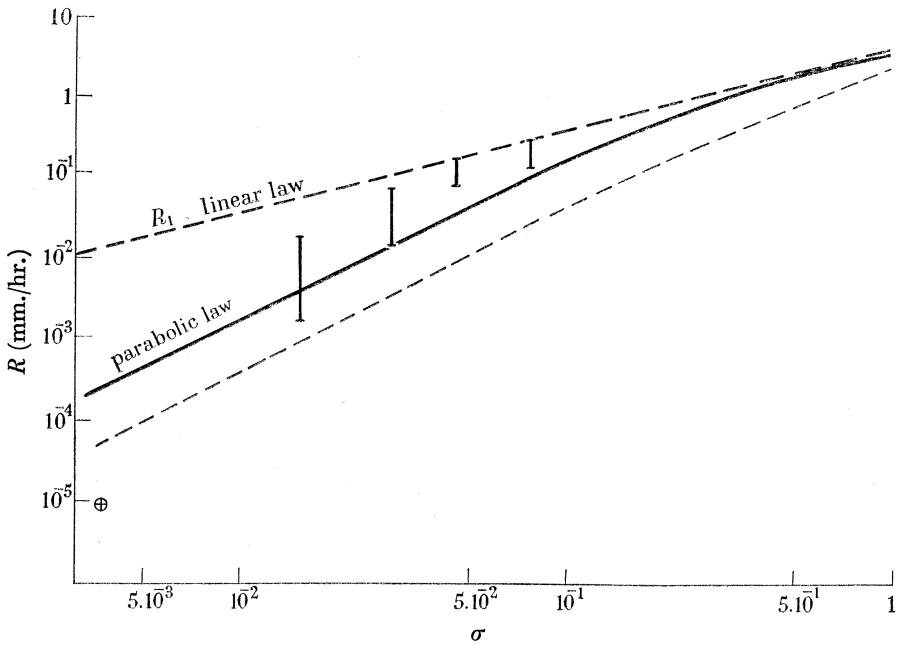

FIGURE 9. The rate of growth of I_2 crystals at 0° C as a function of σ (Volmer & Schultze 1931) in a logarithmic scale. The broken line is the Hertz law with a condensation coefficient $\beta = 0{\cdot}3$. The continuous curve is the rate of growth of a single dislocation (formula (47)) with $x_s = 10^2 a$. The dotted curve is that of a single dislocation assuming $x_0 = 10$, $x_s = 10^3 a$.

would be too small. Another alternative is to suppose that the condition $x_s \gg x_0$ is not satisfied for I_2. In order to decrease the number of degrees of freedom, let us assume that the condensation coefficient β is due only to the factor $c_0(\infty, b)$. That fixes $x_0/x_s \sim 10$. Assuming for $x_s \sim 10^2 a$, one obtains the dotted curve represented in figure 9. As we said before we do not think that a value $x_0/x_s \sim 10$ is actually possible. This point will be decided when the topography of a crystal grown from the vapour is observed. If, as we believe, $x_0 \ll x_s$ the steps must be circular, if $x_0 \gg x_s$ then they must follow the crystallographic orientation, as is observed in the case of growth from solution (Griffin 1950; Frank 1950).

We have been considering the rate of growth of macroscopic surfaces, for which the growth is due essentially to the molecules condensing from the vapour; in this case formula (54) represents the maximum rate of growth for a given surface. When the dimensions of the surface are small, diffusion of molecules from neighbouring surfaces can give an important contribution to its growth, and the rate of growth may be substantially greater than (54).

For instance, Volmer & Estermann (1921) studied the growth of small crystals of Hg at $-63°$ C. The crystals had a plate shape, the thickness h was not observable but was estimated to be of the order of $10^2 a$. The rate of growth of the edges was estimated to be 10^3 times that given by (54). The ratio between the contribution to the growth from diffusion on the flat surface and directly from the vapour should be $2x_s/h$. Therefore we deduce $x_s \sim 10^5 a$ for Hg at $T = 210°$ K, which agrees with the value that we should expect.

12. *Growth from solution*

We consider now, very briefly, the application of the preceding ideas to growth from solution. Although it is clear that from a qualitative point of view there is no essential difference between growth from the vapour and from solution, a quantitative theory of the rate of growth from solution is much more difficult.

First of all, we expect the rate of advance of a step in the crystal surface to be a definite function of the distance x_0 between kinks in the step, because although x_0 is always small, the diffusion of solute molecules towards the kinks, either through the solution, on the surface or in the edge of the step, is now much slower than on the free surface of a crystal. It is difficult to decide the relative importance of these three currents. For instance, the ratio between the current through the solution and on the surface will be represented by the factor $DN_0 a/D_s n_{s0}$, where D and D_s are the diffusion coefficients and N_0 and n_{s0} the saturation concentrations in the solution and on the surface respectively; it is likely that $D > D_s$ but also $N_0 a < n_{s0}$, therefore the factor above may be greater or smaller than 1. Nevertheless, for the time being and in order to simplify the problem, we shall suppose that the contributions from the diffusion on the surface and in the edge can be neglected. Even under these conditions we find another difficulty in the fact that neglect of the motion of the sinks is no longer generally justifiable.

Let us suppose we have a set of parallel steps, at distance y_0 from each other, in one of the close-packed crystallographic directions (for which x_0, the distance between successive kinks, is a maximum). As an approximation the diffusion through the solution can be broken up as follows: At distances $r < x_0$ from each kink we have a hemispherical diffusion field around each kink (provided $D/v_{\text{kink}} \gg x_0$, otherwise the movement of the kink cannot be neglected) with the diffusion potential $(1 - a/r)\,\sigma(x_0)$, where $\sigma(x_0)$ is the supersaturation at a distance x_0; at distances r between x_0 and y_0 from each step we have a semi-cylindrical diffusion field around each step (provided $D/v_{\text{step}} \gg y_0$) with the diffusion potential

$$[\ln (y_0/x_0)]^{-1} [\sigma(x_0) \ln (y_0/r) + \sigma(y_0) \ln (r/x_0)],$$

where $\sigma(y_0)$ is the supersaturation at a distance y_0; and finally, at distances z from the crystal surface between y_0 and δ, the thickness of the unstirred layer at the surface of the crystal, we have a plane diffusion field with the diffusion potential $[(z - y_0)\,\sigma + (\delta - z)\,\sigma(y_0)]\,(\delta - y_0)^{-1}$, where σ is the supersaturation in the stirred solution. The latter diffusion potential applies in any case, but it would be improper to equate the flux calculated from its gradient to the rate of growth R of the crystal unless $D/R \gg \delta$. Usually D/v_{kink}, D/v_{step} and D/R are not very large unless both the concentration and the supersaturation in the solutions are small. We assume in the following considerations that this is the case.

Under these conditions and in terms of the supersaturation $\sigma(x_0)$ the rate of advance of every step is clearly

$$v_\infty = DN_0\Omega 2\pi\sigma(x_0)/x_0. \tag{56}$$

As v_∞ is proportional to the number of kinks per cm., $1/x_0$, the velocity of the step will increase appreciably as the inclination with respect to the close-packed slowest direction increases.

Equating the sum of the hemispherical fluxes going to all the kinks in the step to the semi-cylindrical flux, and equating also the sum of the semi-cylindrical fluxes going to all the steps in the surface to the plane flux, we eliminate $\sigma(y_0)$ and find

$$\sigma(x_0)/\sigma = [1+2\pi a(\delta-y_0)/x_0y_0+(2a/x_0)\ln(y_0/x_0)]^{-1}, \tag{57}$$

which, introduced in (56), gives v_∞ as a function of x_0 and y_0. v_∞ will clearly increase when y_0 increases.

Applying now formulae (43) and (44) for the rate of growth R and the distance between steps y_0 of the growing pyramid, which will be approximately valid in our problem also, we obtain

$$R = DN_0\Omega a\sigma(x_0)/2x_0\rho_c, \tag{58}$$

where $2\rho_c = 2\gamma a/kT\sigma(x_0)$ is the dimension of the critical nucleus and $\sigma(x_0)$ is given by (57). For low supersaturations the third term in the bracket in (57) is the important one; then the rate of growth becomes parabolic. On the contrary, at high supersaturations, the second term in (57) is the important one, and the rate of growth becomes linear:

$$R_1 = DN_0\Omega\sigma/\delta. \tag{59}$$

The change-over from parabolic to linear occurs at a supersaturation σ_1, roughly given by

$$\sigma_1 \sim \gamma x_0/kT\delta. \tag{60}$$

For reasonable values of γ and δ, $\sigma_1 \sim 10^{-3}$. Above σ_1 one should observe only the linear law (59); below σ_1, all the rates of growth between (58) and (59) could be expected. As far as we know there is no experimental evidence for such a critical supersaturation.

On the other hand, we observe frequently (Bunn 1949; Humphreys-Owen 1949) that the rate of growth is substantially smaller than the linear law (59) would suggest; sometimes a crystal surface does not grow at all in spite of the fact that it is in contact with supersaturations as large as $\sigma \sim 0{\cdot}1$. This could possibly be interpreted as being due to the absence of dislocations in the surface or to the presence of so many that the mean distance between them is smaller than $2\rho_c$. In this last case, the number of dislocations per sq.cm. would have to be of the order of $10^{12}\,\mathrm{cm.}^{-2}$, which is high. Moreover, in this case, the dislocations would have to be distributed in a peculiar way, with least density at the centre of each face; for otherwise the growth, when it did occur, would be most rapid at the corners, i.e. dendritic. We are more inclined to think that the number of dislocations involved is quite small, and that they are situated near the middle of the face. The changes in growth rate could be due to rearrangements of the dislocations or to the effect of impurities adsorbed on the steps. The required amount of such impurity is very small indeed. For example, if the number of dislocations per sq.cm. is as high as 10^8, the number of atomic sites on the step-lines connecting them need not exceed 10^{-4} of all sites in the area.

EQUILIBRIUM STRUCTURE OF CRYSTAL SURFACES

PART III. STEPS AND TWO-DIMENSIONAL NUCLEI

13. *Introduction*

We begin with an outline of the theory to be developed in later sections. Some of the statements made in this outline receive their fuller justification later.

It is clear that a crystal will grow only if there are *steps* of monomolecular height in its surface, and growth will take place by the advance of these steps forming new molecular layers. The rate of advance of the steps will depend on their structure when in equilibrium with the vapour; hence the necessity for studying this structure as a preliminary to the study of crystal growth.

Frenkel (1945) has recently shown that such steps, when in equilibrium at temperatures above 0° K, will contain a number of *kinks* (cf. figure 11), i.e. molecular positions from which the energy necessary to take a molecule from the crystal to the vapour is equal to the evaporation energy W. This is true for intermolecular forces of a very general character, as has been shown by Kossel (1927) and Stranski (1928). According to Frenkel, the proportion of molecular positions in the step occupied by kinks is given by a formula of the type

$$e^{-w/kT}, \tag{61}$$

where w is the energy necessary for the formation of a kink in the step. Our first purpose in this part is to study in detail the structure of steps of any crystallographic direction and to estimate the value of w. The concentration of kinks turns out to be in general considerably larger than the concentration of adsorbed molecules in the edge of the step. We consider as a working model a Kossel crystal, a simple cubic structure with first and second nearest neighbour interactions. When the crystal is in real equilibrium with its vapour, a step in equilibrium must be in the mean straight but can have any crystallographic direction.

On the other hand, if the vapour is supersaturated, it is known that there is a two-dimensional nucleus (critical nucleus) which is in unstable equilibrium with the vapour. Our second purpose in this part is to calculate the shape, the dimensions and the total edge free energy of the critical nucleus in equilibrium with a given supersaturation at a given temperature, for the particular case of a (0, 0, 1) surface of a Kossel crystal.

If one assumes that the crystal is perfect, its growth in a supersaturated environment requires the formation of nuclei of critical size, because it is only when they reach this size that they are able to grow freely forming a new molecular layer. It can be proved, on thermodynamical grounds, that the number of critical nuclei created per second must be proportional to $\exp(-A_0/kT)$, where A_0 is half the total edge free energy of a critical nucleus, which will also be called *activation energy for nucleation* (Volmer 1939; Becker & Döring 1935). In the calculation of A_0, the previous authors neglected the configurational entropy, which amounts to supposing that the shape of the critical nucleus is the same as it would be at $T = 0°$ K. Under this assumption, and for the simple case of a (0, 0, 1) surface in a Kossel crystal, the size of the critical (square) nucleus and the activation energy A_0 for nucleation are given by

$$kT \ln \alpha = \phi/l, \quad A_0 = \phi^2/kT \ln \alpha, \tag{62}$$

where α is the saturation ratio, defined as the ratio between the actual concentration in the vapour to the equilibrium value, ϕ the energy of interaction between nearest neighbours and

l^2 the number of molecules in the critical (square) nucleus. Taking account of the entropy factors, we show that the critical nucleus has essentially the same dimensions given in (62) but has rounded corners, which decreases A_0 only by a factor of the order of 0·8 in a typical case. We deduce therefore that the activation energy for nucleation is enormous for the values of α for which growth is observed ($\alpha \sim 1{\cdot}01$; $A_0/kT \sim 3{\cdot}6 \times 10^3$, for the typical value $\phi/kT \sim 6$), and consequently the observed growth at low supersaturations cannot be explained on the basis of a perfect crystal theory.

We believe that the observed rates of growth of crystals can only be explained by recognizing, as has been suggested by Frank (Burton *et al.* 1949; Frank 1949), that those crystals which grow are *not* perfect, and that their lattice imperfections (dislocations) provide steps on the crystal surface making the two-dimensional nucleation unnecessary. If the distance between a pair of dislocations producing a step in the surface is such that a critical nucleus can pass between them the step will grow freely. If that is not the case the step will require a certain activation energy for growth. Using our preceding results we calculate this activation energy, and we show that it is small only when the distance between dislocations is practically equal to the size of the critical nucleus.

In part IV we shall consider the problem of the equilibrium structure of a crystal surface not containing steps, in order to study whether thermal fluctuations are able to produce steps in the surface, in the same way that they produce kinks in a step. The answer will be *no*, provided the temperature is below a certain critical temperature, which for the more close-packed surfaces is of the order of or higher than the melting-point. The problem of the structure of a crystal surface is actually an example of a co-operative phenomenon.

14. *Equilibrium structure of a step*

By a step on a crystal surface we mean a connected line such that there is a difference of level equal to an intermolecular spacing between the two sides of the line.

If the crystal lattice contains no dislocations, then there can only be two varieties of step in the surface; either the step begins and ends on the boundary of the surface or it forms a closed loop on the surface itself (thus bounding a monomolecular elevation or depression on the surface). However, if dislocations are present, it is possible that a step can start on a surface and terminate on a boundary, or it can have both ends in the surface. If a step has an end in the surface, this end must be a place where a dislocation meets the surface with a screw component normal to the surface.

For the sake of simplicity we shall consider a crystal in contact with its vapour, but many of our conclusions will apply for other primary phases; also we shall assume the crystal to be very large compared with the range of molecular forces involved, that is, we shall speak of infinite crystals. We only consider, for simplicity, a (0, 0, 1) face of a simple cubic crystal with forces between molecules of the nearest neighbour or possibly the nearest and next nearest neighbour type. Finally, we neglect altogether the differences in frequency of vibration and rotational free energy of the molecules in different positions in the crystal surface.

If a crystal is then in stable equilibrium with its vapour (the vapour being neither supersaturated nor under-saturated), then it is fairly clear even at this stage (and we prove this later) that a step in equilibrium in the crystal surface will have a constant mean direction

(this direction not necessarily being along a crystallographic axis), and hence under these conditions no finite closed step can be in equilibrium. The latter will only be in equilibrium when the vapour is supersaturated or under-saturated. In this case the equilibrium is unstable. To avoid unnecessary circumlocutions we introduce here the saturation ratio α, defined as the actual vapour concentration divided by the vapour concentration under conditions of stable equilibrium with an infinite crystal surface. Summarizing, then, we expect to find steps of constant mean direction (straight steps) if $\alpha = 1$ and curved steps if $\alpha \neq 1$, the two possibilities being mutually exclusive.

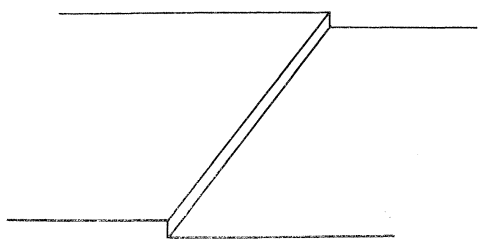

FIGURE 10. Step at $T = 0°$ K.

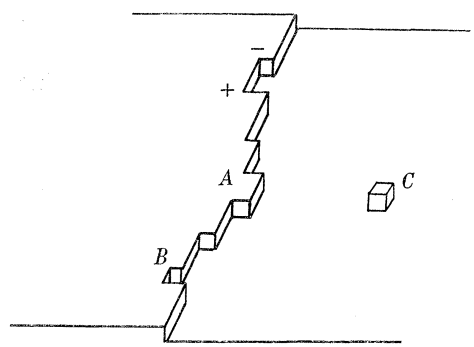

FIGURE 11. Step at $T > 0°$ K.

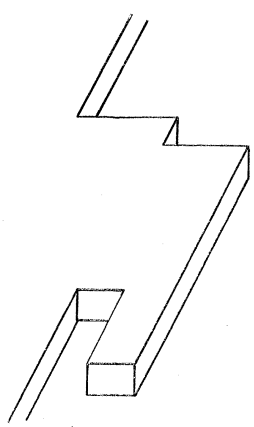

FIGURE 12. Overhangs in a step.

Potential energy considerations show that at 0° K a step will tend to be as straight as possible. This is shown explicitly in § 14·1 (figure 10). As the temperature is raised, a number of kinks appear (+, −), separated by certain distances (figure 11); a certain number of adsorbed molecules (A), and a certain number of vacant step sites (B) also appear. A certain number of adsorbed molecules (C) also appear on the crystal surface proper. We shall see that the concentration of adsorbed molecules and vacant sites in the step is small compared with that of kinks. We require only the knowledge of the concentration of kinks to form a picture of the structure of the step. The representation of the step by kinks, even when we admit kinks of any height, is not capable as it stands of including such a feature as that depicted in

figure 12, which we call an 'overhang'; to this extent our treatment will be slightly inaccurate. However, when the concentration of kinks is small, the concentration of overhangs will be negligible.

In what follows, our unit of length will always be the intermolecular spacing. We distinguish two types of kinks, which we call positive and negative, corresponding to a 'jump' and a 'drop' respectively at the point in question (figure 11). We use the symbol $n_{+r}(x)$ to denote the probability that there is a jump of amount r at a point whose co-ordinate is x. Similarly for $n_{-r}(x)$. We denote by $q(x)$ the probability that there is no jump of any kind at the point x. In the present case there are no geometrical constraints, i.e. at each point in a step, any of the various possibilities can occur independently of what there is at any of the other points. Hence the probability of the occurrence of a given configuration is equal to the product of the probabilities of occurrence of the individual situations which make up the configuration, and we may write as a normalization condition

$$q(x)+\sum_{r=1}^{\infty}\{n_{+r}(x)+n_{-r}(x)\}=1. \tag{63}$$

We define the local mean direction of a step at a point x by the equation

$$h(x)=\tan\theta=\sum_{r=1}^{\infty}r\{n_{+r}(x)-n_{-r}(x)\}\quad(0\leqslant h\leqslant 1), \tag{64}$$

where θ is the smallest angle between the step and the [0, 1] direction. Our problem is now to evaluate the equilibrium values of $q(x)$, $n_{+r}(x)$ and $n_{-r}(x)$ as a function of the temperature T, and also of the first and second nearest neighbour interaction energies ϕ_1 and ϕ_2.

It is possible to prove in a number of ways (see appendix C) that the probabilities n and q must satisfy the thermodynamical relations

$$g_{\pm r}(x)=\{g_{\pm}(x)\}^r\eta_2^{2(r-1)}, \tag{65}$$

$$g_{+}(x)\,g_{-}(x)=\eta_1^2, \tag{66}$$

$$g_{\pm}(x)=g_{\pm}(0)\,\alpha^{\mp x}, \tag{67}$$

where the g represent the relative probabilities

$$g_{\pm r}(x)=n_{\pm r}(x)/q(x); \tag{68}$$

we write $g_{\pm}$ for $g_{\pm 1}$, and we use the notation

$$\eta_{1,2}=\exp(-\phi_{1,2}/2kT). \tag{69}$$

We see, from equation (67), that if $\alpha=1$, and therefore the crystal is in thermodynamical equilibrium with its vapour, all the probabilities are independent of x, and therefore, from (64), the step will have a constant mean direction h. On the contrary, if $\alpha\neq 1$, the step will be curved; its local mean direction is then a function $h(x)$ of position in the step.

14·1. *Equilibrium structure of a straight step.* Let us now consider in more detail the structure of a straight step. Since there is now no dependence on x, we shall omit the variable from our notation. From (63), (65) and (66), using the notation (68), we obtain by summing a geometric series

$$g_{+}+g_{-}=\frac{1+\eta_1^2\eta_2^4-q[1-\eta_1^2\eta_2^2(2-\eta_2^2)]}{q+(1-q)\,\eta_2^2}. \tag{70}$$

In the same way, for a given mean direction h of the step, using (64), (65) and (66), we obtain

$$g_+ - g_- = hq(1-\eta_1^2\eta_2^4)/[q+(1-q)\,\eta_2^2]^2, \tag{71}$$

where we have also used (70) to eliminate $g_+ + g_-$.

From equations (66), (70) and (71) we can express q, n_+ and n_- as functions of η_1, η_2 and h. Equations (65) then enable us to find n_{+r} and n_{-r} as functions of the same quantities, thus completing the solution of our problem. The general expressions are complicated and cumbersome, so we do not give them; instead, we consider some particular cases.

At $T = 0$, we get

$$q = 1-h, \quad n_+ = h, \quad n_- = 0, \quad n_{\pm r} = 0 \quad (r \neq 1),$$

i.e. the step is as straight as it can be.

Before considering higher temperatures, let us see what typical values should be assigned to ϕ_1 and ϕ_2. In our model, the evaporation energy per molecule is $W = 3\phi_1 + 6\phi_2$; assuming $W \sim 0{\cdot}7\,\text{eV}$ (iodine for instance) and $\phi_2/\phi_1 \sim 0{\cdot}2$, we have $\phi_1 \sim 0{\cdot}15\,\text{eV}$ and $\phi_2 \sim 0{\cdot}03\,\text{eV}$. Thus at temperatures of the order of 300° K, we have $\eta_1 \sim 0{\cdot}05$ and $\eta_2 \sim 0{\cdot}6$. Accordingly, at these temperatures, it is reasonable to assume $\eta_2 \sim 1$, which amounts to neglecting the effect of second nearest neighbours. Under these conditions the solution to our problem becomes

$$\left.\begin{aligned} q &= [1+\eta_1^2 - \{(1+\eta_1^2)^2 - (1-\eta_1^2)^2\,(1-h^2)\}^{\frac{1}{2}}]/(1-\eta_1^2)\,(1-h^2), \\ 2g_+ &= 1+\eta_1^2 - q(1-\eta_1^2)\,(1-h), \\ 2g_- &= 1+\eta_1^2 - q(1-\eta_1^2)\,(1+h). \end{aligned}\right\} \tag{72}$$

For $h = 0$, that is to say for the (0, 1) step, equations (66), (70) and (71) give

$$q = (1-\eta_1^2\eta_2^2)/(1+2\eta_1-\eta_1\eta_2^2), \quad n_+ = n_- = q\eta_1. \tag{73}$$

At low temperatures we get

$$q = 1-2\eta_1, \quad n_+ + n_- = 2\eta_1 = 2\exp(-\phi_1/2kT). \tag{74}$$

The expression $n_+ + n_-$ now represents the proportion of step sites occupied by kinks from which the evaporation energy into the vapour is W. Thus, we obtain the same formula as Frenkel (1945) for the concentration of kinks, the energy of formation of those kinks being here $w = \frac{1}{2}\phi_1$. This value for w is, of course, equal to the increase in edge energy of the step by the formation of a kink. Since w is small, we shall have a considerable number of kinks; in fact, if $T \sim 300°\,\text{K}$, $\phi_1 \sim 0{\cdot}15\,\text{eV}$, we shall have one kink for every ten molecules in the step. The concentration of molecules diffusing in the edge of the step is much smaller than that of the kinks, being in fact proportional to η_1^2 which gives one diffusing molecule per 100 molecules in the step, if we use the above values for ϕ_1 and T.

As the inclination of the step increases ($h > 0$) with respect to the [0, 1] direction, the total number of kinks increases, because of the presence of kinks due to geometrical reasons; actually n_+ increases and n_- decreases in such a way that $n_+ + n_-$ increases. For h very small ($h < 2\eta_1$), and at low temperatures, one deduces

$$n_+ + n_- = 2\eta_1\left[1+\frac{h^2}{8\eta_1^2}\right]. \tag{75}$$

On the other hand, as we approach the [1, 1] direction ($h = 1$), the positions in the step from which the evaporation energy is W, are no longer the kinks of height 1 (probability n_+), because of the influence of the second nearest neighbour bonds. Consequently the number of kinks with evaporation energy W reaches a maximum somewhere near $h = 1$, and decreases again being a minimum for the direction [1, 1]. Actually, for the (1, 1) step at low temperatures at which η_1 and η_2 are small, we obtain

$$q = n_{+2} = \eta_2 = \exp(-\phi_2/2kT), \quad n_+ = 1-2\eta_2, \ldots. \tag{76}$$

Now the proportion of step sites from which the evaporation energy is W is represented by $q+n_{+2}$. We obtain again a formula of Frenkel type with an energy of formation $w = \frac{1}{2}\phi_2$ which is extremely small, much smaller than in the case of the (0, 1) step. At higher temperatures, for which $\eta_2 \sim 1$, we obtain

$$q = \frac{1}{2}\frac{1-\eta_1^2}{1+\eta_1^2}, \quad n_+ = \tfrac{1}{4}(1-\eta_1^2), \quad n_- = \frac{1-\eta_1^2}{(1+\eta_1^2)^2}\eta_1^2, \ldots. \tag{77}$$

It can now be seen why we have gone to the trouble of considering second nearest neighbours; we have done so in order to obtain the correct behaviour at low temperatures for the directions near (1, 1). In fact for low temperatures (77) becomes

$$q = \tfrac{1}{2}, \quad n_+ = \tfrac{1}{4}, \quad n_{-r} = 0, \quad n_{+r} = (\tfrac{1}{2})^{r+1},$$

independent of temperature.

14·2. *Free energy of steps*

It is of interest to evaluate the configurational free energy of a straight step. Using standard methods ($S = k \ln W$, $F = U - TS$, etc., W = number of ways in which kinks can be arranged in a step) we obtain the following general expression for the edge free energy per molecule:

$$F = \tfrac{1}{2}(\phi_1+2\phi_2)+\tfrac{1}{2}h\phi_1+kT(\ln q+h\ln g_+), \tag{78}$$

where, of course, q and g_+ are functions of h. This expression is referred to the [0, 1] direction; in order to obtain the free energy per unit length of the step itself, we must divide the expression by $(1+h^2)^{\frac{1}{2}}$.

In the general case the extended form of (78) is exceedingly cumbersome, so we again consider some particular cases. For the (0, 1) step at low temperatures the formula (78) gives

$$F_{01} = \tfrac{1}{2}(\phi_1+2\phi_2)-2kT\eta_1; \tag{79}$$

under the same conditions the corresponding quantity for the (1, 1) step is

$$F_{11} = \phi_1+\phi_2-2kT\ln(1+\eta_2). \tag{80}$$

The contribution of the entropy of the kinks to the edge free energy is small for the (0, 1) step, but for the (1, 1) step it is not negligible. In fact, at temperatures for which $\eta_2 \sim 1$, formula (80) gives $2kT\ln 2 \sim 0{\cdot}07$, or a third of ϕ_1.

At reasonable temperatures the free energy is always smaller for the (0, 1) step than for any other, so we might conclude that steps other than the (0, 1) steps are not in real equilibrium, and that there must be a tendency for these steps to change into (0, 1) steps. If the

steps are infinite, this conclusion would be erroneous. Actually, every step is in equilibrium with the same vapour pressure. Moreover, although the (0, 1) step has the smallest free energy, there is no tendency for other steps to change their orientation, because even the smallest rotation of step requires the transport of an infinite amount of material.

Frenkel (1945) has treated the kinetical problem of the transformation of any step into a (0, 1) step, assuming that only the latter are present in equilibrium, on account of the higher energy of the former. He obtains in this way a time of relaxation independent of the length of the step. This result is clearly incorrect, because the processes allowing a finite step to change its orientation occur only at the corners; consequently the time required for this rotation increases with the length of the step.

15. *The two-dimensional nucleus: activation energy for nucleation*

We have seen in § 14 that if the saturation ratio α is unity then the equilibrium steps are in the mean straight. If $\alpha \neq 1$ we shall find that the equilibrium step forms a closed loop; if $\alpha > 1$ the step bounds a finite incomplete layer of molecules on the surface, in which case we speak of a two-dimensional nucleus, and if $\alpha < 1$ the step bounds a finite hole in an infinite incomplete layer.

The most obvious method for calculating the shape of an equilibrium nucleus would be to use the free-energy formulae and Wulff's theorem.* Although the use of Wulff's theorem is simple in principle, the details prove to be cumbersome. However, the results gleaned in § 14 enable us to find the shape directly.

We know that in general (see appendix C)

$$g_{\pm}(x) = g_{\pm}(0)\, \alpha^{\mp x}, \tag{67}$$

and to complete the explicit determination of g as a function of x it is necessary only to evaluate $g(0)$. So far we have not specified an origin for x; let us now choose it to be the point where the local mean direction of the step is (0, 1). Then, by symmetry,

$$g_{+}(x) = g_{-}(-x).$$

Hence, using (66), we obtain $\quad g_{+}(0) = g_{-}(0) = \eta_1,$

so that with (67) we get $\quad g_{\pm}(x) = \eta_1 \alpha^{\mp x}. \tag{81}$

Invoking once more the normalization condition (63) we obtain

$$q(x) = \frac{1 + (\eta_1 \eta_2^2)^2 - \eta_1 \eta_2^2 (\alpha^x + \alpha^{-x})}{1 - \eta_1^2 \eta_2^2 (2 - \eta_2^2) + \eta_1 (1 - \eta_2^2)\, (\alpha^x + \alpha^{-x})}, \tag{82}$$

using (65) and (81). It is now clear that our information on the structure of the step at every point x is complete.

15·1. *The shape of the equilibrium nucleus*

The local mean direction $h(x)$, and therefore the shape of a step in equilibrium with an external phase of saturation ratio α, is clearly obtained from (4), using (21) and (22). In Cartesian co-ordinates, the shape of the step is represented by the equation

$$y = \int_0^x h(x')\, dx',$$

* In appendix D we offer a new proof of a generalized Wulff's theorem, which will be used later in § 16.

where the origin is at a place where the local mean direction is (0, 1) (see figure 13). Integrating, we find

$$y \ln \alpha = \ln\{(1-\eta_1\eta_2^2\alpha^x)\,(1-\eta_1\eta_2^2\alpha^{-x})/(1-\eta_1\eta_2^2)^2\} - \tfrac{1}{2}\ln\,[H(x)\,H(-x)/\{H(0)\}^2], \quad (83)$$

where $H(x)$ is given by

$$H(x) = \{1-\eta_1^2\eta_2^2(2-\eta_2^2)\}\,\alpha^x + \eta_1(1-\eta_2^2)\,(\alpha^{2x}+1).$$

The second term in (23) can be shown to be always small and negative; when $\eta_2 = 1$ it is zero.

The value of y in (83) becomes infinite when $x = \pm\frac{1}{2}l'$, where l' is given by

$$kT \ln \alpha = (\phi_1 + 2\phi_2)/l' \quad (\alpha > 1). \quad (84)$$

Thus (83) represents a finger-shaped figure (figure 13). It is interesting to note that l' coincides with the dimensions of the equilibrium or critical nucleus when a square shape is assumed [§ 13, formula (62)] and $\phi_2 \ll \phi_1$.

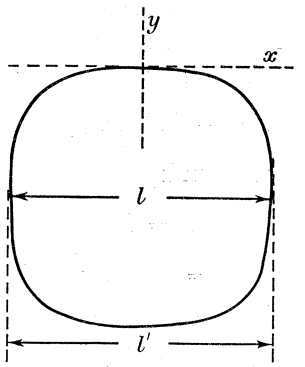

FIGURE 13. Step in equilibrium with supersaturated vapour ($\phi_1/kT \sim 6$).

If in (83) we replace α by its expression as a function of l' from (84), we see that y/l' is a function only of x/l'; hence the shape of the step is independent of α. The value of α fixes the size of the figure. The shape is, of course, dependent on the temperature; at low temperatures the 'corners' become sharper and the 'edges' straighter. At temperatures for which $\eta_2 \sim 1$ the expression for the shape can be written in the form

$$y/l' = (kT/\phi_1)\ln\{1-[\sinh(\phi_1 x/2kTl')/\sinh(\phi_1/4kT)]^2\}. \quad (85)$$

The figure we have obtained is not, of course, entirely correct, in the sense that we should have obtained a closed figure. The reason is the neglect of 'overhangs' (figure 12), which is not a good approximation when the inclination of the step is much greater than $\frac{1}{4}\pi$ with respect to the (0, 1) direction taken as x-axis. Nevertheless, knowledge of the step shape in a range $\frac{1}{4}\pi$ enables us to state the complete shape, because of the square symmetry of the (1, 0, 0) face of the simple cubic lattice. The diameter l of the nucleus obtained in this way (see figure 13) turns out to be given by

$$kT \ln \alpha = (\phi_1 + 2\phi_2 - 4kT\eta_1)/l, \quad (86)$$

to the first order in η_1. The expression in parentheses is seen to be $2F_{01}$ (equation 79), F_{01} being the edge free energy per unit length of the (0, 1) step. This is the result that we should

expect from a correct application of the Gibbs-Thomson formula (see appendix D), and it shows that the shape we have calculated is a good approximation. The difference between l given by (86) and l' given by (84) is practically negligible for ordinary temperatures.

The radius of curvature ρ of the nucleus at the corners when $\eta_2 \sim 1$, is easily shown to be given by

$$\rho/l = -\sqrt{(2)}\,(kT/\phi_1)\tanh^2(\phi_1/2kT). \tag{87}$$

The rounding of the corners at high temperatures is considerable. For the melting-point T_M, for which $kT_M/\phi_1 \sim 0{\cdot}6$, the nucleus would have practically a circular shape. According to (87), the nucleus would become square at $T = 0°$ K. If second nearest neighbours are considered the nucleus would become an octagon.

15·2. *Activation energy for two-dimensional nucleation*

It is easy to show how the activation energy for nucleation A_0 is related to the total edge free energy F_0 of the critical nucleus. Let n be the number of molecules contained in a nucleus, then n will be variable and will have the value n_0 for the critical nucleus itself. Let us suppose that the shape of the nucleus does not change appreciably for values of n around n_0. Then the increase in free energy by the formation of a nucleus containing n molecules will be

$$A = -nkT\ln\alpha + \beta n^{\frac{1}{2}},$$

where β is assumed to be a constant given by

$$F_0 = \beta n_0^{\frac{1}{2}}.$$

Now A has to be a maximum for $n = n_0$, because the critical nucleus is in unstable equilibrium with the vapour of saturation ratio α. This condition fixes the value of

$$n_0 = (\beta/2kT\ln\alpha)^2,$$

and the maximum of A is equal to

$$A_0 = n_0 kT\ln\alpha = \tfrac{1}{2}F_0. \tag{88}$$

The probability for the formation of a critical nucleus is then proportional to $\exp(-A_0/kT)$, and A_0 is called the *activation energy for two-dimensional nucleation.*

In the case of our (0, 0, 1) face in a simple cubic crystal we know that by an application of the Gibbs-Thomson formula (see appendix D) the dimension l of the two-dimensional critical nucleus is given by

$$kT\ln\alpha = 2F_{01}/l, \tag{86}$$

where F_{01} is the edge free energy per molecular position in the direction [0, 1]. The activation energy for two-dimensional nucleation can then be written in the form

$$A_0 = \frac{n_0}{l^2}\frac{(2F_{01})^2}{kT\ln\alpha}. \tag{89}$$

Assuming that the critical nucleus is a square of size l and putting $F_{01} \sim \frac{1}{2}\phi_1$, we deduce the Becker-Döring expression

$$A_0 = \phi_1^2/kT\ln\alpha. \tag{62}$$

Formula (89) differs from (62) essentially by the factor n_0/l^2, the ratio of the actual area of the nucleus to that of the square circumscribed on it. For the typical value $\phi_1/kT \sim 6$ we obtain graphically from figure 13 that $n_0/l^2 \sim 0{\cdot}86$. This shows that the actual activation for

two-dimensional nucleation is reduced with respect to (62) only by a small factor, which is not sufficient to account for the observed growth rate at low supersaturations.

16. *Steps produced by dislocations*

As a final application of the generalized Wulff theorem (see appendix D) we evaluate the activation energy for nucleation in the presence of screw dislocations.

A real crystal is supposed not to have a perfect lattice, but to contain a number of lattice imperfections in the form of dislocations, and Frank (1949) has shown that when dislocations having a screw component normal to the surface terminate in the crystal surface, they ensure the permanent existence of steps in the surface during growth. Every dislocation is

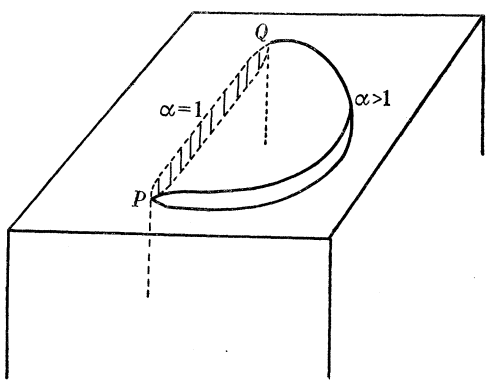

FIGURE 14. Step between two screw dislocations P and Q terminating in the surface.

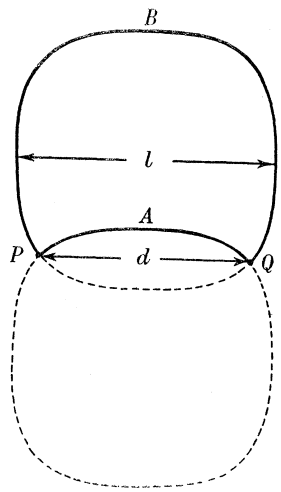

FIGURE 15. Equilibrium positions of a step between two dislocations P and Q: PAQ stable, PBQ unstable.

the origin of a step, which finishes usually in another dislocation of different sign. Therefore we must study the behaviour of a step between two screw dislocations of opposite sign. A picture of the surface in this case is shown in figure 14. We shall suppose for definiteness that the line joining the dislocations is in the [0, 1] direction, and we let the distance between the dislocations be d (figure 15). In real equilibrium ($\alpha = 1$) the step will remain straight between the two dislocations (figure 14), having the structure of a piece of step (0, 1). If $\alpha > 1$ the step will become curved (figure 14), and its shape, seen from above, under equilibrium conditions, is the same as part of the shape of a 'free' nucleus passing through the dislocations P, Q (figure 15). (Our calculations show in fact (appendix C) that the kink density at a point in a step depends only on conditions in the immediate neighbourhood of this point.) The diameter of this free nucleus will be l, given by (89) or approximately by (62). If $l > d$, there are two possible equilibrium positions: PAQ which is stable, and PBQ which is unstable. For growth we require the transition $PAQ \rightarrow PBQ$, and the activation energy A_d for this is half the edge free energy of the piece PBQ minus half the edge free energy of the piece PAQ. This quantity is easily evaluated graphically. To find the free energy of a piece of boundary we have merely to evaluate the area of the sector contained by

the piece and the lines joining its ends to the centre of the nucleus, as a function of d/l (see appendix D). This we have done for $\phi_1/kT \sim 6$, and figure 16 shows the ratio of A_d to the activation energy A_0 for ordinary nucleation. The curve has a vertical tangent at $l = d$, which means that we have to go to values of l very close to d in order to obtain a reasonably small value for the activation energy. Of course if $l < d$, the activation energy is zero. The dotted curve in figure 16 is obtained if we assume that the free equilibrium nucleus is a square.

Hence we conclude that given a certain saturation ratio α, and therefore a value l for the dimensions of the critical nucleus, all the steps connecting dislocations distant $d < l$ will not move at all, and those connecting dislocations distant $d > l$ will be able to move freely without requiring an activation energy.

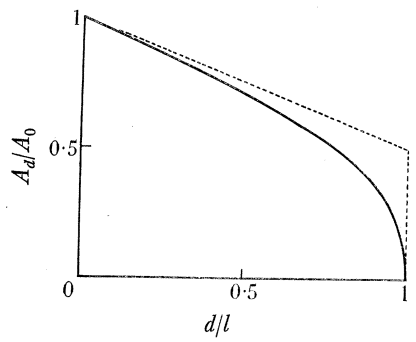

FIGURE 16. Activation energy A_d for the growth of a step between two dislocations a distance d apart.

PART IV. STRUCTURE OF A CRYSTAL SURFACE AS A CO-OPERATIVE PHENOMENON

17. *Introduction*

Following an idea put forward by Frenkel (1945), we discussed in part III the structure of the edge of an incomplete molecular layer on a crystal surface, which we call a 'step'. We found that such an edge contains in equilibrium at temperature T a large number of 'kinks'. The results of this part enable us to describe the structure at a temperature T of surfaces of high index, which contain steps even at the absolute zero of temperature. Frenkel appears also to have concluded that a surface of low index, and thus flat at the absolute zero, would acquire at a finite temperature a definite number of such steps. This we believe to be incorrect. We shall show in this part that the problem of the structure of a surface is different from that of a step, being actually a problem in co-operative phenomena. The result of our investigations is that a surface of low index will remain flat, and not acquire any steps, below a certain transition temperature; above this temperature the surface becomes essentially rough, a large number of steps appearing.

The problem of the structure of a step is actually one-dimensional; we were dealing with situations spread over a line. As we pointed out in § 14, we could assign independent probabilities for the existence of given features (kinks) at each point in the step, i.e. the range of possible states at each point is independent of the states at all the other points. In the two-dimensional problem which concerns us, this is no longer the case. This can be seen in the following way.

We are interested in the difference of levels between neighbouring molecules. If two neighbouring molecules differ in level by r molecular spacings, we speak of a *jump* of magnitude r. It is clear that the number of places where jumps can occur is greater than the number of molecules in the surface; hence the probability of having a jump between two given molecules cannot be independent of the jumps occurring in all the other positions. Figure 17 shows a $(0, 0, 1)$ surface of a simple cubic crystal. At $T>0$ the surface will contain a certain number of jumps or differences of levels. The levels of the molecules can of course be assigned independently; however, the jumps cannot. For suppose we trace out a closed path *ABCDEFA* in the surface, then the magnitude of the jump at any point on the path must be uniquely fixed by the magnitudes of the jumps at the remaining points on the path.

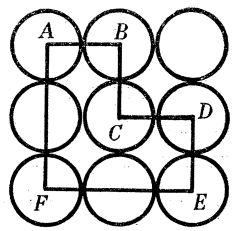

FIGURE 17

We shall consider the surface structure problem as solved when the surface potential energy at equilibrium is known as a function of temperature. For instance, if we consider a simple cubic model with nearest neighbour interactions ϕ, then a completely flat $(0, 0, 1)$ surface has a surface potential energy $\frac{1}{2}\phi$ per molecule. If, however, the surface contains a jump of magnitude r, then there will be an extra contribution to the surface potential energy of amount $\frac{1}{2}r\phi$. In general, we shall define the *surface roughness* s as $(U-U_0)/U_0$, where U_0 is the surface potential energy per molecule of the flat surface ($T=0$) and U that of the actual surface; s is equal to the average number of bonds per molecule parallel to the surface.

In the case of a $(0, 0, 1)$ surface in a simple cubic crystal, mentioned above, the problem of finding $U-U_0$, which we call the configurational potential energy, is seen to be equivalent to finding the same quantity for a square lattice of units each capable of taking a range μ of states, such that the energy of interaction between two neighbouring units is a certain function $u(\mu, \mu')$ of their states. In the simple case considered we have

$$u(\mu, \mu') = \tfrac{1}{2}\phi\,|\,\mu-\mu'\,| \quad (\mu, \mu' = 0, \pm 1, \pm 2, \ldots). \tag{90}$$

Our problem, then, is an example of the so-called standard problem of co-operative phenomena in crystal lattices; given a lattice composed of identical units, each capable of a number of states μ, such that the energy of interaction between neighbouring units i, j is a function of μ_i and μ_j, what is the partition function per unit of the lattice?

18. *Co-operative phenomena in crystal lattices*

It seems to be characteristic of co-operative problems that the thermodynamical functions are non-analytic functions of the temperature; they thus possess discontinuities or infinities

in themselves or in their derivatives. The temperature at which these singularities occur are called *transition temperatures*. But this result is by no means generally proved. It is conceivable that in certain cases there will be a critical region where some of the thermodynamical functions change very rapidly without having a singularity.

So far, only particular cases of the general co-operative problem in lattices have been completely solved: those in which μ is capable of two values only, and the lattice is two-dimensional. The partition function is completely known only in the case of a rectangular lattice with equal or different interactions in the two crystallographic directions (Onsager 1944; Onsager & Kaufmann 1946). In this case a single singularity is known to exist and its position is also known. Under the assumption that a single transition temperature exists for any symmetrical (equal interaction in all directions) two-dimensional lattice, its value is known (Wannier 1945), again with the limitation that μ is two-valued.

For our purpose, only the potential energy U is required. There are, in fact, several approximate methods for finding U, the best known of which is that due to Bethe (1935). These methods have been applied extensively (Wannier 1945) to the Ising model of a two-dimensional ferromagnet. However, the rigorous solution for a rectangular lattice, due to Onsager (1944, 1946), is qualitatively different from all the approximate solutions. In the approximate methods both the potential energy and the specific heat can be discontinuous functions of temperature; the correct treatment shows that both are continuous, but the specific heat has a logarithmic infinity at a temperature some 10 % below that at which Bethe's method predicted a discontinuity. The reasons for this discrepancy have been discussed by Wannier (1945). These results have thrown considerable doubt on the predictions of approximate methods, especially when they predict a latent heat, i.e. that the potential energy is also discontinuous. Broadly speaking, it is characteristic of these approximations that the calculated quantities are evaluated more accurately on the low-temperature side of the transition temperature than on the high side.

The exact Onsager solution was applied to the case of a two-dimensional ferromagnet; the same solution could be applied with little change to an adsorbed monolayer on a perfectly flat crystal surface. It seems not unreasonable to suppose that the behaviour of a monolayer will be similar to that of the crystal surface itself. Such an interpretation means that we suppose that the molecules in the crystal surface are capable of two levels only. This means that if we include adsorbed molecules or nuclei in the model, holes are excluded. The two-level model of a crystal surface is undoubtedly an over-simplification, but it has the advantage that we shall be able to use the results of Onsager's treatment for several types of symmetrical and unsymmetrical surface lattices (§ 19). The generalization of Onsager's method to more than two levels seems to be very difficult; hence, in order to study how the transition temperature changes with the number of levels, we generalize Bethe's method to a many level problem in § 20.

19. *Two-level model of a crystal surface*

In appendix E we shall give a short mathematical account of the interpretation of Onsager's solution from the point of view of our problem. In this section we shall state the results and discuss their physical consequences.

In the case of a two-dimensional lattice with z nearest neighbours and equal interaction energy ϕ in all directions (symmetrical case), Wannier (1945) has shown that, assuming there is a transition temperature T_c, it will be given by the general formula

$$\mathrm{gd}\, H_c = \pi/z, \quad H_c = \phi/2kT_c, \tag{91}$$

where gd is the Gudermannian function defined by

$$\mathrm{gd}\, x \equiv 2\tan^{-1} e^x - \tfrac{1}{2}\pi \equiv 2\tan^{-1}(\tanh \tfrac{1}{2}x).$$

In the simplest case of a square lattice ($z = 4$), (91) becomes

$$\sinh H_c = 1,$$

or

$$\eta_c = e^{-H_c} = \sqrt{(2)} - 1 \sim 0{\cdot}41, \quad \frac{kT_c}{\phi} = (2\ln\cot\tfrac{1}{8}\pi)^{-1} \sim 0{\cdot}57. \tag{92}$$

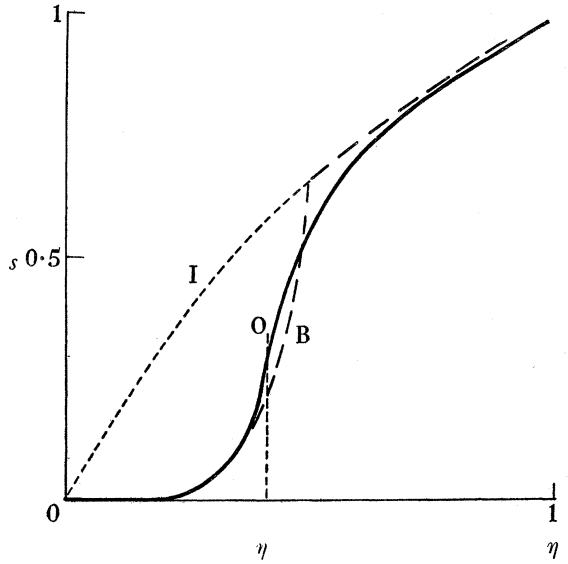

FIGURE 18. The surface roughness s of a square surface lattice as a function of η for a two-level model. O, Onsager's solution; B, Bethe's solution; I, assuming no geometrical constraints.

In this case Onsager and Onsager & Kaufmann have found the exact partition function of the lattice for all temperatures. The configurational potential energy per molecule $U - U_0$ or the surface roughness $s = 2(U - U_0)/\phi$ (see § 17) is found to be given by the formula

$$s = 1 - \tfrac{1}{2}\left(1 + \frac{2}{\pi}k_2 K_1\right)\coth H, \tag{93}$$

where

$$K_1 = K(k_1) = \int_0^{\frac{1}{2}\pi} [1 - k_1^2 \sin^2\omega]^{-\frac{1}{2}}\, d\omega$$

is the complete elliptic integral of the first kind, and

$$k_2 = 2\tanh^2 H - 1, \quad k_1 = \frac{2\sinh H}{\cosh^2 H}.$$

A graph of s against $\eta = \exp(-H) = \exp(-\phi/2kT)$ is given in figure 18. The curve possesses a vertical tangent at the transition temperature given by (92). For low temperatures or small η, (93) becomes

$$s = 4\eta^4. \tag{94}$$

This result shows that at low temperatures the jumps existing in the surface are due essentially to adsorbed molecules; in fact, the proportion of molecular positions on the surface occupied by adsorbed molecules is $\eta^4 = \exp(-2\phi/kT)$; as every adsorbed molecule has four horizontal bonds, the number of these bonds per molecule due to adsorbed molecules turns out to be equal to (94). In an actual crystal surface there will also be vacant surface sites in number equal to that of adsorbed molecules, therefore s should be $8\eta^4$; the reason why (94) is only half of that is, clearly, the assumption of a two-level model. In fact there will also be on the crystal surface nuclei of adsorbed molecules and holes consisting of more than one vacant surface site, but their concentration will be very small at low temperatures. Provided that is so, they can be considered as independent entities, and their concentration is proportional to η^6 for nuclei (or holes) of two adsorbed molecules (or vacant surface sites) and to higher powers of η for greater nuclei (or holes). As the temperature approaches the transition point, the concentration of these nuclei becomes larger and they cannot be considered as independent entities; the problem must then be considered as a co-operative phenomenon.

It is interesting to compare (93) with the result that we would have obtained if we had assumed no geometrical constraints in the surface; it is easy to see that under these conditions s would have been given by

$$s = 2\eta/(1+\eta), \tag{95}$$

which is represented by the dotted curve in figure 18.

In the case of a triangular lattice ($z = 6$, close-packed plane) (91) becomes

$$\exp 2H_c = 3,$$

or

$$\eta_c = 1/\sqrt{3} \sim 0{\cdot}58, \quad kT_c/\phi = (\ln 3)^{-1} \sim 0{\cdot}91. \tag{96}$$

This value for the transition temperature was obtained directly by Wannier & Onsager by an elegant method (Wannier 1945) assuming that a single transition temperature exists.

Examples of square surface lattices are the (1, 0, 0) face both in simple cubic and face-centred cubic lattices. An example of a triangular surface lattice is the (1, 1, 1) in the face-centred cubic lattice. In all these cases the nearest neighbour interactions in the surface itself are the same as the nearest neighbour interactions inside the crystal. The transition temperatures (92) or (96) for these surfaces are very high and seem to be of the same order of magnitude or higher than the melting-point T_M of the crystal. In fact, for the solid state of the rare gases for which a nearest neighbour interaction model can be considered as a reasonable approximation, we find from the experimental values $kT_M/\phi \sim 0{\cdot}7$. We deduce that these surfaces, if the crystal is perfect, must remain essentially flat for all temperatures below the melting-point, apart, of course, from the presence of adsorbed molecules and vacant surface sites.

Another interesting case is that of surfaces for which the nearest neighbour interactions in the surface itself are not only first but also second nearest neighbour bonds, as, for instance, (1, 1, 0) both for simple cubic and face-centred cubic lattices. Then the surface lattice is rectangular and the interactions are ϕ_1 (first nearest neighbour bond) in one direction and ϕ_2 (second nearest neighbour bond) in the other direction. The exact partition function for this lattice has also been given by Onsager (1944). He has shown that the potential energy (or our

surface roughness) follows a curve similar to figure 18, with a vertical tangent at a transition temperature given by

$$\sinh H_{1c} \sinh H_{2c} = 1, \qquad H_{1c} = \phi_1/2kT_c, \quad H_{2c} = \phi_2/2kT_c.$$

This formula can be written in the form

$$\frac{2kT_c}{\phi_1} \ln \coth \frac{\phi_1}{4kT_c} = \frac{\phi_2}{\phi_1}. \tag{97}$$

Figure 19 gives kT_c/ϕ_1 as a function of the ratio ϕ_2/ϕ_1 between bond energies. We see that for a given ϕ_1 the transition temperature decreases rather slowly as ϕ_2 decreases; it is only for ratios of the order $\phi_2/\phi_1 \sim 0{\cdot}1$ that T_c is smaller than (92) by a factor $\frac{1}{2}$. This is probably the case for homopolar crystals. Thus the transition temperature for these surfaces should be of the order of one-half of the melting-point. It could be interpreted as a surface melting of second nearest neighbour bonds.

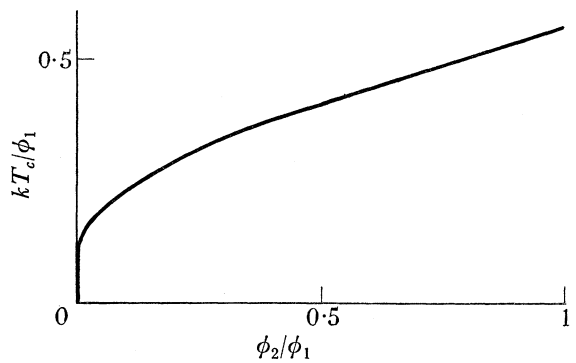

FIGURE 19. Transition temperature for a rectangular unsymmetrical lattice as a function of the ratio between the bond energies in both directions.

Finally, in the case of surfaces containing only second nearest neighbour bonds, as, for instance, (1, 1, 1) for simple cubic crystals, the transition temperature (7) is much lower; it is of the order of ϕ_2/ϕ_1 times the melting-point. At ordinary temperatures these surfaces would therefore be above their transition temperature.

The configurational surface free energy is, in all cases, very small below and at the transition temperature. Above this temperature it decreases roughly linearly with rise of temperature, the slope being $-k \ln 2$ approximately. Therefore the differences in surface free energy between the different faces of a crystal will decrease more and more as the temperature rises and the critical temperatures of the high index surfaces are surpassed, since high index faces have higher surface energies but lower transition temperatures.

The existence of a transition temperature, when it is below the melting-point, should have an observable effect on the adsorption properties of the surface, which clearly depends on the surface roughness. Actually the presence of adsorbable substance will change the equilibrium structure of the surface itself, and its transition temperature. We hope to treat this point in detail elsewhere. Meanwhile, a possible experimental method of testing the existence of a transition temperature would be to prepare, say, a metal crystal with one of

its less dense-packed surfaces exposed, anneal at various temperatures *in vacuo*, quench and test the adsorption properties of the surface. A sharp change in the latter would be expected when the annealing temperature crosses the transition temperature of the surface.

Similar considerations would apply to the influence of the catalytic properties of the surface of some solids on the kinetics of chemical reactions between adsorbed substances, in the cases when the catalytic activity is restricted to 'active' points on the surface. Frenkel (1945) suggested that these 'active' points should be identified with the presence of jumps on the surface, assuming that the adsorption of the reacting molecules in the edge of the steps decreases the activation energy for their chemical reaction.

On the other hand, the existence of a transition temperature will not have any influence on the kinetics of growth of the crystal surface. It would if the crystal were perfect. Below the transition temperature the only mechanism of growth would be a two-dimensional nucleation, which we know (part III) is always a very slow process at low supersaturations. Above the transition temperature the growth will be proportional to the supersaturation. Actually the fact that real crystals are imperfect guarantees the presence of the steps required to explain the observed growth at low supersaturations and below the transition temperature; Frank (1949) has shown that, during growth, a dislocation or group of dislocations terminating in the surface sends out closed loops of step in such a way that at any instant the surface is covered by a very high density of steps, practically independently of the number of dislocations present (provided there is at least one). Therefore, even if we observe the growth of a surface for which the critical temperature is below the melting-point, there would hardly be any difference between the rate of growth below and above the critical temperature.

20. *Many-level model: Bethe's approximation*

The two-level model of a crystal surface is clearly an over-simplification. We expect that with a many-level model, which corresponds to the actual crystal surface, the transition temperature should be lowered. In order to study this point we extend in this section Bethe's method to our many-level problem. In this method we assume that in a given region, arbitrarily chosen, the probabilities in which we are interested are independent; we then insert correction factors to take account of the geometrical constraints, and attempt to evaluate them by the requirement of self-consistency.

We shall limit ourselves, for simplicity, to the study of the structure of a (0, 0, 1) surface of a simple cubic crystal. Figure 20 shows a group of five molecules in the crystal surface, whose levels are i, j, k, l, m (at $T = 0$ we would have $i = j = k = l = m = 0$). Let the probability for this configuration be $p(i;j,k,l,m)$, p not being normalized. We assume that

$$p(i;j,k,l,m) = \eta^{|i-j|+|i-k|+|i-l|+|i-m|}\,\epsilon(j)\,\epsilon(k)\,\epsilon(l)\,\epsilon(m), \quad \eta = \exp\left(-\frac{\phi}{2kT}\right), \tag{98}$$

where ϕ is as usual the nearest neighbour interaction. The factors containing η represent the Boltzmann factors, and the functions ϵ are the correction factors which take into account the influence of geometrical constraints of the outside region on the molecules considered. The factors $\epsilon(x)$ will be less than unity unless $x = 0$; in this case we take $\epsilon(0) = 1$. The level zero corresponds to Bethe's 'right atom', the other levels to different kinds of 'wrong atoms'. By symmetry, $\epsilon(x) = \epsilon(-x)$.

The total probability $p(x)$, for the central molecule to be at the level x, whatever the values of j, k, l, m, is

$$p(x) = \sum_{jklm} p(x;j,k,l,m) = \{f(x)\}^4, \tag{99}$$

where

$$f(x) = \sum_j \eta^{|x-j|}\epsilon(j), \tag{100}$$

and the summations are carried out over all possible levels. Clearly $f(x) = f(-x)$. Following Bethe, the self-consistency condition is that the probability $p(x)$ for the central molecule to be at the level x must be equal to that for one of the molecules in the outer shell to be also at this level. Therefore $p(x)$ can also be written as

$$p(x) = \sum_{i,klm} p(i;x,k,l,m) = \epsilon(x)\sum_i \eta^{|x-i|}\{f(i)\}^3, \tag{101}$$

where we have used (98) and (100). Hence from (99) and (101) we obtain

$$f^4(x) = \epsilon(x)\sum_i \eta^{|x-i|}f^3(i), \quad f^r(x) \equiv \{f(x)\}^r. \tag{102}$$

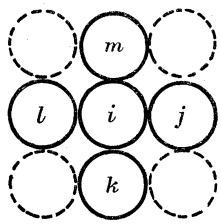

FIGURE 20

The correction factors $\epsilon(x)$ have to be determined from the equations (100) and (102). Now if we divide (102) by $f^3(0)$, use (100), and introduce the functions $g(x) = [f(x)/f(0)]^3$, the equations (102) transform into the system of linear equations

$$g(x)\sum_i \eta^{|x-i|}\epsilon(i) = \epsilon(x)\sum_i \eta^{|x-i|}g(i),$$

which have the only solution

$$\epsilon(x) = g(x) = [f(x)/f(0)]^3. \tag{103}$$

This form of the conditions that $\epsilon(x)$ must satisfy is very convenient for numerical calculations.

The potential energy U, and therefore the surface roughness $s = 2U/\phi$, can also be written in a general form. In fact, the energy corresponding to the configuration of figure 20 is

$$\tfrac{1}{2}\phi\{|i-j|+|i-k|+|i-l|+|i-m|\},$$

and therefore the potential energy per molecule U of the surface will be

$$U = \frac{1}{2}\frac{\phi}{2}\frac{\sum\{|i-j|+|i-k|+|i-l|+|i-m|\}p(i;j,k,l,m)}{\sum p(i;j,k,l,m)}, \tag{104}$$

where the summations are carried out over all values of i, j, k, l, m. Using (98) and (100) the potential energy or the surface roughness can be written in the form

$$s = \tfrac{1}{2}\eta\frac{\partial}{\partial\eta}\ln\sum_i f^4(i), \tag{105}$$

where the use of the sign of partial differentiation is to indicate that ϵ is to be treated as constant during the differentiation. Once the $\epsilon(x)$ are known from equations (103) the surface roughness factor is determined from (105).

20·1. *Two-level problem*

Let us first consider, as an introduction, the two-level case, which is the problem initially considered by Bethe (1935). In this case, from (100) ($i = 0, 1$),

$$f(0) = 1+\epsilon_1\eta, \quad f(1) = \epsilon_1+\eta; \qquad \epsilon(0) = 1, \quad \epsilon(1) = \epsilon_1,$$

and formula (103) becomes Bethe's equation

$$\epsilon_1 = \left(\frac{\epsilon_1+\eta}{1+\epsilon_1\eta}\right)^3, \tag{106}$$

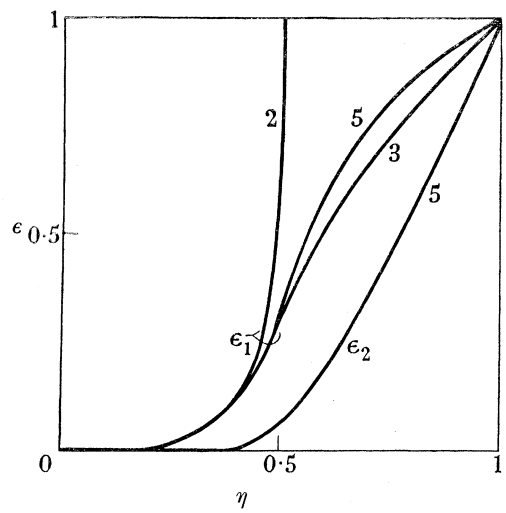

FIGURE 21. Bethe's factors ϵ for the two, three, and five levels.

giving ϵ_1 as a function of η. Figure 21 gives ϵ_1 (curve 2) as a function of η. ϵ_1 is smaller than 1 only for values of η smaller than 0·5. Above $\eta = 0{\cdot}5$ the only solution of (106) is $\epsilon_1 = 1$. The temperature corresponding to $\eta = 0{\cdot}5$ has been interpreted as the transition temperature of the corresponding co-operative phenomenon:

$$\eta_c = 0{\cdot}5, \quad kT_c/\phi = (2\ln 2)^{-1} \sim 0{\cdot}72. \tag{107}$$

This value is higher than the value $kT_c/\phi \sim 0{\cdot}57$ (92) given by the correct treatment of Onsager. On the other hand, the fact that $\epsilon_1 = 1$ above $\eta = 0{\cdot}5$ cannot be interpreted from a physical point of view, and shows only that the method is not correct. Actually $\epsilon_1 = 1$ means, from the point of view of our problem, that the geometrical constraints have disappeared above the transition temperature, and this is obviously impossible. According to the definition of the factors ϵ, they must be smaller than 1 at all temperatures.

The surface roughness is now given by

$$s = \frac{4\epsilon_1\eta}{1+\epsilon_1^4}\,\frac{1}{1+\epsilon_1\eta}. \tag{108}$$

For low temperatures, $s = 4\eta^4$, the same expression as is given by Onsager's treatment. Above $\eta = 0{\cdot}5$, s is given by formula (95) corresponding to the hypothesis of independency of the probabilities or $\epsilon_1 = 1$. The expression (108) has been represented in figure 18, for comparison with Onsager's result.

20·2. *Three-level problem*

The simplest many-level problem which corresponds to the structure of a crystal surface is the three-level problem. In this case, using (100) ($i = 1, 0, -1$),

$$f(0) = 1+2\epsilon_1\eta, \quad f(1) = f(-1) = \eta+\epsilon_1(1+\eta^2); \qquad \epsilon(0) = 1, \quad \epsilon(1) = \epsilon(-1) = \epsilon_1.$$

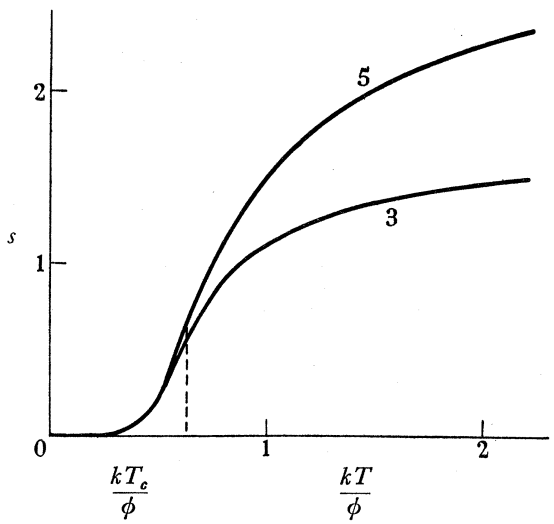

FIGURE 22. The surface roughness s for a three-level and five-level problem, as a function of kT/ϕ.

The general formula (103) now gives the equation

$$\epsilon_1 = \left[\frac{\eta+(1+\eta^2)\,\epsilon_1}{1+2\eta\epsilon_1}\right]^3 \tag{109}$$

for the calculation of ϵ_1 as a function of η. The result is represented in figure 21 (curve 3). In this case $\epsilon_1 = 1$ is not a solution of (109) for any finite temperature, as we should expect on physical grounds. On the other hand, ϵ_1 has no singularity allowing the definition of a transition temperature. To decide where this transition temperature is we must wait till s is known.

The value of s is easily calculated from (105):

$$s = \frac{8\eta\epsilon_1}{1+2\epsilon_1^4}\,\frac{1+\epsilon_1\eta}{1+2\epsilon_1\eta}. \tag{110}$$

The result is represented in figure 22 as a function of kT/ϕ; the curve has a point of inflexion at a temperature given by

$$\eta_c = 0{\cdot}45, \quad kT_c/\phi \sim 0{\cdot}63. \tag{111}$$

This temperature can be interpreted as the transition temperature of the three-level problem. It is substantially lower than the transition temperature corresponding to the two-level Bethe problem, but still higher than Onsager's value. The derivative of s with respect to T (which would correspond to the specific heat in our problem) would have a maximum at this transition temperature, but not a singularity.

At low temperatures (110) becomes

$$s = 8\eta^4,$$

which represents the jumps due to the presence in the surface of adsorbed molecules *and* vacant surface sites, which were not allowed in a two-level model. At high temperatures s becomes now larger than 1 (in fact, its maximum value for $\eta = 1$ is 1·8). The reason for that is again that we have now the possibility of jumps of height 2 intermolecular distances, and therefore the number of bonds parallel to the surface per molecule (equal to s) can now be greater than 1.

20·3. *Many-level problem*

It is interesting to see how the surface roughness behaves with increasing number of levels. In the case of five levels, one obtains the equations

$$\epsilon_1 = \left(\frac{\eta+(1+\eta^2)\,\epsilon_1+\eta(1+\eta^2)\,\epsilon_2}{1+2\eta\epsilon_1+2\eta^2\epsilon_2}\right)^3, \quad \epsilon_2 = \left(\frac{\eta^2+\eta(1+\eta^2)\,\epsilon_1+(1+\eta^4)\,\epsilon_2}{1+2\eta\epsilon_1+2\eta^2\epsilon_2}\right)^3 \tag{112}$$

for the calculation of $\epsilon_1 = \epsilon(1) = \epsilon(-1)$ and $\epsilon_2 = \epsilon(2) = \epsilon(-2)$. The surface roughness s is given by

$$s = \frac{8\eta}{1+2\epsilon_1^4+2\epsilon_2^4}\,\frac{\epsilon_1+\eta(\epsilon_1^2+2\epsilon_2)+(1+3\eta^2)\,\epsilon_1\epsilon_2+2\eta^3\epsilon_2^2}{1+2\eta\epsilon_1+2\eta^2\epsilon_2}. \tag{113}$$

The values of ϵ_1 and ϵ_2 are represented in figure 21 as functions of η and those of s in figure 22 as functions of kT/ϕ. The curve s has again a point of inflexion, defining the transition temperature at a value of kT_c/ϕ which cannot be distinguished from (111). The inclination of the tangent increases and hence the height of the maximum for the derivative of s. We notice that the difference in behaviour between three and five levels is rather small from the point of view of the location of the transition temperature. The reason for that is that the new parameters ϵ which we introduce to represent the new levels are very small in the neighbourhood of the critical point.

The calculations can be carried on to any number of levels. In the vicinity of the transition temperature there is practically no further change. Also the parameters ϵ do not become 1, at any rate for temperatures for which $\eta < 0{\cdot}8$, in spite of the fact that for an infinite number of levels $\epsilon(x) \equiv 1$ is a solution of equations (100) and (102).

The change in the value of the transition temperature, according to Bethe's method, occurs therefore at the passage from two to three levels. Although we also expect to have a decrease in the correct transition temperature, when the number of levels is increased, we do not know whether this decrease will be as substantial as it is in Bethe's approximation, owing to the anomalous behaviour of the two-level problem in this approximation.

APPENDICES

APPENDIX A. INFLUENCE OF THE MEAN DISTANCE x_0 BETWEEN KINKS ON THE RATE OF ADVANCE OF STEPS

A1. *Single step*

We suppose the kinks to be regularly distributed on the step at distances x_0 from each other (figure 23). Let us suppose D_s is independent of direction in the surface; we have to solve equation (14) or

$$x_s^2 \nabla^2 \psi = \psi, \quad \psi = \sigma - \sigma_s, \tag{A1}$$

with the boundary condition $\psi = 0$ for $y = \pm\infty$. We suppose also that there is a current in the edge of the step, governed by the diffusion constant D_e, which is large enough for the current passing directly from the surface to the kinks to be neglected. Since ψ must be periodic in x, with period x_0, the required solution of (A1) is

$$\psi(x, y) = \sigma\beta \sum_{n=0}^{\infty} c_n e^{\mp l_n y} \cos k_n x; \qquad k_n = 2\pi n/x_0, \quad l_n^2 = x_s^{-2} + k_n^2. \tag{A2}$$

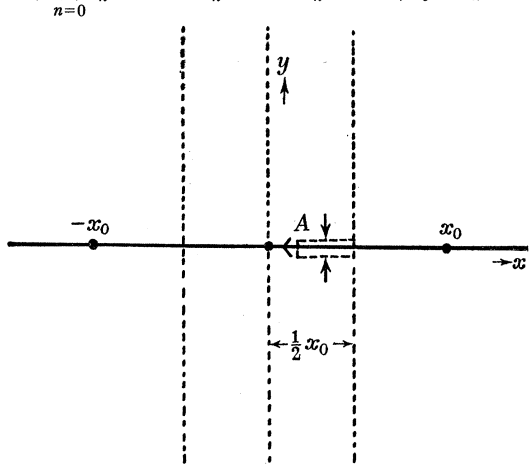

FIGURE 23. Step ($y = 0$) with kinks at a distance x_0 from each other.

The minus sign corresponds to $y > 0$, and the plus sign to $y < 0$; the coefficients c_n have to be determined. The current going into one kink ($x = 0$ for instance) will be equal to the current

$$j = D_s n_{s0} (\partial\psi/\partial y)_{y=0}$$

going from the surface to the edge integrated between $-\frac{1}{2}x_0$ and $\frac{1}{2}x_0$. The velocity of the step will then be the result of the current going into all the kinks, and turns out to be

$$v_\infty = 2\sigma x_s \nu \exp(-W/kT)\beta c_0, \tag{A3}$$

which is the general expression (19) given in § 4. We have now to calculate the factor c_0.

In the edge of the step we shall have a supersaturation σ_e and an expression $\psi_e = \sigma - \sigma_e$, which will be a function of x. In general, $\psi(x, 0) = \beta_1 \psi_e(x)$, where $\beta_1 < 1$ is a retarding factor similar to (17). If the interchange of molecules between the edge and its immediate neighbourhood is rapid, $\beta_1 = 1$. Hence

$$\beta_1 \psi_e(x) = \sigma\beta \sum_{n=0}^{\infty} c_n \cos k_n x. \tag{A4}$$

Near the kinks ($x = 0$ for instance) we shall have $\psi_e(0) = \beta_2\sigma$, where β_2 is another retarding factor corresponding to the interchange between edge and kink. Putting $\beta = \beta_1\beta_2$, we have the condition

$$\sum_{n=0}^{\infty} c_n = 1. \tag{A5}$$

The current in the edge passing through the point A (figure 23), whose co-ordinate is x, is given by

$$j_e = -D_e(dn_e/dx) = -D_e n_{e0}\sigma\beta_2 \sum_{n=0}^{\infty} c_n k_n \sin k_n x, \tag{A6}$$

where (A4) has been used. On the other hand, this current must be equal to that going from the surface to the edge between x and $\frac{1}{2}x_0$, that is to say

$$2D_s n_{s0}\int_x^{\frac{1}{2}x_0} (\partial\psi/\partial y)_{y=0}\,dx = -2D_s n_{s0}\sigma\beta\left[c_0(\tfrac{1}{2}x_0 \operatorname{sgn} x - x)/x_s - \sum_{n=1}^{\infty} (c_n l_n/k_n)\sin k_n x\right], \tag{A7}$$

where $\operatorname{sgn} x$ is 1 for $x>0$, -1 for $x<0$ and 0 for $x = 0$. Equating (A6) and (A7) we obtain the coefficients $c_n (n>0)$ as functions of c_0:

$$c_n/c_0 = (4bc/n^2)\,[1+(2c/n)\,(1+b^2/n^2)^{\frac{1}{2}}]^{-1}, \tag{A8}$$

with the abbreviations

$$b = x_0/2\pi x_s, \quad c = x_0 a/2\pi x_e^2, \quad x_e^2 = D_e n_{e0} a/D_s n_{s0}\beta_1. \tag{A9}$$

From (A5) and (A8) we obtain

$$1/c_0 = 1+4bc\sum_{n=1}^{\infty}\{n^2[1+(2c/n)\,(1+b^2/n^2)^{\frac{1}{2}}]\}^{-1}. \tag{A10}$$

The series in (A10) can be approximated to by an integral

$$\sum_{n=1}^{\infty}\{n^2[1+(2c/n)\,(1+b^2/n^2)^{\frac{1}{2}}]\}^{-1} \simeq \int_0^1 \frac{dx}{1+2cx(1+b^2x^2)^{\frac{1}{2}}},$$

which can be evaluated using the transformation $\tan\theta = bx$. The final result for c_0 is

$$\frac{1}{c_0} = 1+2bc(b^2+c^2)^{-\frac{1}{2}}\{f_1(x_1, u_m)+f_2(x_2, u_m)\}, \tag{A11}$$

where
$$f_1(x_1, u_m) = 2(x_1^2-1)^{-\frac{1}{2}}\tan^{-1}\{u_m(x_1^2-1)^{\frac{1}{2}}/(x_1-u_m)\},$$
$$f_2(x_2, u_m) = (1-x_2^2)^{-\frac{1}{2}}\ln\{(u_m(1+(1-x_2^2)^{\frac{1}{2}})+x_2)/(u_m(1-(1-x_2^2)^{\frac{1}{2}})+x_2)\},$$
$$u_m = b/\{1+(1+b^2)^{\frac{1}{2}}\}, \quad x_1 = c/b+(c^2/b^2+1)^{\frac{1}{2}}>1, \quad x_2 = -c/b+(c^2/b^2+1)^{\frac{1}{2}}<1.$$

For $x_0\to\infty$, we obtain the result for widely separated kinks; it is easy to see that c_0 is then proportional to $1/x_0$, or to the number of kinks per cm.

The method used to calculate the current going into the kinks is correct, provided the current via the edge is important or $x_e>a$. In the limiting case when $x_e\sim a$ the result of this calculation should be the same as if the current via the edge were neglected altogether. In § 4 we have seen that x_e is of the order of a; under these conditions, and assuming $x_0\gg a$ and $x_s\gg a$, one obtains from (A9) that $c\gg 1$ and $c/b\gg 1$; then, the rather complicated expression (A11) reduces to

$$1/c_0 = 1+2b\ln\{4c/(1+(1+b^2)^{\frac{1}{2}})\}, \tag{A12}$$

which is the formula (21) of § 4.

A2. *Parallel sequence of steps*

We suppose the steps and kinks are disposed as in figure 24, the kinks forming a rectangular lattice. Let the distance between kinks be x_0 and that between steps y_0. Between steps the same continuity equation (A1) holds. Again we have periodicity in the x-direction, hence in the interval

$$-\tfrac{1}{2}y_0<y<\tfrac{1}{2}y_0, \quad -\tfrac{1}{2}x_0<x<\tfrac{1}{2}x_0,$$

we have the solution

$$\psi(x,y)=\sigma\beta\sum_{n=0}^{\infty}c_n\frac{\cosh l_n y}{\cosh \tfrac{1}{2}l_n y_0}\cos k_n x, \tag{A13}$$

where k_n and l_n have the same significance as in (A2). The velocity of every step will be the result of the current going into every kink, equal to the current going from the surface to the step in the range x_0. The velocity turns out to be

$$v_\infty=2\sigma x_s \nu e^{-W/kT}\tanh(y_0/2x_s)\,\beta c_0, \tag{A14}$$

which is the general formula (24) given in § 5. To calculate c_0 we have again the condition

$$\sum_{n=0}^{\infty}c_n=1 \tag{A15}$$

as before. To evaluate all the $c_n(n>0)$ as functions of c_0, we use the same method as in § A1, and from (A15) we deduce for c_0 the rather complicated expression

$$1/c_0=1+4bc\tanh(y_0/2x_s)\sum_{n=1}^{\infty}\{n^2[1+(2c/n)\,(1+b^2/n^2)^{\frac{1}{2}}\tanh((n/2e)\,(1+b^2/n^2)^{\frac{1}{2}})]\}^{-1}, \tag{A16}$$

where b and c are given by (A9) and

$$e=x_0/2\pi y_0. \tag{A17}$$

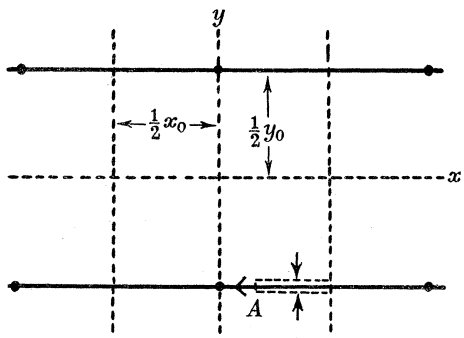

FIGURE 24. Sequence of steps distant y_0 from each other with kinks distant x_0.

In the limiting case when $x_e\sim a$, and therefore $c\gg 1$, the series in (A16) can be approximately evaluated, replacing the $\tanh x$ by $x/(1+x)$. The approximated result is

$$1/c_0=1+2b\tanh(y_0/2x_0)\,[\ln(4c/(1+(1+b^2)^{\frac{1}{2}}))+(2e/b)\tan^{-1}b], \tag{A18}$$

which is the formula (25) given in § 5.

APPENDIX B. THE MUTUAL INFLUENCE OF A PAIR OF GROWTH SPIRALS

We now reconsider, in more detail, the interaction of the growth spirals of a pair of dislocations (like or unlike) whose separation is at least a moderate multiple of ρ_c. We have seen (§ 9·1) that their resultant activity will equal that of one dislocation except in so far as

influences transmitted along the step from the point of meeting modify the rate of rotation of the separate spirals. To examine this effect we first consider a simpler case.

A circular expanding step, whose position is defined by $r = r_1(t)$, is helped on over a small portion of its length, e.g. by meeting another small closed loop of step (a small island nucleus). Re-entrant portions of the curve fill in rapidly, so that we then have $r = r_1(t) + f(\theta, t)$, where θ is the angular polar co-ordinate and t the time. We suppose f small compared with r_1, and $\partial r/\partial\theta = r'$ small enough for its square to be neglected in expressions for curvature (35) and normal velocity (36):

$$1/\rho = (r^2+2r'^2-rr'')\,(r^2+r'^2)^{-\frac{3}{2}} \sim 1/r - r''/r^2 \sim 1/r_1 - \partial^2 f/\partial s^2,$$

$$v = (\partial r/\partial t)\, r(r^2+r'^2)^{-\frac{1}{2}} \sim \partial r/\partial t = \partial r_1/\partial t + \partial f/\partial t.$$

Here s is the arc distance $r\theta$. By equation (34) we have then

$$\partial r_1/\partial t + \partial f/\partial t = v_\infty - v_\infty \rho_c/r_1 + v_\infty \rho_c \partial^2 f/\partial s^2.$$

Subtracting the corresponding equation obtained when f is zero, we have

$$\frac{\partial f}{\partial t} = v_\infty \rho_c \frac{\partial^2 f}{\partial s^2}.$$

This is simply the diffusion equation, with an effective diffusivity $v_\infty \rho_c$. Whatever the initial form of f, provided it is confined to a small portion of the circumference and disregarding the closed nature of the curve (as is right, since we are going to apply the result to a spiral instead of a circle), its solution tends rapidly to the form

$$f = A(4\pi\rho_c v_\infty t)^{-\frac{1}{2}} \exp\,(-s^2/4\rho_c v_\infty t),$$

for which $\int_{-\infty}^{\infty} f\,ds$ has the constant value A. Thus the growth increment remains constant in area but gradually spreads out along the step.

This result should be approximately valid for deformations of the spiral also, except close to the centre, where r' is no longer negligible. We apply it, then, to a growth spiral which, once in every turn, meets another based on a dislocation a distance l away. Each time this happens the resulting concave region of the growth front fills up rapidly, making an area of increment which we estimate roughly as $(4-\pi)\,l^2/8$ from the difference in area between two circular quadrants and a rectangle. This occurs $\omega/2\pi$ times a second at a distance, measured along the step, approximately $l^2/16\rho_c$ from the dislocation. These growth increments now diffuse along the step, but at the same time the spiral continues to rotate, so that while the increment spreads, its centre recedes from the dislocation, the arc distance being expressible approximately as

$$s = \rho_c(l/4\rho_c + \omega t)^2.$$

Near the centre of the spiral the concept of an area diffusing along a line fails; the growth increment which diffuses into the centre is used up in extending the step line faster than would occur spontaneously.

Supposing the diffusion law continued to hold as far as the centre of the spiral and on some fictitious line beyond it, the value of f at this point resulting from one meeting of the growth fronts at a time $t = 0$ would be approximately

$$f_d = \{(4-\pi)\,l^2/16(\pi\rho_c v_\infty t)^{\frac{1}{2}}\} \exp\,[-\rho_c(l/4\rho_c + \omega t)^4/4v_\infty t].$$

This is zero for small or large t, and has a maximum very nearly at the maximum of the exponential factor which occurs at $t = l/12\omega\rho_c$. Inserting this value of t, and at the same time writing $\omega = \epsilon v_\infty/2\rho_c$, where ϵ is a factor representing the increase of rate of rotation over that of an unperturbed single spiral, we have

$$f_{d,\,\max.} = [(4-\pi)/16]\,(6\epsilon l^3/\pi\rho_c)^{\frac{1}{2}} \exp[-(\tfrac{1}{2}\epsilon)\,(l/3\rho_c)^3].$$

We may alternatively focus attention on the area of incremental growth which would have diffused past the centre, on the same assumptions. This is

$$F_d = [(4-\pi)\,l^2/16]\,\mathrm{erfc}\,[(l/4\rho_c+\omega t)^2\,(4v_\infty t/\rho_c)^{-\frac{1}{2}}],$$

where $\mathrm{erfc}\,(x)$ is the complementary error function $1-\mathrm{erf}\,(x)$. As a function of time this has its maximum value at $t = l/12\omega\rho_c$, and is then

$$F_{d,\,\max.} = [(4-\pi)\,l^2/16]\,\mathrm{erfc}\,[(\tfrac{1}{2}\epsilon)^{\frac{1}{2}}\,(l/3\rho_c)^{\frac{1}{2}}].$$

Consideration of either of these expressions, $f_{d,\,\max.}$ or $F_{d,\,\max.}$, suffices to show that the influence transmitted into the centre is quite negligible if l much exceeds $3\rho_c$.

For variations of l/ρ_c the first of these functions is a maximum precisely, the second very nearly, when $(l\epsilon^{\frac{1}{3}}/3\rho_c) = 1$. The corresponding maximum values are $0{\cdot}234\rho_c$ and $0{\cdot}155\epsilon^{-\frac{2}{3}}\rho_c^2$. We may crudely estimate the order of magnitude of the amount of extra rotation produced by such an increment by dividing by $2\pi\rho_c$ in the first case or $\pi\rho_c^2$ in the second, obtaining $0{\cdot}037$ or $0{\cdot}049\epsilon^{-\frac{2}{3}}$ of a turn. This occurs once in every turn, i.e. $\epsilon \sim 1{\cdot}04$ or $1{\cdot}05$. This result is not directly valuable, for the maxima occur at a separation too small for the validity of approximations used in the treatment; but it does show that at greater separations where the approximations are reasonably valid (say $l > 4\pi\rho_c$) the interaction is quite negligible.

The calculation affirms the surmise that when ρ_c is steadily reduced below the critical value $\frac{1}{2}l$ above which the activity of an unlike pair of dislocations is zero, the activity first rises above that of a single dislocation before settling down to equality with it; but it leaves much doubt as to the actual magnitude of the maximum excess. It is probably a few units per cent, and if it later turns out that importance attaches to the actual value, a step-by-step trajectory calculation must be carried out.

Appendix C. Proof of certain formulae in the statistics of kinks

To prove formulae (65), (66) and (67) in the text, we consider particular processes (figures 25, 26, 27, 28) and we apply the principle of detailed balancing.

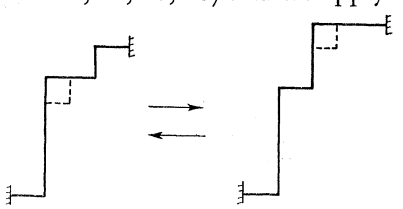

Figure 25

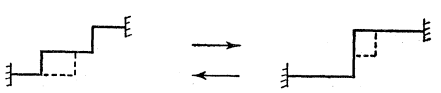

Figure 26

Figure 27

Figure 28

Let us first consider the process shown in figure 25. The molecule denoted by a square is the one which moves. The positions in the shaded regions are supposed to remain the same during the process. In this case the energies of the two configurations are the same, so the probabilities for their occurrence are equal. Hence

$$n_{+r}(x)\, q(x+1)\, n_+(x+2) = n_{+(r-1)}(x)\, n_{+2}(x+1)\, q(x+2). \tag{C1}$$

Here we have written n_+ for n_{+1}. Later we write g_+ for g_{+1}. It is convenient to introduce a function defined by

$$g_{\pm r}(x) = n_{\pm r}(x)/g(x). \tag{C2}$$

Then (A1) can be written

$$g_{+r}(x)\, g_+(x+2) = g_{+(r-1)}(x)\, g_{+2}(x+1). \tag{C3}$$

For the process of figure 26, we need to supply an energy ϕ_2 in going from the left-hand to the right-hand diagram. Hence

$$g_{+2}(x+1) = g_+(x)\, g_+(x+2)\, \eta_2^2, \tag{C4}$$

where we have again used (C2) and also the abbreviation

$$\eta_{1,2} = \exp(-\phi_{1,2}/2kT). \tag{C5}$$

Substituting the value (C4) of $g_{+2}(x+1)$ in (C3) we obtain

$$g_{+r}(x) = \{g_+(x)\}^r\, \eta_2^{2(r-1)}, \tag{C6}$$

as is easily shown by induction on r. Formula (C6) is formula (65) of the text.

We now need an equation relating neighbouring positions. Comparing (C4) and (C6) ($r = 2$) we obtain, immediately,

$$\{g_+(x)\}^2 = g_+(x-1)\, g_+(x+1). \tag{C7}$$

From the process illustrated by figure 27 we obtain

$$g_+(x+1)\, \eta_1^2 = g_+(x)\, g_-(x+1)\, g_+(x+2),$$

and using the property (C7) we obtain

$$g_+(x)\, g_-(x) = \eta_1^2, \tag{C8}$$

which is formula (66) in the text.

The general solution of the functional equation (C7) is easily proved to be

$$g_+(x) = g_+(0)\, e^{cx}, \tag{C9}$$

where $g_+(0)$ and c are arbitrary constants. We now investigate the dependence of the constant c in (C9) on the supersaturation, or more specifically the saturation ratio α defined by the equation

$$N = \alpha N_0 = \alpha(\eta_1\eta_2)^4. \tag{C10}$$

Here N is the occupation probability for an adsorbed molecule on the surface, and

$$N_0 = \exp\{-2(\phi_1+\phi_2)/kT\}$$

is clearly the value of N when $\alpha = 1$. Since we are speaking of equilibrium, N is independent of position in the surface. From the process represented by figure 28 we obtain

$$N = g_+(x)\, g_-(x+1)\, \eta_1^2\eta_2^4, \tag{C11}$$

and combining this result with (C8), (C9) and (C10) we obtain

$$\alpha = e^{-c},$$

and therefore (A9) becomes

$$g_+(x) = g_+(0)\, \alpha^{-x}, \tag{C12}$$

which is equation (67) given in the text.

Appendix D. Wulff's theorem

'In a crystal at equilibrium, the distances of the faces from the centre of the crystal are proportional to their surface free energies per unit area.'

A great deal has been written on the general form of this theorem, and von Laue (1943) has given a critical review of the subject. There is no really satisfactory proof of the three-dimensional Wulff theorem even now. The proof for the two-dimensional case given here is believed to have merits not to be found in any earlier proof.

The problem is to find the relation between the shape of the two-dimensional equilibrium nucleus, and the polar diagram of the free energy of a boundary element as a function of its orientation. The shape is fixed by the condition of minimum total free energy for a given area of nucleus. Let (r, ϕ) be the polar co-ordinates (figure 29) of a point T of the crystal boundary S, and let (x, y) be the corresponding Cartesian co-ordinates. Construct a tangent to S at T, and let OM be a perpendicular from the origin to the tangent (length p). Let $f(\theta)$ be the edge free energy per unit length of the element of boundary at T. The line element for the boundary in parametric form is

$$ds = (\dot{x}^2+\dot{y}^2)^{\frac{1}{2}}\,dt, \tag{D1}$$

where the dot denotes differentiation with respect to the parameter t. We now choose θ as the parameter. Then the total edge free energy F and area n_0 (number of molecules) of our nucleus are given by

$$F = \int (\dot{x}^2+\dot{y}^2)^{\frac{1}{2}} f(\theta)\,d\theta, \quad n_0 = \frac{1}{2}\int (x\dot{y}-y\dot{x})\,d\theta, \tag{D2}$$

respectively. From figure 29,

$$p = x\cos\theta + y\sin\theta. \tag{D3}$$

Let us find the locus of M as T goes over the whole of the curve S. This will give the 'pedal' of S, which is determined by (D3) and the equation obtained from it by partial differentiation with respect to θ. Conversely, if the pedal is known, i.e. p is given as a function of θ, then the (x, y) equation of S can be obtained from the equations

$$\left.\begin{aligned} x &= p\cos\theta - \dot{p}\sin\theta, \\ y &= p\sin\theta + \dot{p}\cos\theta. \end{aligned}\right\} \tag{D4}$$

Using these expressions we can write (D2) in the form

$$F = \int (p+\ddot{p})f\,d\theta, \quad n_0 = \frac{1}{2}\int (p+\ddot{p})\,p\,d\theta. \tag{D5}$$

The problem now is to minimize F subject to the condition of n_0 being constant. Introducing the Lagrange multiplier λ, the appropriate Euler equation giving the minimum condition is

$$\frac{\partial Q}{\partial p} - \frac{d}{d\theta}\left(\frac{\partial Q}{\partial \dot{p}}\right) + \frac{d^2}{d\theta^2}\left(\frac{\partial Q}{\partial \ddot{p}}\right) = 0,$$

where

$$Q = \tfrac{1}{2}(p+\ddot{p})\,p - \lambda(p+\ddot{p})f.$$

These two equations reduce to

$$p+\ddot{p} = \lambda(f+\ddot{f}), \tag{D6}$$

and the solution of this differential equation is

$$p(\theta) = C\sin(\theta-\beta) + \lambda f(\theta),$$

where C and β are arbitrary constants. Now the first term on the right possesses the period 2π; so that if we choose the origin in such a way that the crystal possesses some rotational symmetry with respect to it (centre of the crystal), we see that $C = 0$. Hence

$$p(\theta) = \lambda f(\theta), \tag{D7}$$

which shows that up to a constant factor the polar diagram of the edge free energy is the pedal of the equilibrium shape of the crystal.

The foregoing theorem, which is a generalization of Wulff's theorem, enables us to study the properties of the critical nucleus in a very general way. First we deduce from (D5), (D6) and (D7) the total edge free energy F_0 of our nucleus:

$$F_0 = 2n/\lambda. \tag{D8}$$

The constant λ can be determined in the following way. Assuming that the shape of the nucleus does not change in the neighbourhood of the equilibrium dimensions, it was shown in §15·2 (formula 88) that the total edge free energy of the critical nucleus is given by

$$F_0 = 2n_0 kT \ln \alpha. \tag{D9}$$

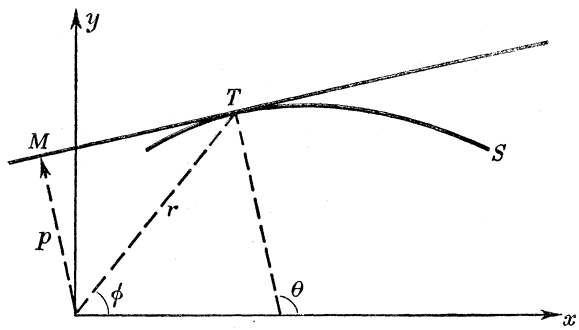

FIGURE 29

Therefore, from (D8) and (D9), $1/\lambda = kT \ln \alpha$,

and (D7) becomes $$kT \ln \alpha = f(\theta)/p(\theta). \tag{D10}$$

This equation represents not only a generalization of Wulff's theorem, but also a generalization of the Gibbs-Thomson formula—in two dimensions of course. Knowing $f(\theta)$, equation (D10) gives $p(\theta)$, and hence the shape of the critical nucleus is derived by the following geometrical construction. Draw a radius vector from the origin to the curve of $p(\theta)$ and construct a perpendicular to the radius vector at the point of intersection with the curve. Then the envelope of these perpendiculars, when the radius vector describes a complete revolution, defines the shape of the critical nucleus. Naturally, the curve of $p(\theta)$ will be closed if the free energy per unit length is single-valued. We emphasize here that θ is generally not the same as ϕ, the polar angle in the shape diagram (figure 29).

For the particular points of the step for which the tangent to the shape is normal to the radius vector, $\theta = \phi$ and $p(\theta) = r(\phi)$, and equation (D10) becomes

$$kT \ln \alpha = f(\phi)/r(\phi), \tag{D11}$$

showing that the distance from the centre to one of these particular points is proportional to the edge free energy per unit length at this point, which is the ordinary form of Wulff's theorem. If f or r is independent of ϕ then (D11) becomes the Gibbs–Thomson equation in two dimensions.

It is possible to give a simple expression for the radius of curvature of the nucleus at a point whose polar angle is ϕ in terms of the values of $f(\theta)$ and $f''(\theta)$ at the corresponding point in the edge free-energy diagram. The result is

$$\rho(\phi) = \{f(\theta)+f''(\theta)\}/kT\ln\alpha, \tag{D12}$$

the unit of length again being the intermolecular spacing.

The solution (D7) has been obtained on the assumption that S and its pedal possess continuously turning tangents. When there are sharp corners in S, the solution also applies for all pieces of S possessing continuously turning tangents. However, it may turn out that more than one free-energy diagram corresponds to a given S. To illustrate this, let us consider the polygonal equilibrium shape shown in figure 30, where S is the boundary of the crystal and O is its centre.

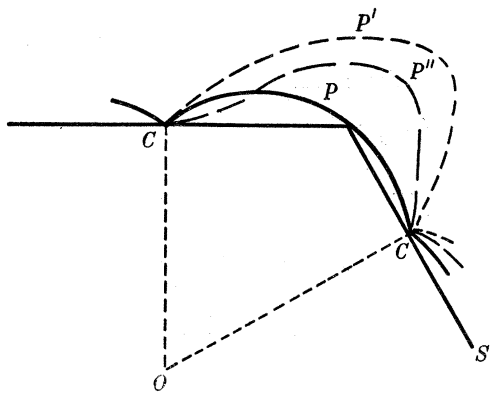

FIGURE 30

It is easily seen geometrically that if the free-energy diagram is that figure P obtained by finding the pedal of S (a number of circular arcs, if S is polygonal), then any curve P' lying entirely outside P, but coinciding with P at the cusps C, will give the same S, namely that given by P. If, however, the free-energy diagram lies entirely inside P, but coincides with P at the cusps C, then we obtain a shape for the crystal S' (different from S) which possesses neither sharp corners nor straight edges, and there is a one-to-one correspondence between S' and the free-energy diagram, so that given S' the free-energy diagram is determined uniquely and vice versa. This is the case in the particular model which we have been considering in part III. In the intermediate cases when the free-energy diagram P'' lies partly within and partly without P, then the corresponding crystal shape S'' will have sharp corners with or without straight segments in the boundary, depending on the actual form P''.

At $T=0$ we expect most crystals to be polygonal (or polyhedral, in three dimensions). The question arises: Are the corners rounded when $T>0$, or can it happen that the equilibrium form remains polyhedral? If the potential energy were like P' in figure 30, and if the entropy correction were insufficient to bring the free-energy diagram within P, then sharp

corners would remain. This seems to be the case for ionic crystals. Shuttleworth (1949) has calculated the potential energies per unit area of the (1, 1, 0) and (1, 0, 0) faces of a number of ionic crystals and finds that their ratio is always greater than 2. Thus it would require temperatures probably above the melting-point to give rounded edges. In the case of metals near their melting-point, it is probable that the free-energy diagram will be within P, therefore the edges will become rounded.

Appendix E. An outline of the matrix method of treating co-operative problems

Here we give a brief account of the mathematics leading to (93). The general methods are due to Montroll (1941), Kramers & Wannier (1941), Onsager (1944), Onsager & Kaufmann (1946) and Wannier (1945). We consider a chain of identical units, each capable of a range of states μ. Let the chain be $m+1$ units long, so that there are m bonds connecting them (figure 31). Let the state of the rth unit be μ_r. If the units are in given fixed states, each bond contributes $u(\mu_{r+1}, \mu_r)$ to the total energy of the chain, so that the total energy of the chain is

$$\epsilon_i = u(\mu_{m+1}, \mu_m) + u(\mu_m, \mu_{m-1}) + \ldots + u(\mu_2, \mu_1). \tag{E1}$$

Hence the partition function for the chain is

$$\begin{aligned} f_{m+1} &= \sum_i \exp(-\epsilon_i/kT) \\ &= \sum_{\mu_{m+1}} \sum_{\mu_m} \ldots \sum_{\mu_2} \sum_{\mu_1} V(\mu_{m+1}, \mu_m)\, V(\mu_m, \mu_{m-1}) \ldots V(\mu_2, \mu_1), \end{aligned} \tag{E2}$$

where

$$V(\mu, \mu') = \exp\{-u(\mu, \mu')/kT\}, \tag{E3}$$

and the summations in (E2) are carried out over all possible values of all the μ's. Since (E2) is in the form of a matrix product, (E3) can be regarded as a matrix, μ being a row index, and μ' a column index.

Figure 31

If we define

$$\Phi_{m+1}(\mu_{m+1}) = \sum_{\mu_m} \sum_{\mu_{m-1}} \ldots \sum_{\mu_1} V(\mu_{m+1}, \mu_m)\, V(\mu_m, \mu_{m-1}) \ldots V(\mu_2, \mu_1), \tag{E4}$$

we see from (E2) that

$$\Phi_{m+1}(\mu_{m+1}) = \sum_{\mu_m} V(\mu_{m+1}, \mu_m)\, \Phi_m(\mu_m). \tag{E5}$$

Φ_{m+1} may be called the partial partition function relative to the state μ_{m+1}, and we see that (E5) gives the effect on the partial partition function of a chain by the addition of another unit. The complete partition function f_{m+1} is of course given by

$$f_{m+1} = \sum_{\mu_{m+1}} \Phi_{m+1}(\mu_{m+1}). \tag{E6}$$

If the chain is very long, the ratios between the various components of Φ_{m+1} will be the same as those between the corresponding components of Φ_m, so that in the limit as m becomes very large we obtain

$$\Phi_{m+1}(\mu) = \lambda \Phi_m(\mu). \tag{E7}$$

Hence from (E 6) $$f_{m+1} = \lambda f_m, \tag{E 8}$$

so that λ must be the partition function per unit. Combining (E 5), (E 6) and (E 7) we are confronted by the following eigenvalue problem for λ:

$$\sum_{\mu'} V(\mu, \mu')\, \psi(\mu') = \lambda \psi(\mu), \tag{E 9}$$

which can be written in the contracted notation

$$(V, \psi)\,(\mu) = \lambda \psi(\mu). \tag{E 10}$$

By (E 3) the elements of V are all positive, and by (E 4) the components of ψ (i.e. the components of Φ) are all positive. This enables us to conclude by theorems due to Frobenius (1908, 1909) that λ is the largest eigenvalue of V. The results used here are that a matrix with positive elements has a largest eigenvalue which is simple and greater in absolute magnitude than any other eigenvalue, and that, moreover, the eigenvector belonging to it has components of only one sign. We may choose this sign to be positive. This eigenvector is the only one with this property.

E 1. *The one-dimensional, two-level case*

As a preliminary to the solution of our two-dimensional, two-level problem, we first find the V for the corresponding one-dimensional problem. In this problem the interaction energy between two neighbouring molecules is zero if they have the same level and $\frac{1}{2}\phi_1$ if not. We designate one of the possible levels by $\mu = +1$ and the other by $\mu = -1$. The 'interaction' energy between two neighbours can then be put in the form

$$u(\mu, \mu') = \frac{\phi_1}{2} \frac{1 - \mu\mu'}{2}, \tag{E 11}$$

which gives 0 if $\mu = \mu'$ and $\frac{1}{2}\phi_1$ otherwise. Hence from (E 3)

$$V(\mu, \mu') = \exp\{\tfrac{1}{2} H(\mu\mu' - 1)\}, \tag{E 12}$$

where $$H = \phi_1 / 2kT. \tag{E 13}$$

The operator V in (E 12) has the following effect on a general function (which we may interpret, if we please, as the partial partition function):

$$(V, \psi)\,(\mu) = \psi(\mu) + e^{-H} \psi(-\mu), \tag{E 14}$$

using the contracted notation. If we define an operator C by the equation

$$(C, \psi)\,(\mu) = \psi(-\mu), \tag{E 15}$$

we can write V as $$V = 1 + e^{-H} C, \tag{E 16}$$

using (E 14). From (E 15) $$C^2 = 1, \tag{E 17}$$

so C has the eigenvalues ± 1, showing that V has the eigenvalues $1 \pm e^{-H}$. The upper sign gives the largest eigenvalue, and hence the partition function per molecule.

In order to use these results in the treatment of the two-dimensional problem, we write V in the form $$V = A e^{\frac{1}{2}\bar{H} C}, \tag{E 18}$$

which is possible in view of (E 17), since we have, using (E 17) and (E 18),

$$V = A(\cosh \tfrac{1}{2}\bar{H} + C \sinh \tfrac{1}{2}\bar{H}).$$

Thus, from (E16), $$A^2 = 1 - e^{-2H} = 2e^{-H}\sinh H, \tag{E19}$$

$$\coth \tfrac{1}{2}\bar{H} = e^{H}. \tag{E20}$$

Hence $$V = (2e^{-H}\sinh H)^{\frac{1}{2}} \exp(\tfrac{1}{2}\bar{H}C), \tag{E21}$$

where H is given by (E20).

E2. *The two-dimensional, two-level case: rectangular lattice*

In order to treat the two-dimensional case we consider n parallel chains of the same type as before. We shall build up the two-dimensional lattice in two steps by the addition of complete columns of molecules. Thus our 'unit' is the column. In the first stage we include only the 'horizontal' bonds (left-hand, figure 32), and in the second stage we insert the 'vertical' bonds (right-hand, figure 32). We associate with the last element in each chain (the jth chain) the variable μ, which can take the values ± 1. A complete set of values assigned

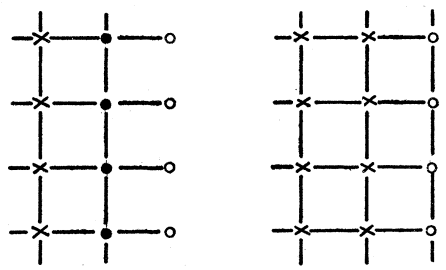

FIGURE 32

to the n variables describes a configuration $(\mu) = (\mu_1, \ldots, \mu_n)$ of the last column, which constitutes our unit in the sense of figure 31. Thus the operator which describes the addition of a new column with the horizontal bonds only is

$$V_1 = (2e^{-H}\sinh H)^{\frac{1}{2}n} \exp(\tfrac{1}{2}\bar{H}B) \tag{E22}$$

from (E21), where $$B = \sum_{j=1}^{n} C_j, \tag{E23}$$

and the individual operators C_j have the effect

$$(C_j, \psi)\,(\mu_1, \ldots, \mu_j, \ldots, \mu_n) = \psi(\mu_1, \ldots, -\mu_j, \ldots, \mu_n). \tag{E24}$$

We now wish to find the operator which represents the insertion of the vertical interactions, as in the right-hand figure (figure 32). The total energy corresponding to the inclusion of the vertical bonds will be

$$u(\mu_1, \ldots, \mu_n) = \sum_{j=1}^{n-1} \frac{\phi_2}{2}\left(\frac{1 - \mu_j\mu_{j+1}}{2}\right), \tag{E25}$$

where $\frac{1}{2}\phi_2$ is the strength of the vertical bond when it is not zero. We assume for generality that ϕ_1 and ϕ_2 are not necessarily equal. The effect of the interaction is to multiply the general term in the partial partition function, represented by one of the 2^n vector components $\psi(\mu_1, \ldots, \mu_n)$ by the appropriate factor

$$\exp\{-u(\mu_1, \ldots, \mu_n)/kT\}.$$

The corresponding operator is represented by a diagonal matrix. It can be constructed from the simple operators $S_1, \ldots, S_n$ which multiply ψ by the sign of its first, ..., nth argument as follows:

$$(S_j, \psi)\,(\mu_1, \ldots, \mu_j, \ldots, \mu_n) = \mu_j \psi(\mu_1, \ldots, \mu_j, \ldots, \mu_n), \tag{E 26}$$

$$A = \sum_{j=1}^{n-1} S_j S_{j+1}, \tag{E 27}$$

$$V_2 = \exp\{-\tfrac{1}{2}(n-1)\,H'\}\exp(\tfrac{1}{2}H'A), \tag{E 28}$$

where

$$H' = \phi_2/2kT.$$

Hence the operator associated with our problem is

$$V = V_2 V_1 = \exp(-\tfrac{1}{2}nH)\exp\{-\tfrac{1}{2}(n-1)\,H'\}\,(2\sinh H)^{\frac{1}{2}n}\exp(\tfrac{1}{2}H'A)\exp(\tfrac{1}{2}\bar{H}B). \tag{E 29}$$

The largest eigenvalue of V is then the partition function per column of the lattice, and its nth root is the partition function per molecule.

Onsager (1944) has shown that the largest eigenvalue λ_M of $\exp(H'A)\exp(\bar{H}B)$ is given by

$$2\ln\lambda_M = \gamma(2\pi/n) + \gamma(4\pi/n) + \ldots + \gamma(2\pi) + c, \tag{E 30}$$

where $|c| \leqslant H'$ and

$$\cosh\gamma(\omega) = \cosh 2H' \cosh 2\bar{H} - \sinh 2H' \sinh 2\bar{H}\cos\omega. \tag{E 31}$$

This leads to the conclusion that, in our case, the partition function per molecule λ is given by

$$\ln\lambda = -F/kT = \tfrac{1}{2}\ln(2\sinh H) - \tfrac{1}{2}(H+H') + \frac{1}{2\pi}\int_0^\pi \gamma(\omega)\,d\omega, \tag{E 32}$$

where

$$\cosh\gamma(\omega) = \cosh H' \operatorname{cosh}\bar{}\, H - \sinh H' \operatorname{sinh}\bar{}\, H \cos\omega \tag{E 33}$$

when $n \to \infty$. This result is exact, the effect of c disappearing by division with n and the summation converging to a definite integral.

In the special case of quadratic symmetry, $H = H'$, and these results reduce to

$$\cosh\gamma(\omega) = \cosh H \coth H - \cos\omega, \tag{E 34}$$

since it follows from (E 20) that

$$\sinh H \sinh\bar{H} = \cosh H \tanh\bar{H} = \cosh\bar{H}\tanh H = 1 \tag{E 35}$$

and

$$\ln\frac{\lambda e^H}{2\cosh H} = \frac{1}{2\pi}\int_0^\pi \ln\tfrac{1}{2}\{1+\sqrt{(1-k_1^2\sin^2\omega)}\}\,d\omega, \tag{E 36}$$

where

$$k_1 = (2\sinh H)/\cosh^2 H. \tag{E 37}$$

We cannot reduce (E 36) any further, but the potential energy per molecule U can be given in terms of the tabulated functions. We have

$$U = -\frac{\phi}{2}\frac{d}{d\bar{H}}(\ln\lambda), \tag{E 38}$$

which yields

$$S = 2U/\phi = -\frac{d}{dH}(\ln\lambda).$$

From (E 36), (E 37) and (E 38) we finally obtain

$$S = 1 - \frac{1}{2}\left(1 + \frac{2}{\pi} k_2 K_1\right) \coth H, \tag{E 39}$$

where
$$k_1^2 + k^2 = 1, \quad K_1 = K(k_1) = \int_0^{\frac{1}{2}\pi} (1 - k_1^2 \sin^2 \omega)^{-\frac{1}{2}} \, d\omega, \tag{E 40}$$

the latter integral being the complete elliptic integral of the first kind; formula (E 39) is the formula (93) in the text.

References

Andrews, M. R. 1927 *J. Phys. Chem.* **30**, 1947.
Becker, R. & Döring, W. 1935 *Ann. Phys., Lpz.*, **24**, 719.
Bethe, H. A. 1935 *Proc. Roy. Soc.* A, **150**, 552.
Bunn, C. W. 1949 *Disc. Faraday Soc.* no. 5, 132.
Burton, W. K. & Cabrera, N. 1949 *Disc. Faraday Soc.* no. 5, 33, 40.
Burton, W. K., Cabrera, N. & Frank, F. C. 1949 *Nature*, **163**, 398.
Centnerszwer, M. 1913 *Z. phys. Chem.* **85**, 99.
Frank, F. C. 1949 *Disc. Faraday Soc.* no. 5, 48, 67.
Frank, F. C. 1950 *Phil. Mag.* **41**, 200.
Frenkel, J. 1945 *J. Phys. U.S.S.R.* **9**, 392.
Frobenius, G. 1908 *S.B. preuss. Akad. Wiss.* **1**, 471.
Frobenius, G. 1909 *S.B. preuss. Akad. Wiss.* **2**, 514.
Gibbs, J. W. 1878 *Collected works*, 1928, p. 325, footnote. London: Longmans Green and Co.
Gillespie, L. J. & Fraser, L. H. D. 1936 *J. Amer. Chem. Soc.* **56**, 2260.
Griffin, L. J. 1950 *Phil. Mag.* **41**, 196.
Hertz, H. 1882 *Ann. Phys., Lpz.*, **17**, 193.
Humphreys-Owen, S. P. F. 1949 *Proc. Roy. Soc.* A, **197**, 218.
Knudsen, M. 1915 *Ann. Phys., Lpz.*, **47**, 697.
Kossel, W. 1927 *Nachr. Ges. Wiss. Göttingen*, p. 135.
Kramers, H. A. & Wannier, G. H. 1941 *Phys. Rev.* **60**, 252, 263.
von Laue, M. 1943 *Z. Kristallogr.* **105**, 124.
Mackenzie, J. K. 1950 Thesis, Bristol.
Miers, Sir H. A. 1903 *Proc. Roy. Soc.* **71**, 439.
Miers, Sir H. A. 1904 *Phil. Trans.* A, **202**, 459.
Montroll, E. W. 1941 *J. Chem. Phys.* **9**, 706.
Onsager, L. 1944 *Phys. Rev.* **65**, 117.
Onsager, L. & Kaufmann, B. 1946 *Report on Int. Conf. on Fundamental Particles and Low Temperatures, Cambridge*, 1946. Vol. 2, Physical Society. Low Temperatures, 1947.
Shuttleworth, R. 1949 *Proc. Phys. Soc.* A, **62**, 167.
Stranski, I. N. 1928 *Z. phys. Chem.* **136**, 259.
Stranski, I. N. & Kaischew, R. 1934 *Z. phys. Chem.* (B), **26**, 31.
Volmer, M. 1939 *Kinetik der Phasenbildung*. Dresden und Leipzig: Steinkopff.
Volmer, M. & Estermann, I. 1921 *Z. Phys.* **7**, 13.
Volmer, M. & Schultze, W. 1931 *Z. phys. Chem.* (A), **156**, 1.
Wannier, G. H. 1945 *Rev. Mod. Phys.* **17**, 50.
Wyllie, G. 1949 *Proc. Roy. Soc.* A, **197**, 383.

4

CABRERA N., CELLI V., GOODMAN F.O. AND MANSON R.
SCATTERING OF ATOMS BY SOLID SURFACES I.
SURFACE SCIENCE 19, 67 (1970).

SURFACE SCIENCE 19 (1970) 67–92 © North-Holland Publishing Co., Amsterdam

SCATTERING OF ATOMS BY SOLID SURFACES. I

N. CABRERA*†, V. CELLI*, F. O. GOODMAN** and R. MANSON*
University of Virginia, Charlottesville, Virginia 22903, U.S.A.

Received 1 May 1969

A quantum mechanical theory of the scattering of atoms by solid surfaces is presented. The theory is applied to a detailed discussion of elastic scattering (diffraction) processes, and the extension to inelastic scattering (phonon exchange) processes is discussed briefly. A great advantage of the theory is that scattering intensities of any size are easily handled; the moduli of the scattering matrix elements are not restricted to be small. If the results are expanded to lowest order in these moduli, then the "first order distorted wave Born approximation" is recovered. An example of the results obtained is that the intensity of the specularly scattered beam is by no means always larger than other diffracted intensities; this result is in agreement with experiments, and is a decided improvement over the usual first order treatments.

1. Introduction

The scattering of atoms by solid surfaces is by no means well understood, either experimentally or theoretically. If a sufficiently high level of understanding of this scattering could be reached, there is no doubt that atom–surface scattering could form a very useful tool indeed for studies of the properties of the single surface atomic layer of a solid. This is because, under normal conditions, incident atoms do not penetrate substantially beyond the first surface layer of a solid. These remarks are particularly true in view of the advent of controllable nearly-monoenergetic atomic beams[1–4]). As an example, such studies could be used to investigate surface phonon spectra of solids[5]). Low energy electron diffraction, while an exceedingly useful tool in its own right, does not yield much information concerning the *single* surface layer, because even electrons of quite low energy penetrate many solid surface layers.

For experiments of this nature to be useful, it is essential that a sufficiently good theory be available to interpret the results. It is clear that the *basis* of any complete theory of atom–surface scattering must be a quantum mechanical theory of inelastic scattering. However, the classical mechanical

* Department of Physics.
† On leave at the Escuela de Fisica y Matematicas, Instituto Politecnico, Unidad Profesional de Zacatenco, Mexico 14, D.F., Mexico.
** Department of Aerospace Engineering and Engineering Physics.

theory[6–9]) is in a considerably better state than is the quantum theory[10,11]). This situation is understandable because the classical theory can deal relatively easily, and perhaps correctly, with those large atom–surface energy and momentum transfers which are relevant to much recent research; examples are the drag forces on artificial earth-satellites and the efficiency of cryopumps. In quantum language, these transfers are results of "many-phonon" processes, which are not at all well understood. However, even one-phonon processes have not been adequately dealt with, although some theoretical progress has been made[10,11]). Perhaps the most remarkable statement which can be made in this context is that even *zero*-phonon processes (that is completely elastic diffraction processes) do not yet have an adequate theoretical interpretation.

Conventional quantum atom–surface elastic scattering theory, as used, for example, by Lennard-Jones and his coworkers[12]), is based on a first order distorted wave Born approximation. That this approach is inadequate for a useful description of experimental elastic scattering data is shown by the following remarks. This first order approximation is not valid if the total non-specular flux is large; that is, it is valid only if the specular beam contains considerably more flux than do all the other beams together. However, recent experimental data, for example those of Fisher and his coworkers[4]), show that the specular beam does not always contain the largest flux. Indeed, at least for not too glancing an incidence, the specular flux is usually *less* than the flux of even a *single* diffracted beam; in fact, the specular beam occasionally seems to vanish completely, even though first-order diffracted beams are at the same time readily visible.

The authors' view is that, before an adequate quantum theory of *inelastic* atom–surface scattering can be developed, an adequate *elastic* theory must be developed. Then, hopefully, many-phonon processes may be incorporated into the theory in a natural manner, starting perhaps with one-phonon processes. Eventually, it is hoped that the results of the classical theory may be obtained, by means of a limiting procedure, from the many-phonon quantum theory. The object of this paper is to present a new theory of elastic scattering which, it is hoped, will form the basis for the future work described above. The extension to inelastic scattering is discussed briefly.

2. Development of notation

The instantaneous potential energy of interaction of an atom (called the "gas atom") with a solid is denoted by $V(\boldsymbol{r}, \boldsymbol{u})$ where $\boldsymbol{r}$ is the position of the gas atom and $\boldsymbol{u}$ represents the displacements of all the solid atoms. The value of $V(\boldsymbol{r}, \boldsymbol{u})$ averaged over the thermal motions of the solid atoms is

denoted by $v(r)$, which is called the "thermally-averaged potential energy function"; this is written as follows:

$$v(r) = \langle V(r, u) \rangle . \tag{2.1}$$

It is the function $v(r)$ rather than $V(r, u)$ which is important in our elastic scattering theory; $V(r, u)$ becomes important in the inelastic scattering theory (see, for example, section 7).

Where k is the incident wave-vector, M is the mass, and $\Psi(r)$ is the wave-function of the gas atom, the Schrödinger equation is

$$(\nabla^2 + k^2 - 2Mv(r)/\hbar^2)\, \Psi(r) = 0. \tag{2.2}$$

The z-direction is chosen as the outward normal to the surface, and R is defined as the two-dimensional position-vector (x, y) of the gas atom parallel to the surface; that is,

$$r = (x, y, z) = (R, z). \tag{2.3}$$

The solid surface is assumed perfect in the usual sense; that is, the surface atoms are assumed to form a perfect, two-dimensional, infinite, periodic array. Incident atoms are assumed unable to penetrate beyond this surface layer under normal conditions. These assumptions result in a two-dimensional reciprocal lattice, each vector of which is parallel to the surface; the reciprocal lattice vectors are denoted by G, G'.

We define

$$v_G(z) = L^{-2} \int_{\text{surface}} v(r)\, e^{-iG \cdot R}\, d^2R, \tag{2.4}$$

where L^2 = surface area; the inverse of (2.4) is

$$v(r) = \sum_G v_G(z)\, e^{iG \cdot R}. \tag{2.5}$$

The convention is introduced that sums over reciprocal lattice vectors G are over all G, including $G=0$, unless otherwise indicated. The wave-function $\Psi(r)$ may be expanded as follows:

$$\Psi(r) = \sum_G \Psi_G(z)\, e^{i(K+G) \cdot R}, \tag{2.6}$$

where K is the component (k_x, k_y) of k parallel to the surface:

$$k = (k_x, k_y, k_z) = (K, k_z). \tag{2.7}$$

For future reference, we note that

$$k_z^2 = k^2 - K^2. \tag{2.8}$$

It is observed from the above definitions that a three-dimensional vector

is denoted by a lower case letter, for example $\boldsymbol{k}$. The corresponding two-dimensional vector, parallel to the surface, is denoted by the corresponding capital letter, for example $\boldsymbol{K}$; the z-component, perpendicular to the surface, is denoted by a subscript z, for example k_z. This notation is made explicit in (2.7). The only exception to this notation is the vector $\boldsymbol{r}$, the z-component of which is denoted simply by z; see (2.3). A reciprocal lattice vector, for example $\boldsymbol{G}$, has no three-dimensional counterpart in this theory.

Substitution of (2.5) and (2.6) into (2.2) gives

$$\sum_{\boldsymbol{G}} \left(\frac{\mathrm{d}^2 \Psi_{\boldsymbol{G}}}{\mathrm{d}z^2} + k_{\boldsymbol{G}z}^2 \, \Psi_{\boldsymbol{G}} - \frac{2M}{\hbar^2} \sum_{\boldsymbol{G}'} v_{\boldsymbol{G}-\boldsymbol{G}'} \, \Psi_{\boldsymbol{G}'} \right) \mathrm{e}^{\mathrm{i}\boldsymbol{G}\cdot\boldsymbol{R}} = 0 , \tag{2.9}$$

where $k_{\boldsymbol{G}z}$ is defined by analogy with (2.8):

$$k_{\boldsymbol{G}z}^2 = k^2 - (\boldsymbol{K} + \boldsymbol{G})^2 . \tag{2.10}$$

Thus we note from (2.8) and (2.10) that k_z and k_{0z} are identical.

Each term of the outer summation in (2.9) vanishes separately:

$$\left(\frac{\mathrm{d}^2}{\mathrm{d}z^2} + k_{\boldsymbol{G}z}^2 - \frac{2M}{\hbar^2} v_0 \right) \Psi_{\boldsymbol{G}} = \frac{2M}{\hbar^2} \sum_{\boldsymbol{G}' \neq \boldsymbol{G}} v_{\boldsymbol{G}-\boldsymbol{G}'} \, \Psi_{\boldsymbol{G}'} . \tag{2.11}$$

The interpretation of $v_0(z)$ follows from (2.4) with $\boldsymbol{G}=\boldsymbol{0}$; that is, $v_0(z)$ is the thermally-averaged potential energy function, $v(r)$, averaged over the directions x and y parallel to the surface. The potential $v_0(z)$ is associated with a complete set, $\phi_\alpha(z)$, of eigenstates. Greek subscripts α, β stand for both states of negative energy and states of positive energy; negative-energy states are denoted by subscripts m, n and positive-energy states by subscript q. The Schrödinger equation defining the $\phi_\alpha(z)$ is

$$\left(\frac{\mathrm{d}^2}{\mathrm{d}z^2} + \alpha^2 - \frac{2M}{\hbar^2} v_0(z) \right) \phi_\alpha(z) = 0 , \tag{2.12}$$

where

$$\alpha^2 \equiv q^2 \quad \text{if} \quad \alpha = q , \tag{2.13a}$$

and

$$\alpha^2 \equiv -k_n^2 \quad \text{if} \quad \alpha = n . \tag{2.13b}$$

With these definitions, the eigenvalue, E_α, of the energy of the state α is

$$E_\alpha = \hbar^2 \alpha^2 / 2M , \tag{2.14}$$

for both negative-energy states ($E_n \leqslant 0$) and positive-energy states ($E_q \geqslant 0$). Normalization of any state is by means of "box normalization", the cubic

box having side L, where $L\to\infty$:

$$\lim_{L\to\infty}\int_{-\frac{1}{2}L}^{\frac{1}{2}L}|\phi_\alpha(z)|^2\,\mathrm{d}z=1\,. \tag{2.15}$$

Hence, the positive-energy states may be called "continuum states", and the negative-energy states "bound states". The number of bound states is denoted by B.

It is convenient to choose the ϕ_α to be real. For q sufficiently small, the potential $v_0(z)$ gives rise to total reflection and the asymptotic forms of the $\phi_\alpha(|z|\to\infty)$ are:

$$\phi_n(|z|\to\infty)=0,\qquad \phi_q(z\to-\infty)=0\,, \tag{2.16a}$$

and

$$\phi_q(z\to\infty)=2L^{-\frac{1}{2}}\cos(qz+\xi_q)\,, \tag{2.16b}$$

where ξ_q is a (non-arbitrary) phase.

The energy of a bound state is E_n, but the *total* energy of an atom in the state is larger than E_n by an amount equal to the kinetic energy associated with its motion parallel to the surface. This total energy is denoted by E_{nG}, where

$$E_{nG}=E_n+\hbar^2(\mathbf{K}+\mathbf{G})^2/2M\,. \tag{2.17}$$

This energy need not be equal to the incident energy, denoted by E:

$$E=\hbar^2k^2/2M\,, \tag{2.18}$$

of the atom because the atom is in the bound state only temporarily. On the other hand, the total energy of the atom in a final diffracted state *is* equal to E. The term "diffracted state" is understood to include the specular state.

The following addition to the notation is made: reciprocal lattice vectors associated with final diffracted states may be denoted by $\mathbf{F}, \mathbf{F}'$; that is, $\mathbf{G}, \mathbf{G}'$ stand for *any* reciprocal lattice vectors, whereas $\mathbf{F}, \mathbf{F}'$ stand *only* for those linking the initial state to final diffracted states. The zero reciprocal lattice vector, which links the initial state to the specular state, is included as one of the $\mathbf{F}$. As with $\mathbf{G}$, sums over $\mathbf{F}$ are over all $\mathbf{F}$, including $\mathbf{F}=\mathbf{0}$, unless otherwise indicated explicitly. We note that $\mathbf{F}, \mathbf{F}'$ may be associated with bound states as well as with diffracted states, although energy cannot then be conserved in the bound states.

The final energy of an atom in a diffracted state, $\mathbf{F}$, is equal to its incident energy, E. The component of the final wave-vector of this atom parallel to the surface is $(\mathbf{K}+\mathbf{F})$, and it follows from (2.10) and (2.18) that k_{Fz} may be interpreted as the magnitude of the component normal to the surface.

Therefore, if, for a particular G, we obtain $k_{Gz}^2 \geqslant 0$ from (2.10), this G is associated with a diffracted state and $F \equiv G$; if, on the other hand, $k_{Gz}^2 < 0$, this G is not associated with a diffracted state and there is no F equal to G. Combining this result with (2.8) and (2.10), we obtain the condition for a diffracted state:

$$k_{Fz}^2 = k_z^2 - F^2 - 2\boldsymbol{K}\cdot\boldsymbol{F} \geqslant 0\,. \tag{2.19}$$

To simplify the notation slightly, we note that q in (2.16b) may stand for k_{Fz}, and that the following definitions may be made without ambiguity:

$$\phi_F \equiv \phi_q, \quad \xi_F \equiv \xi_q, \quad \text{etc.} \quad \text{if} \quad q = k_{Fz}\,. \tag{2.20}$$

For example, ξ_0 stands for ξ_q where $q = k_z = k_{0z}$.

3. Derivation of the scattering equations

3.1. General formalism

Ψ_G is expanded in terms of the ϕ_α as follows:

$$\Psi_G = \sum_\alpha c_{G\alpha}\,\phi_\alpha\,. \tag{3.1}$$

Substituting (3.1) into (2.11), we obtain

$$\sum_\alpha c_{G\alpha}(k_{Gz}^2 - \alpha^2)\,\phi_\alpha = (2M/\hbar^2)\sum_{G'\neq G}\sum_\alpha c_{G'\alpha}\,v_{G-G'}\,\phi_\alpha\,. \tag{3.2}$$

Multiplying both sides of (3.2) by $\phi_\beta^*\,(=\phi_\beta)$ and integrating over z in the usual manner, we obtain

$$c_{G\alpha}(k_{Gz}^2 - \alpha^2) = (2M/\hbar^2)\sum_{G'\neq G}\sum_\beta c_{G'\beta}(\beta\,|v_{G-G'}|\,\alpha)\,, \tag{3.3}$$

where the matrix element is defined by

$$(\beta\,|v_G|\,\alpha) = \lim_{L\to\infty}\int_{-\frac{1}{2}L}^{\frac{1}{2}L} \phi_\beta^*(z)\,v_G(z)\,\phi_\alpha(z)\,\mathrm{d}z\,. \tag{3.4}$$

Eq. (3.3) determines $c_{G\alpha}$ uniquely except where $\alpha = k_{Gz}$, when the ambiguity is resolved by demanding that $\Psi(\boldsymbol{r})$ describe an incoming plane wave of wave-vector $\boldsymbol{k}$ and outgoing scattered waves. We obtain

$$c_{G\alpha}\exp(-\mathrm{i}\xi_0) = \delta_{\alpha,0}\,\delta_{G,0} + (2M/\hbar^2)\,(k_{Gz}^2 - \alpha^2 + \mathrm{i}\varepsilon)^{-1}\,(G\,\alpha\,|t|\,0\,k_z)\,, \tag{3.5}$$

where $\varepsilon > 0$ and we ultimately take the limit as $\varepsilon \to 0$, and where $(G\,\alpha\,|t|\,0\,k_z)$ is a t-matrix[13]), defined by

$$(G\alpha\,|t|\,0\,k_z)\exp(\mathrm{i}\xi_0) = \sum_{G'\neq G}\sum_\beta c_{G'\beta}(\alpha\,|v_{G-G'}|\,\beta)\,. \tag{3.6}$$

Substitution of (3.5) into (3.1) yields the following formula for the Ψ_G:

$$\Psi_G \exp(-i\xi_0) = \phi_0\,\delta_{G,0} + \frac{2M}{\hbar^2}\sum_{\alpha}\frac{(G\,\alpha\,|t|\,0\,k_z)\,\phi_\alpha}{(k_{Gz}^2 - \alpha^2 + i\varepsilon)}, \tag{3.7}$$

where the equation for the t-matrix is obtained by substituting for $c_{G'\beta}$ in (3.6) from (3.5):

$$(G\,\alpha\,|t|\,0\,k_z) = (\alpha\,|v_G|\,k_z)(1-\delta_{G,0}) + \frac{2M}{\hbar^2}\sum_{G'\neq G}\sum_{\beta}\frac{(\alpha\,|v_{G-G'}|\,\beta)\,(G'\,\beta\,|t|\,0\,k_z)}{(k_{G'z}^2 - \beta^2 + i\varepsilon)}. \tag{3.8}$$

Let us consider the summation over continuum states in (3.7):

$$S_1 \equiv \sum_{q}\frac{(G\,q\,|t|\,0\,k_z)\,\phi_q}{(k_{Gz}^2 - q^2 + i\varepsilon)}. \tag{3.9}$$

It is shown in Appendix A that the following results may be considered as exact:

$$k_{Gz}^2 < 0: \quad S_1(z\to\infty) = 0, \tag{3.10a}$$

$$k_{Gz}^2 > 0: \quad S_1(z\to\infty) = -(iL^{\frac{1}{2}}/2k_{Fz})(F\,k_{Fz}\,|t|\,0\,k_z)\exp[i(k_{Fz}z + \xi_F)], \tag{3.10b}$$

where F is used instead of G to emphasize that $k_{Gz}^2 > 0$ implies that $G = F$ is associated with a final diffracted state; see (2.19). It follows that $\Psi_F(z\to\infty)$, which is the asymptotic form as $z\to\infty$ of the diffracted beam F, is given essentially by the t-matrix, defined by (3.6) and (3.8).

3.2. Further development of notation

We now introduce dimensionless quantities, in terms of which our results may be conveniently expressed. These quantities are written in terms of two parameters, an inverse-length parameter, denoted by a, and an energy parameter, denoted by D. For example, these two parameters could be (and will be later) Morse interaction potential parameters[14]). Keeping, where convenient, to the notation of Lennard-Jones and his coworkers[12]), the following definitions are made:

$$\mu_G \equiv k_{Gz}/a, \quad \mu_0 \equiv k_z/a, \quad \text{etc.}, \tag{3.11}$$

$$d^2 \equiv 2MD/\hbar^2 a^2, \tag{3.12}$$

and

$$\lambda_m^G \equiv 2M(E - E_{mG})/\hbar^2 a^2. \tag{3.13}$$

Dimensionless matrix elements are defined as follows for $G \neq G'$:

$$A_{GG'}^{GG'} = A_{FF'}^{FF'} = \frac{aL}{4(\mu_F \mu_{F'})^{\frac{1}{2}}} \frac{d^2}{D} (k_{Fz} | v_{F-F'} | k_{F'z}), \tag{3.14}$$

$$A_{Gm}^{GG'} = A_{Fm}^{FG'} = \frac{(aL)^{\frac{1}{2}}}{2\mu_F^{\frac{1}{2}}} \frac{d^2}{D} (k_{Fz} | v_{F-G'} | m), \tag{3.15}$$

$$A_{mG'}^{GG'} = A_{mF}^{GF} = \frac{(aL)^{\frac{1}{2}}}{2\mu_F^{\frac{1}{2}}} \frac{d^2}{D} (m | v_{G-F} | k_{Fz}), \tag{3.16}$$

and

$$A_{mn}^{GG'} = \frac{d^2}{D} (m | v_{G-G'} | n), \tag{3.17}$$

where a G or F subscript on A stands for state k_{Gz} or k_{Fz}. Dimensionless t-matrix elements are defined in a similar manner:

$$D_G^G = D_F^F = \frac{aL}{4(\mu_0 \mu_F)^{\frac{1}{2}}} \frac{d^2}{D} (F\, k_{Fz} | t | 0\, k_z) \tag{3.18}$$

and

$$D_G^m = \frac{\mathrm{i}(aL)^{\frac{1}{2}}}{2\lambda_m^G \mu_0^{\frac{1}{2}}} \frac{d^2}{D} (G\, m | t | 0\, k_z), \tag{3.19}$$

where a G or F superscript on D stands for state k_{Gz} or k_{Fz}. The asymptotic form as $z \to \infty$ of the wave-function is now written explicitly in terms of the dimensionless quantities D_G^α by use of (3.10):

$$L^{\frac{1}{2}}\, \Psi_0(z \to \infty) = \exp(-\mathrm{i}k_z z) + (1 - 2\mathrm{i}D_0^0) \exp[\mathrm{i}(k_z z + 2\xi_0)], \tag{3.20}$$

and

$$(L\mu_F/\mu_0)^{\frac{1}{2}}\, \Psi_F(z \to \infty) = -2\mathrm{i}\, D_F^F \exp[\mathrm{i}(k_{Fz} z + \xi_0 + \xi_F)]. \tag{3.21}$$

The part, $c_{Gm}\phi_m$, denoted here by Ψ_G^m, of Ψ_G associated with the bound state m may be written explicitly in terms of D_G^m:

$$(aL/\mu_0)^{\frac{1}{2}}\, \Psi_G^m(z) = -2\mathrm{i}\, D_G^m \phi_m(z) \exp(\mathrm{i}\xi_0). \tag{3.22}$$

3.3. Approximate scattering equations

In order to develop an approximate solution of the t-matrix eq. (3.8), we consider the summation over continuum states therein:

$$S_2 \equiv \sum_q \frac{(\alpha | v_{G-G'} | q)\, (G'\, q | t | 0\, k_z)}{(k_{G'z}^2 - q^2 + \mathrm{i}\varepsilon)}. \tag{3.23}$$

The work so far has been *exact*; for example, Ψ_G is given exactly by (3.1)

if (3.3) is solved for c_{Gz}, and (3.8) is the exact t-matrix equation. However, unlike the summation S_1 in (3.9), the summation S_2 cannot be done exactly, and some approximation is necessary. The approximation used here is discussed in Appendix B, and amounts to calculating S_2 by keeping only the imaginary part of $(k_{G'z}^2 - q^2 + i\varepsilon)^{-1}$, that is $-i\pi\delta(k_{G'z}^2 - q^2)$. The result is

$$k_{G'z}^2 < 0: \quad S_2 \simeq 0, \tag{3.24a}$$

$$k_{G'z}^2 > 0: \quad S_2 \simeq -(iL/4k_{Fz})(\alpha\,|v_{G-F}|\,k_{Fz})(F\,k_{Fz}\,|t|\,0\,k_z), \tag{3.24b}$$

where F is used instead of G' for the reason stated just after (3.10b). Using this approximation in (3.8), we obtain the following approximate t-matrix equation, written in terms of the D_G^α defined by (3.18) and (3.19):

$$i\,\lambda_\alpha^G\,D_G^\alpha = -A_{\alpha 0}^{G0}(1-\delta_{G,0}) + i\sum_{G'\neq G}\sum_\beta A_{\alpha\beta}^{GG'}\,D_{G'}^\beta, \tag{3.25}$$

where λ_G^G, as yet undefined, is defined for convenience by

$$\lambda_G^G = i. \tag{3.26}$$

In practice, the calculation would be restricted to a consideration of, say, R non-zero reciprocal lattice vectors and B bound states, resulting in, say, the specular beam plus N other diffracted beams. [R is even because reciprocal lattice vectors must be chosen in pairs. If G is chosen, then in order that $v(r)$ be real it follows from (2.5) that $-G$ must be chosen also; the reality of $v(r)$ is then assured because it follows from (2.4) that $v_G = v_{-G}^*$.] To proceed, it is convenient to reduce the number of equations in (3.25) by eliminating D_0^α from the set; we have

$$\lambda_\alpha^0\,D_0^\alpha = \sum_{G'\neq 0}\sum_\beta A_{\alpha\beta}^{0G'}\,D_{G'}^\beta. \tag{3.27}$$

Substituting (3.27) into the right hand side of (3.25) for $G \neq 0$, we obtain the following $(N+BR)$ simultaneous equations for the remaining $D_G^\beta (G \neq 0)$:

$$\sum_{G'\neq 0}\sum_\beta X_{\alpha\beta}^{GG'}\,D_{G'}^\beta = A_{\alpha 0}^{G0}\begin{cases} G = F = 1, 2, \ldots, N;\ \beta = G = F, \\ G = 1, 2, \ldots, R;\ \beta = m = 1, 2, \ldots, B, \end{cases} \tag{3.28}$$

where

$$X_{\alpha\beta}^{GG'} \equiv A_{\alpha 0}^{G0}\,A_{0\beta}^{0G'} + i\,A_{\alpha\beta}^{GG'} + i\sum_m A_{\alpha m}^{G0}\,A_{m\beta}^{0G'}/\lambda_m^0, \tag{3.29}$$

where the $A_{\alpha\beta}^{GG}$, which are as yet undefined, are defined for convenience as follows:

$$A_{\alpha\alpha}^{GG} = -\lambda_\alpha^G, \tag{3.30a}$$

and

$$A_{\alpha\beta}^{GG} = 0 \quad \text{if} \quad \alpha \neq \beta. \tag{3.30b}$$

We may note that, with these definitions, our approximate t-matrix equation (3.25) may be written

$$\mathrm{i}\sum_{G'}\sum_{\beta} A_{\alpha\beta}^{GG'} D_{G'}^{\beta} = A_{\alpha 0}^{G0}(1-\delta_{G,0}). \tag{3.31}$$

The $X_{\beta\alpha}^{GG}$, for example, are given by

$$X_{FF}^{GG} = |A_{F0}^{G0}|^2 + 1 + \mathrm{i}\sum_{m} |A_{Fm}^{G0}|^2/\lambda_m^0, \tag{3.32a}$$

$$X_{mm}^{GG} = |A_{m0}^{G0}|^2 - \mathrm{i}\lambda_m^G + \mathrm{i}\sum_{n} |A_{mn}^{G0}|^2/\lambda_m^0, \tag{3.32b}$$

$$X_{\alpha\beta}^{GG} = A_{\alpha 0}^{G0}\, A_{0\beta}^{0G} + \mathrm{i}\sum_{m} A_{\alpha m}^{G0}\, A_{m\beta}^{0G}/\lambda_m^0 \quad \text{if} \quad \alpha \neq \beta. \tag{3.32c}$$

In fact, it is almost always a good approximation to set $\lambda_m^0 = \infty$, when the disappearance of the last terms of X in (3.29) and (3.32) causes considerable simplification. Reasons for this are discussed further in section 4.3.

We may emphasize that D_0^0 and D_0^m, which appear, respectively, in the expression (3.20) for $\Psi_0(z\to\infty)$ and in (3.22) for $\Psi_0^m(z)$, are obtained in terms of the $D_G^\alpha(G\neq 0)$ in (3.28) from (3.27); that is,

$$D_0^0 = -\mathrm{i}\sum_{G\neq 0}\sum_{\alpha} A_{0\alpha}^{0G} D_G^\alpha, \tag{3.33}$$

and

$$D_0^m = \sum_{G\neq 0}\sum_{\alpha} A_{m\alpha}^{0G} D_G^\alpha/\lambda_m^0. \tag{3.34}$$

We note that D_0^m vanishes if $\lambda_m^0 = \infty$.

3.4. Intensities and unitarity

An "intensity", R_F, is defined for each of the outgoing (specular and diffracted) beams:

$$R_F \equiv (L\mu_F/\mu_0)\,|\Psi_F^+(z\to\infty)|^2, \tag{3.35}$$

where Ψ_F^+ denotes the outgoing part of Ψ_F; it follows from (3.20) and (3.21) that

$$R_F = |\delta_{F,0} - 2\mathrm{i}D_F^F|^2. \tag{3.36}$$

The intensities are defined so that

$$R_F = \frac{\text{flux of atoms in the diffracted beam } F}{\text{incident flux of atoms}}, \tag{3.37}$$

and it follows that the R_F must satisfy the relation

$$\sum_F R_F = 1. \tag{3.38}$$

The relation (3.38) corresponds to the unitarity condition of the t-matrix theory[13]); it is proved from the above work in Appendix C.

4. Application to some special cases

It is instructive and interesting to illustrate the results of section 3 by specializing them to cases in which only a small number, R, of non-zero reciprocal lattice vectors and a small number, B, of bound states are considered. This specialization implies also a small number, $N+1$, of outgoing beams, because $N \leqslant R$.

4.1. $R=0, B=0, N=0$

This is the simplest possible case, that of complete specular reflection; we obtain

$$L^{\ddagger}\,\Psi_0(z\to\infty) = \exp(-ik_z z) + \exp[i(k_z z + 2\xi_0)], \tag{4.1}$$

and

$$R_0 = 1\,. \tag{4.2}$$

4.2. $R=2, B=0, N=1$

Here we have just two reciprocal lattice vectors, one of which is linked to a diffracted beam, with no bound states

$$L^{\ddagger}\,\Psi_0(z\to\infty) = \exp(-ik_z z) + \exp(ik_z z)\left[\frac{1-|A_{F0}^{F0}|^2}{1+|A_{F0}^{F0}|^2}\right], \tag{4.3}$$

$$(L\mu_F/\mu_0)^{\ddagger}\,\Psi_F(z\to\infty) = -i\exp[i(k_{Fz}z + \xi_0 + \xi_F)]\left[\frac{2A_{F0}^{F0}}{1+|A_{F0}^{F0}|^2}\right], \tag{4.4}$$

$$R_F = 1 - R_0 = \left[\frac{2|A_{F0}^{F0}|}{1+|A_{F0}^{F0}|^2}\right]^2. \tag{4.5}$$

4.3. $R=2, B=1, N=0, \lambda_m^0=\infty$

The only outgoing beam is the specular beam, but passages through a single bound state are allowed by two reciprocal lattice vectors. The assumption that λ_m^0 is large results in considerable simplification, and is generally valid because it follows from (2.8), (2.17), (2.18) and (3.13) that

$$a^2\lambda_m^0 = k_z^2 - 2ME_m/\hbar^2\,. \tag{4.6}$$

Now $k_z^2 \geqslant 0$ and $E_m \leqslant 0$, and the only conditions under which λ_m^0 could be small are either very low incident energy or very glancing incidence (k_z^2 small) coupled with the existence of a bound state very near the top of the potential

well ($-E_m$ small).

$$L^{\frac{1}{2}}\,\Psi_0(z\to\infty) = \exp(-\mathrm{i}k_z z) + \exp[\mathrm{i}(k_z z + 2\xi_0)] \times \times \left[\frac{1 - \mathrm{i}\,|A_{m0}^{G0}|^2\,(1/\lambda_m^G + 1/\lambda_m^{-G})}{1 + \mathrm{i}\,|A_{m0}^{G0}|^2\,(1/\lambda_m^G + 1/\lambda_m^{-G})}\right], \tag{4.7}$$

$$(aL/\mu_0)^{\frac{1}{2}}\,\Psi_G^m(z) = \exp(\mathrm{i}\xi_0)\,\phi_m(z)\left[\frac{2A_{m0}^{G0}/\lambda_m^G}{1 + \mathrm{i}\,|A_{m0}^{G0}|^2\,(1/\lambda_m^G + 1/\lambda_m^{-G})}\right], \tag{4.8}$$

$$R_0 = 1\,. \tag{4.9}$$

We note that we cannot in general assume that λ_m^G or λ_m^{-G} is large as we did in (4.6) for λ_m^0. In fact, it follows from (3.13) that λ_m^G is a measure of how far the incident state is from resonance with a bound state m through the reciprocal lattice vector G; for example, $\lambda_m^G = 0$ at *exact* resonance. The result that λ_m^0 can never vanish follows from the fact that the incident state cannot resonate exactly with a bound state without participation of a non-zero reciprocal lattice vector.

4.4. $R = R'$, $\lambda_m^0 = \infty$

A general result for B bound states and $N(\leqslant R')$ diffracted beams can be written in simple form with the (severe) restriction that the R' non-zero reciprocal lattice vectors are chosen so that none can be written as a difference of two others. With this restriction, the second term of X in (3.29) is zero (there is no reciprocal lattice vector $G - G'$). As in the previous section, we set $\lambda_m^0 = \infty$ for simplicity, when only the first term of X in (3.29) remains

$$L^{\frac{1}{2}}\,\Psi_0(z\to\infty) = \exp(-\mathrm{i}k_z z) + \exp[\mathrm{i}(k_z z + 2\xi_0)]\,(2 - \Delta)/\Delta\,, \tag{4.10}$$

$$(L\mu_F/\mu_0)^{\frac{1}{2}}\,\Psi_F(z\to\infty) = -\,\mathrm{i}\exp[\mathrm{i}(k_{F_z} z + \xi_0 + \xi_F)]\,2A_{F0}^{F0}/\Delta\,, \tag{4.11}$$

and

$$(aL/\mu_0)^{\frac{1}{2}}\,\Psi_G^m(z) = \exp(\mathrm{i}\xi_0)\,\phi_m(z)\,2A_{m0}^{G0}/\lambda_m^G\Delta\,, \tag{4.12}$$

where

$$\Delta \equiv 1 + \sum_{F\neq 0} |A_{F0}^{F0}|^2 + \mathrm{i}\sum_{G\neq 0}\sum_m |A_{m0}^{G0}|^2/\lambda_m^G\,, \tag{4.13}$$

$$R_F = 4\,|A_{F0}^{F0}/\Delta|^2\,, \tag{4.14a}$$

$$R_0 = 1 - \sum_{F\neq 0} R_F\,. \tag{4.14b}$$

5. The thermally-averaged potential energy function

5.1. General considerations

Let us consider the details of the calculation of the thermally-averaged potential energy function, $v(r)$, from the instantaneous potential function,

$V(r, u)$, via (2.1). The function $V(r, u)$ is itself assumed to be obtained by a summation, over all atoms of the solid, of a pairwise potential energy function, denoted by $U(r-r_n-u_n)$, where r is the gas atom position, r_n is the equilibrium position of the solid atom n and u_n its displacement from equilibrium. Hence,

$$V(r, u) = \sum_n U(r - r_n - u_n). \tag{5.1}$$

We recall the notation (2.3) and similarly define

$$r_n = (R_n, z_n) \tag{5.2}$$

for the equilibrium positions and

$$p = (P, p_z) \tag{5.3}$$

for wave-vectors. We write

$$V(r, u) = (L/2\pi)^3 \sum_n \int U_p \exp[ip\cdot(r - r_n - u_n)]\, d^3p, \tag{5.4}$$

where

$$U_p \equiv L^{-3} \int U(r) \exp(-ip\cdot r)\, d^3r, \tag{5.5}$$

and integrals are understood to be between the limits $\pm\infty$ unless otherwise indicated. Therefore, the thermally-averaged value, $v(r)$, of $V(r, u)$ is given by

$$v(r) = (L/2\pi)^3 \sum_n \int U_p \exp[ip\cdot(r - r_n)] \langle \exp(-ip\cdot u_n)\rangle\, d^3p. \tag{5.6}$$

It is a well-known result that[15])

$$\langle \exp(ip\cdot u_n)\rangle = \exp\langle -\tfrac{1}{2}(p\cdot u_n)^2\rangle \equiv \exp[-W(n, p)], \tag{5.7}$$

where W is a Debye–Waller exponent:

$$W(n, P, p_z) \equiv \langle \tfrac{1}{2}(p\cdot u_n)^2\rangle \tag{5.8}$$

$$= \tfrac{1}{2}(p_x^2\langle u_{xn}^2\rangle + p_y^2\langle u_{yn}^2\rangle + p_z^2\langle u_{zn}^2\rangle). \tag{5.9}$$

From (2.3), (5.3), (5.6) and (5.7), we have

$$v(r) = (L/2\pi)^3 \sum_n \int d^2P\, dq \times$$
$$\times U_{P,q} \exp[iP\cdot(R - R_n)] \exp[iq(z - z_n)] \exp[-W(n, P, q)], \tag{5.10}$$

where q stands for the dummy variable p_z, and where both z_n and $W(n, p, q)$ are understood to be independent of n_x and n_y.

Using the result that

$$\sum_{n_x}\sum_{n_y}\exp(\mathrm{i}\boldsymbol{P}\cdot\boldsymbol{R}_n) = N_s(2\pi/L)^2\sum_{\boldsymbol{G}}\delta(\boldsymbol{P}-\boldsymbol{G}), \tag{5.11}$$

where N_s is the number of surface atoms, we obtain

$$v(\boldsymbol{r}) = N_s(L/2\pi)\sum_{\boldsymbol{G}}\exp(\mathrm{i}\boldsymbol{G}\cdot\boldsymbol{R})$$

$$\times\sum_{n_z}\int \mathrm{d}q\; U_{G,q}\exp(\mathrm{i}qz)\exp(-\mathrm{i}qz_n)\exp[-W(n,G,q)]. \tag{5.12}$$

From (2.5 and (5.12), we obtain

$$v_G(z) = (N_sL/2\pi)\int \exp(\mathrm{i}qz)\,U_{G,q}\sum_{n_z}\exp[-W(n,G,q)]\exp(-\mathrm{i}qz_n)\,\mathrm{d}q\,. \tag{5.13}$$

When $W=0$, v is to be interpreted as V:

$$V_G(z) = N_s(L/2\pi)\int \exp(\mathrm{i}qz)\,U_{G,q}\sum_{n_z}\exp(-\mathrm{i}qz_n)\,\mathrm{d}q\,. \tag{5.14}$$

If we define

$$V_{G,q} = L^{-1}\int V_G(z)\exp(-\mathrm{i}qz)\,\mathrm{d}z\,, \tag{5.15}$$

it follows from (5.14) that

$$V_{G,q} = N_sU_{G,q}\sum_{n_z}\exp(-\mathrm{i}qz_n). \tag{5.16}$$

For simplicity, we make the approximation that W is independent of n_z, replacing $W(n,G,q)$ by $W(G,q)$:

$$W(G,q) \equiv \tfrac{1}{2}(G^2\langle u_x^2\rangle + q^2\langle u_z^2\rangle), \tag{5.17}$$

where we have set

$$\langle u_{xn}^2\rangle = \langle u_{yn}^2\rangle = \langle u_x^2\rangle \quad \text{for all } n\,, \tag{5.18a}$$

and

$$\langle u_{zn}^2\rangle = \langle u_z^2\rangle \quad \text{for all } n\,. \tag{5.18b}$$

With the approximations (5.17) and (5.18), it follows from (5.13) and (5.16) that

$$v_G(z) = \exp(-\tfrac{1}{2}G^2\langle u_x^2\rangle)(L/2\pi)\int \exp(\mathrm{i}qz)\,V_{G,q}\exp(-\tfrac{1}{2}q^2\langle u_z^2\rangle)\,\mathrm{d}q\,. \tag{5.19}$$

Substituting for $V_{G,q}$ in (5.19) from (5.15) and carrying out the q-integration,

we obtain

$$v_G(z) = \frac{\exp(-\frac{1}{2}G^2\langle u_x^2\rangle)}{(2\pi\langle u_z^2\rangle)^{\frac{1}{2}}} \int V_G(z') \exp\left(-\frac{(z'-z)}{2\langle u_z^2\rangle}\right) dz' . \quad (5.20)$$

5.2. The Morse potential representation

We represent $V_0(z)$ by a Morse potential[14]), and $V_G(z)$ by the corresponding exponential repulsion if $G \neq 0$:

$$V_0(z) = D' \{\exp[2a(z'_m - z)] - 2\exp[a(z'_m - z)]\}, \quad (5.21)$$

$$V_G(z) = \kappa'_G D' \exp[2a(z'_m - z)] \quad \text{if } G \neq 0. \quad (5.22)$$

Let us consider the general term

$$V_G(z) = A\exp(-bz). \quad (5.23)$$

Inserting (5.23) into (5.20), we obtain

$$v_G(z) = \exp(-\tfrac{1}{2}G^2\langle u_x^2\rangle)\exp(\tfrac{1}{2}b^2\langle u_z^2\rangle)\, V_G(z). \quad (5.24)$$

Therefore, with the expressions (5.21) and (5.22), our thermally-averaged $v_0(z)$ remains a Morse potential, with the same a but with modified D and z_m; our thermally-averaged $v_G(z)$, for $G \neq 0$, remains an exponential repulsion, with modified κ_G, D and z_m:

$$v_0(z) = D\{\exp[2a(z_m - z)] - 2\exp[a(z_m - z)]\}. \quad (5.25)$$

and

$$v_G(z) = \kappa_G D \exp[2a(z_m - z)] \quad \text{for } G \neq 0, \quad (5.26)$$

where

$$\kappa_G \equiv \kappa'_G \exp(-\tfrac{1}{2}G^2\langle u_x^2\rangle), \quad (5.27)$$

$$D \equiv D' \exp(-a^2\langle u_z^2\rangle), \quad (5.28)$$

and

$$z_m \equiv z'_m + \tfrac{3}{2}a\langle u_z^2\rangle. \quad (5.29)$$

5.3. Eigenstates and matrix elements

With $v_0(z)$ given by the Morse potential (5.25), the eigenstates ϕ_n, defined by (2.12)–(2.16), are[16,17])

$$L^{\frac{1}{2}}\phi_q(z) = \left|\frac{\Gamma(\frac{1}{2} - d + i\mu)}{\Gamma(2i\mu)}\right| \zeta^{-\frac{1}{2}} W_{d,i\mu}(\zeta), \quad (5.30)$$

and

$$a^{-\frac{1}{2}}\phi_n(z) = \left[\frac{(2d-1-2n)\,n!}{(2d-1-n)\,!^3}\right]^{\frac{1}{2}} e^{-\frac{1}{2}\zeta}\zeta^{d-\frac{1}{2}-n} L_{2d-1-n}^{2d-1-2n}(\zeta), \quad (5.31)$$

where μ is defined to conform to the notation (3.11),

$$\mu = q/a\,, \tag{5.32}$$

ζ is defined by

$$\zeta = 2d\exp[a(z_m - z)]\,, \tag{5.33}$$

and where $W_{a,b}(\zeta)$ and $L_b^a(\zeta)$ are, respectively, the confluent hypergeometric function[16]) of ξ and the generalized Laguerre polynomial function[17]) of ζ. The eigenvalues, E_a, are given by (2.13) and (2.14) where k_n for a bound state is given by

$$k_n = a(d - \tfrac{1}{2} - n), \quad n = 0, 1, 2, \ldots \quad (n \leqslant d - \tfrac{1}{2}). \tag{5.34}$$

With the above representation of the potentials $v_G(z)$, the matrix elements (3.14)–(3.17) may be expressed as follows

$$\begin{aligned}\frac{A_{FF'}^{FF'}}{\kappa_{F-F'}} = \frac{\pi}{4}\frac{[\sinh(2\pi\mu_F)\sinh(2\pi\mu_{F'})]^{\frac{1}{2}}}{[\cosh(2\pi\mu_F) - \cosh(2\pi\mu_{F'})]} \times \\ \times\left[(\mu_F^2 - \mu_{F'}^2 + 2d)\left|\frac{\Gamma(\frac{1}{2} - d + i\mu_{F'})}{\Gamma(\frac{1}{2} - d + i\mu_F)}\right| + \right. \\ \left. + (\mu_F^2 - \mu_{F'}^2 - 2d)\left|\frac{\Gamma(\frac{1}{2} - d + i\mu_F)}{\Gamma(\frac{1}{2} - d + i\mu_{F'})}\right|\right],\end{aligned} \tag{5.35}$$

$$\begin{aligned}\frac{A_{Fm}^{FG}}{\kappa_{F-G}} = \frac{A_{mF}^{GF}}{\kappa_{G-F}} = \frac{\pi^{\frac{1}{2}}}{4}\left[\frac{(2d - 2m - 1)}{m!\,(2d - m - 1)\,!}\right]^{\frac{1}{2}} \times \\ \times\left[\frac{\sinh(2\pi\mu_F)}{\cosh(2\pi\mu_F) + \cos(2\pi d)}\right]^{\frac{1}{2}} \times \\ \times(\mu_F^2 + (d - \tfrac{1}{2} - m)^2 + 2d)\,|\Gamma(\tfrac{1}{2} + d + i\mu_F)|\,,\end{aligned} \tag{5.36}$$

$$\begin{aligned}\frac{A_{mn}^{GG'}}{\kappa_{G-G'}} = \frac{(-)^{m-n}}{4}\left[\frac{(2d - m - 1)\,!\,m!}{(2d - n - 1)\,!\,n!}(2d - 2m - 1)(2d - 2n - 1)\right]^{\frac{1}{2}} \times \\ \times[(m - n)(2d - m - n - 1) + 2d] \qquad \text{if } m \geqslant n\,.\end{aligned} \tag{5.37}$$

If $A_{mn}^{GG'}$ for $n > m$ is required, then m and n are interchanged in (5.37).

6. Discussion of the elastic scattering theory

6.1. Relationship to the distorted wave Born approximation

If the results of sections 3 and 4 are expanded to lowest order in the matrix elements, the first order (distorted wave Born approximation) results are

recovered. For example, from section 4.2 we obtain

$$R_0 \simeq 1 - 4X, \tag{6.1a}$$

and

$$R_F \simeq 4X, \tag{6.1b}$$

where

$$X \equiv |A_{F0}^{F0}|^2, \tag{6.2}$$

provided that $X \ll 1$. There is little difference between the first-order results (6.1) and our results (4.5) if $X \ll 1$, that is, if the matrix element modulus is "small"; of course, this is the motivation behind first order theory. The point here is that the present theory leads to sensible results no matter how large are the matrix element moduli.

For example, two particularly interesting results follow from (4.5): (i) for certain values of the matrix element A_{F0}^{F0}, the intensity of the specular beam is considerably less than that of the diffracted beam; indeed, if $|A_{F0}^{F0}| = 1$, the specular beam vanishes and all outgoing atoms pass into the diffracted beam: (ii) for *both* very small *and* very large values of $|A_{F0}^{F0}|$, the specular intensity approaches unity and, of course, has a minimum for intermediate $|A_{F0}^{F0}|$; for the special case (4.5), this minimum is zero, as observed in (i).

6.2. Resonances with bound states

A result of considerable importance concerns the case of "resonance" of the incident beam with a bound state; for $E = E_{mG}$ we obtain exact resonance, with $\lambda_m^G = 0$ from (3.13). It follows from the above results [for example, (4.13) and (4.14) and their generalizations] that, when exact resonance occurs, the intensity of the specular beam rises sharply, and that of each of the other beams falls. On the other hand, it has been known for some time that, experimentally, the intensity of the specular beam generally *falls* as resonance is approached[18,19]). This fall in the specular intensity is undoubtedly due to inelastic scattering of the gas beam, the probability of which is greatly increased if the gas atoms resonate into a bound state, because of the extra time they stay (while travelling over the surface in the bound state) in close proximity to the surface. The theory developed so far considers only elastic scattering, and all gas atoms are either specularly scattered or diffracted, independently of the time they spend in intermediate bound states. The above points regarding the effects of inelastic scattering are considered further in section 7.

6.3. Surface resonances

The phenomena which we call "surface resonances" are most easily discussed with reference to the actual forms, (5.35) and (5.36), of the matrix

elements. These resonances refer to the behavior of the diffraction as a diffracted beam just appears above, or just disappears below, the surface. (We note from (2.19) and (3.11) that a diffracted beam is allowed if $\mu_G^2>0$, and is not allowed if $\mu_G^2<0$.) This behavior depends critically on d, the parameter defined by (3.12) where, of course, a and D are now the Morse potential parameters; two extreme types of behavior are possible, with a gradually-varying spectrum in between. We restrict attention for the moment to the example in section 4.4.

The first, and simpler, extreme type of behavior occurs in general when d is not nearly half an odd integer, say when $d\simeq$integer. Then, $|A_{m0}^{G0}|^2/\lambda_m^G$ varies smoothly in general as μ_G^2 passes through zero, and $|A_{F0}^{F0}|^2\to$constant $\times\mu_F$ as $\mu_F^2\to 0+$. It follows from (4.13) and (4.14) that, as a diffracted beam, say F', disappears, the intensity $R_{F'}$ falls rapidly, but smoothly, to zero, all the other intensities $R_F(F\neq F')$ increasing rapidly, but smoothly, to pick up on new curves.

As d becomes closer to half an odd integer, the behaviors of the R_F become more complicated. If

$$d = n + \tfrac{1}{2} + \delta_n, \tag{6.3}$$

where $|\delta_n|$ is small, the relevant matrix elements have the following forms for small $|\mu_G^2|$ or μ_F^2:

$$\frac{|A_{F0}^{F0}|^2}{\kappa_F^2} = \frac{\mu_F}{(\delta_n^2+\mu_F^2)}\,X, \tag{6.4a}$$

and

$$\frac{|A_{n0}^{G0}|^2}{\kappa_G^2\lambda_n^G} = \frac{2\delta_n}{(\delta_n^2+\mu_G^2)}\,X, \tag{6.4b}$$

where

$$X \equiv \frac{\pi}{16}\coth(\pi\mu_0)\,\frac{(\mu_0^2+1+2n)^2}{n!^2}\,|\Gamma(n+1+i\mu_0)|^2, \tag{6.4c}$$

and where we note that the bound state n does not exist unless $\delta_n\geq 0$. At $\delta_n=0$ exactly, we obtain, again for small $|\mu_G^2|$ or μ_F^2:

$$|A_{F0}^{F0}|^2 \to \kappa_F^2 X/\mu_F \tag{6.5a}$$

and

$$|A_{n0}^{G0}|^2/\lambda_n^G \to 0. \tag{6.5b}$$

For this special extreme case ($d=$half an odd integer), nothing spectacular happens as one of the μ_G^2, say $\mu_{G'}^2$, increases through negative values to zero, but, for $\mu_{G'}^2=\mu_{F'}^2=0$, $|A_{F'0}^{F'0}|^2$ tends to infinity and R_0 jumps discontinuously to unity, all the $R_F(F\neq 0)$ dropping to zero. R_0 falls and $R_F(F\neq 0)$ rises as $|A_{F'0}^{F'0}|^2$ decreases through moderate values, and in fact R_0 then displays a

minimum, $R_{F'}$ displaying a corresponding maximum; for smaller values of $|A_{F'0}^{F'0}|^2$, R_0 increases rapidly to later pick up on a smooth curve, this increase being accompanied by a corresponding decrease of $R_{F'}$. If δ_n is not exactly zero, these results are somewhat modified, although the resonance phenomena persist provided that $|\delta_n|$ is not too large. Similar resonances as $\mu_G^2 \to 0$ have been discussed by McRae[10]) for the case of low energy electron diffraction.

Fig. 1 illustrates the behavior of the intensities as functions of $\mu_{G'}^2$ where

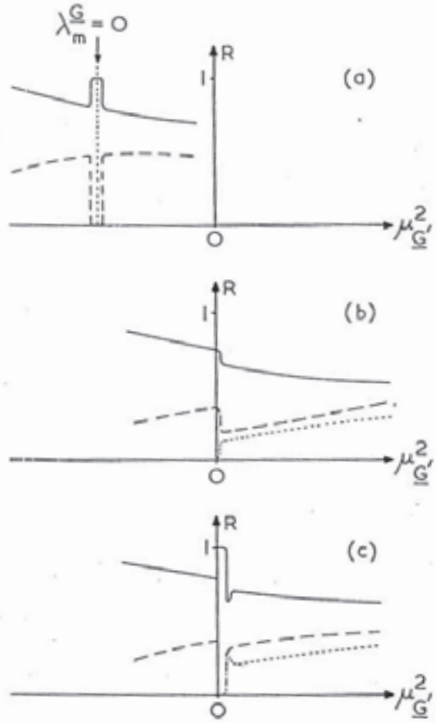

Fig. 1. The behavior of the intensities R_0(——), R_F(------) and $R_{F'}$(·····) as functions of $\mu^2{}_{G'}$ where some of the resonance phenomena, discussed in section 6, occur. (a) R_0 and R_F when a resonance with the bound state m occurs via the reciprocal lattice vector G for a special case of the type discussed in section 4.4. (b) R_0, $R_{F'}(F' = G')$ and $R_F(F \neq G')$ as the diffracted beam F' appears above the surface (at $\mu^2{}_{G'} = \mu^2{}_{F'} = 0$) when $d \simeq$ integer. (c) The same as (b) when $d =$ half an odd integer.

some of these resonance phenomena occur. Fig. 1a shows R_0 and R_F when a resonance with the bound state m occurs via the reciprocal lattice vector G for a special case of the type discussed in section 4.4. Fig. 1b describes R_0, $R_{F'}(F' = G')$ and $R_F(F \neq G')$ as the diffracted beam F' appears above the surface (at $\mu_{G'}^2 = \mu_{F'}^2 = 0$) for a case in which the "surface resonance" de-

scribed above does not occur (that is, $d \simeq$ integer, say). Fig. 1c illustrates the same case as does fig. 1b, except that now $d =$ half and odd integer exactly.

We note that these surface resonances, discussed here for $\mu_G^2 \to 0$, occur also when $\mu_0^2 \to 0$ that is, they occur as tangential incidence is approached. However, resonances of this type are not as important because the incidence must be too close to tangential to be feasible experimentally.

7. Extension to inelastic scattering

We consider in this section the effects of excitation and de-excitation of thermal vibrations in the solid by an impinging gas atom; the need to consider the thermal vibrations is already foreshadowed by our use of the thermally-averaged potential, v, in section 2. The formal theory is a direct generalization of that developed in sections 2 and 3, and many intermediate steps are omitted.

The wave-function, $\Psi(\boldsymbol{r}, \boldsymbol{u})$ may be expanded as follows:

$$\Psi(\boldsymbol{r}, \boldsymbol{u}) = \sum_{K', \alpha, \nu} c_{K', \alpha, \nu} \, \phi_\alpha(z) \, \mathrm{e}^{\mathrm{i}K' \cdot R} \, \Phi_\nu(\boldsymbol{u}), \tag{7.1}$$

where $\Phi_\nu(\boldsymbol{u})$ is a vibrational wave-function of the solid, ν runs over vibrational quantum numbers, and the sum over K' replaces that over G in (2.6). Of course, K' assumes all values and not just those $K+G$. We introduce a shorthand index, f or g, for all the quantum numbers K', α, ν; we use g in general, and f when we wish to stress that we are dealing with a final outgoing state (this notation parallels the F, G notation of section 3). The label 0 is reserved for the quantum numbers of the initial (or specular) state.

The analogue of (3.5) is

$$c_g \, \mathrm{e}^{-\mathrm{i}\xi_0} = \delta_{g,0} + (E_0 - E_g + \mathrm{i}\varepsilon)^{-1} \, t_{g0}, \tag{7.2}$$

where E_0 and E_g include the vibrational energies; the analogue of (3.6) is

$$t_{g0} \, \mathrm{e}^{\mathrm{i}\xi_0} = \sum_{g' \neq g} c_{g'} \, V_{gg'}. \tag{7.3}$$

Our t-matrix equation, the analogue of (3.8), is obtained by substituting for $c_{g'}$ in (7.3) from (7.2):

$$t_{g0} = V_{g0}(1 - \delta_{g,0}) + \sum_{g' \neq g} \frac{V_{gg'} t_{g'0}}{(E_0 - E_{g'} + \mathrm{i}\varepsilon)}. \tag{7.4}$$

The notation is further refined so that $g = b$ stands for a quantum number set associated with a bound state and $g = c$ with a continuum state; we note that f is always associated with a continuum state. Then, dimensionless quantities may be defined by direct analogy with (3.11)–(3.19) and (3.26).

Care must be taken over interpreting the definitions, some of which are presented here explicitly:

$$\mu_c \equiv k_{cz}/a, \quad \mu_f \equiv k_{fz}/a, \quad \text{etc.} \tag{7.5}$$

$$\lambda_b \equiv 2M(E_0 - E_b)/\hbar^2 a^2, \tag{7.6}$$

$$\lambda_c \equiv \mathrm{i}, \tag{7.7}$$

$$A_{cc'} \equiv \frac{aL}{4(\mu_c \mu_{c'})^{\frac{1}{2}}} \frac{d^2}{D} V_{cc'} \quad \text{for } c \neq c', \tag{7.8}$$

$$A_{cb} \equiv \frac{(aL)^{\frac{1}{2}}}{2\mu_c^{\frac{1}{2}}} \frac{d^2}{D} V_{cb}, \tag{7.9}$$

$$A_{bb'} \equiv \frac{d^2}{D} V_{bb'} \quad \text{for } b \neq b', \tag{7.10}$$

$$D_c \equiv \frac{aL}{4(\mu_0 \mu_c)^{\frac{1}{2}}} \frac{d^2}{D} t_{c0}, \tag{7.11}$$

and

$$D_b \equiv \frac{\mathrm{i}(aL)^{\frac{1}{2}}}{2\lambda_b \mu_0^{\frac{1}{2}}} \frac{d^2}{D} t_{b0}. \tag{7.12}$$

The final intensities have the same form as those (3.36):

$$R_f \equiv R_f(K_f, k_{fz}, v_f) = |\delta_{f,0} - 2\mathrm{i}\, D_f|^2. \tag{7.13}$$

The final quantum numbers are not arbitrary, but must satisfy the condition of energy conservation:

$$\hbar^2(K_f^2 + k_{fz}^2) + 2ME_{\mathrm{vib}}(v_f) = \hbar^2(K_0^2 + k_{0z}^2) + 2ME_{\mathrm{vib}}(v_0). \tag{7.14}$$

In the elastic treatment, the vibrational energy is unchanged and therefore disappears from (7.14), $K_f - K_0$ is equal to a reciprocal lattice vector, $\boldsymbol{F}$, and (7.14) reduces to (2.10). The initial and final vibrational states of the solid are not observed in experiments to date; we must, therefore, average (7.13) over initial phonon states and sum over final phonon states.

As in section 3, an approximate, but unitary, t-matrix may be obtained by keeping only the imaginary part of $(E_0 - E_{g'} + \mathrm{i}\varepsilon)^{-1}$, that is $-\mathrm{i}\pi\delta(E_0 - E_{g'})$, in the integral over continuum states in (7.4); in this way, the following analogue of (3.25) is obtained for all g:

$$\mathrm{i}\lambda_g D_g = -A_{g0}(1 - \delta_{g,0}) + \mathrm{i} \sum_{g' \neq g} A_{gg'} D_{g'}, \tag{7.15}$$

where we recall the definition (7.7).

In the case of elastic scattering, where the parallel momentum of the gas atom may change only by discrete amounts, the solution of (7.15) is straightforward, and some solutions are discussed in section 4. The case of inelastic scattering is more difficult since both the energy and momentum of the gas atom may change continuously over wide ranges of values. However, if we are willing to make the restriction that the gas atom exchanges only a single phonon with the solid, the solution of (7.15) is again straightforward. For example, if we consider a system with no diffraction and only "one-phonon beams", p, scattered around the specular beam, 0, the (unitary) dimensionless t-matrix, D_g, is given by the following set of equations:

$$D_0 = -\mathrm{i}\sum_p A_{0p}D_p, \tag{7.16a}$$

and

$$D_p = A_{p0}(1 - \mathrm{i}D_0), \tag{7.16b}$$

where $\sum_p$ implies summations over both K_p and v_p, and where v_p differs from v_0 only by the emission or absorption of a single phonon. From (7.13) and (7.16) it follows that the intensities are given by

$$R_0 = 1 - \sum_p R_p, \tag{7.17a}$$

and

$$R_p = \frac{4|A_{p0}|^2}{(1 + \sum_{p'} |A_{p'0}|^2)^2}. \tag{7.17b}$$

As a less trivial example, let us consider a system in which, in addition to undergoing inelastic processes, a gas atom may be diffracted into a bound state, b. With the one-phonon approximation, we obtain from (7.15)

$$\mathrm{i}D_0 = A_{0b}D_b + \sum_p A_{0p}D_p, \tag{7.18a}$$

$$-\mathrm{i}\lambda_b D_b = A_{b0}(1 - \mathrm{i}D_0) - \mathrm{i}\sum_p A_{bp}D_p, \tag{7.18b}$$

and

$$D_p = A_{p0}(1 - \mathrm{i}D_0) - \mathrm{i}A_{pb}D_b. \tag{7.18c}$$

The intensities, R_p, are found as usual by solving (7.18) for the D_p and substituting into (7.13).

These intensities, as well as those (7.17), must still be averaged over initial phonon states and summed over final phonon states; this has not yet been done. A reasonable approximation, which preserves unitarity, is to average separately each term in the numerators and denominators of the resulting expressions for the D_p. Then, diffraction matrix elements such as A_{b0} become matrix elements of the thermally-averaged potential defined by (2.1),

while averages of summations such as $\sum_p |A_{p0}|^2$ may be found using methods developed by Van Hove[21]). These averaging problems are not discussed further in this paper.

In order to obtain a simple qualitative picture of the effects of a bound state resonance on inelastic scattering, and in particular on the specular intensity, let us simplify (7.18) by assuming that, near the resonance, phonon exchange is important only when the gas atom is already in the bound state. With this simplification in mind, we set $A_{0p}=A_{p0}=0$ in (7.18) and derive from (7.13) that

$$R_0 = 1 - \sum_p R_p , \tag{7.19a}$$

and

$$R_p = \frac{4|A_{pb}A_{b0}|^2}{\lambda_b^2 + (|A_{b0}|^2 + \sum_{p'} |A_{p'b}|^2)^2} . \tag{7.19b}$$

Assuming that the matrix elements are sufficiently slowly-varying around the resonance, we obtain the important qualitative result that R_0 has a *minimum* and each R_p a maximum at exact resonance, when $\lambda_b=0$. This result should be contrasted with the corresponding results for elastic scattering in sections 3 and 4, in which R_0 has a *maximum* ($R_0=1$) at exact resonance. That the experimentally-observed minimum in R_0 at resonance[19, 18]), discussed in section 6.2, is a result of inelastic, rather than of elastic, scattering was suggested by Lennard-Jones and Devonshire[22]).

Acknowledgments

The authors wish to acknowledge several stimulating discussions on the subject of this paper with Dr. S. S. Fisher. The work was supported by the U.S. Air Force under Grant No. AFOSR-68-1569, and by the National Aeronautics and Space Administration under Grant No. NGR 47-005-046.

Appendix A. Evaluation of S_1 in (3.9)

In the limit of $L\to\infty$, (3.9) may be written as an integral:

$$S_1(z\to\infty) = \frac{L^{\frac{1}{2}}}{2\pi}\int_0^\infty \frac{(G\,q\,|t|\,0\,k_z)}{(k_{Gz}^2 - q^2 + i\varepsilon)}\left[e^{i(qz+\xi_q)} + e^{-i(qz+\xi_q)}\right] dq , \tag{A1}$$

where we have taken the limit as $z\to\infty$ and substituted for ϕ_q from (2.16b). The contours chosen for evaluation of these integrals are shown in fig. A1. Contour A is chosen for the first integral, and contour B for the second.

Then, for a very general t-matrix [that is, for a very general $v(r)$], the contributions to the integrals from those parts of the contours which do not lie on the real axis vanish in the limit of $z \to \infty$. For this to be rigorously true, it is sufficient that the t-matrix has no singularities on the positive real axis;

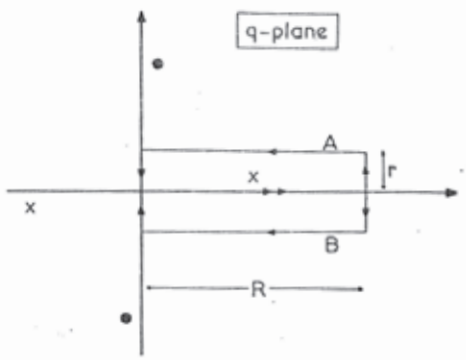

Fig. A1. Contours chosen for the integrals in (A1). The limits are $R \to \infty$ and $r > \varepsilon/2k_{Gz} \to 0$. (● poles for $k^2_{Gz} < 0$; × poles for $k_{Gz} > 0$).

this will be so for a physically realistic $v(r)$. The only contribution to the integrals, then, comes from the pole at $q = (k^2_{Gz} + i\varepsilon)^{\frac{1}{2}}$ when $k^2_{Gz} \geqslant 0$, and the result (3.10) is obtained.

Appendix B. Evaluation of S_2 (3.23)

In the limit of $L \to \infty$, (3.23) may be written as an integral:

$$S_2 = \frac{L}{2\pi} \int_0^\infty \frac{(\alpha \,|v_{G-G'}|\, q)\,(G'\, q\,|t|\, 0\, k_z)}{(k^2_{G'z} - q^2 + i\varepsilon)}\, dq\,, \tag{B1}$$

and the contour chosen for its evaluation is shown in fig. B1. It is assumed that the integral is equal to one-half of this contour integral, and that the only significant contribution to this contour integral is from the pole at $q = (k^2_{G'z} + i\varepsilon)^{\frac{1}{2}}$ when $k^2_{G'z} \geqslant 0$. The result (3.24) follows.

That this is only an approximation is clear, for example, from the fact that the contribution when $k^2_{G'z} < 0$ is ignored; this is equivalent to ignoring the beams which are "diffracted into the surface". The approximation is more serious, however, as singularities of both $(\alpha|v_{G-G'}|\, q)$ and $(G'\, q|t|\, 0\, k_z)$ in the upper half of the q-plane are ignored also.

The contributions when $k^2_{G'z}<0$ could easily be included in the above formalism; for simplicity, however, they are not considered further in this paper.

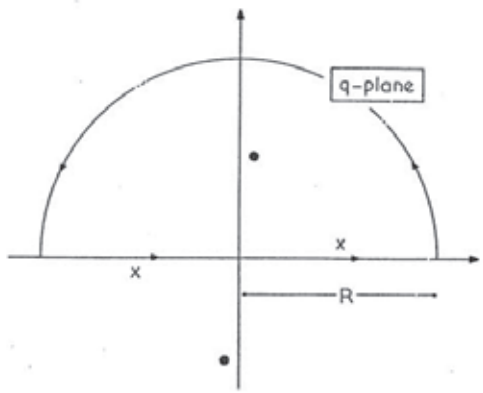

Fig. B1. Contour chosen for the integral in (B1). The limit is $R\to\infty$. (● poles for $k^2{}_{G'z}<0$; × poles for $k^2{}_{G'z}>0$).

Appendix C. Proof of unitarity (3.38)

In this appendix we use: (i) the convention of summation over repeated indices α and β and (ii) the convention that summations over F, G and G' do *not* include the zero reciprocal lattice vector.

Then, from (3.33), (3.36) and (3.38), we observe that we are required to prove that

$$2Z \equiv |1 - 2\sum_G A^{0G}_{0\alpha}\, D^{\alpha}_G|^2 - 1 + 4\sum_F |D^F_F|^2 = 0. \tag{C1}$$

We have

$$Z = -\sum_G (D^{\alpha^*}_G\, A^{G0}_{\alpha 0} + A^{0G}_{0\alpha}\, D^{\alpha}_G) + 2\sum_{G,\,G'} D^{\beta^*}_{G'}\, A^{G'0}_{\beta 0}\, A^{0G}_{0\alpha}\, D^{\alpha}_G + 2\sum_F |D^F_F|^2. \tag{C2}$$

It follows from (3.28) and (3.29) that we may define an X^G_α such that

$$X^G_\alpha = \sum_{G'} A^{G0}_{\alpha 0}\, A^{0G'}_{0\beta}\, D^{\beta}_{G'} + \mathrm{i}\sum_{G,\,G'\neq G} A^{GG'}_{\alpha\beta}\, D^{\beta}_{G'} + \mathrm{i} A^{GG}_{\alpha\beta}\, D^{\beta}_G + \mathrm{i}\sum_{m,\,G'} A^{G0}_{\alpha m}\, A^{0G'}_{m\beta}\, D^{\beta}_{G'}/\lambda^0_m - A^{G0}_{\alpha 0} = 0. \tag{C3}$$

Therefore,

$$0 = \sum_G (X^G_\alpha\, D^{\alpha^*}_G + X^{G^*}_\alpha\, D^{\alpha}_G)$$
$$= \sum_{G,\,G'} (D^{\alpha^*}_G\, A^{G0}_{\alpha 0}\, A^{0G'}_{0\beta}\, D^{\beta}_{G'} + D^{\beta^*}_{G'}\, A^{G'0}_{\beta 0}\, A^{0G}_{0\alpha}\, D^{\alpha}_G)$$

$$+ \mathrm{i} \sum_{G,\, G' \neq G} (D_G^{\alpha *} A_{\alpha\beta}^{GG'} D_{G'}^{\beta} - D_{G'}^{\beta *} A_{\beta\alpha}^{G'G} D_G^{\alpha})$$

$$+ \mathrm{i} \sum_{G} (D_G^{\alpha *} A_{\alpha\beta}^{GG} D_G^{\beta} - D_G^{\beta *} A_{\beta\alpha}^{GG *} D_G^{\alpha})$$

$$+ \mathrm{i} \sum_{m,\, G,\, G'} (D_G^{\alpha *} A_{\alpha m}^{G0} A_{m\beta}^{0G'} D_{G'}^{\beta} - D_{G'}^{\beta *} A_{\beta m}^{G'0} A_{m\alpha}^{0G} D_G^{\alpha}) / \lambda_m^0$$

$$- \sum_{G} (D_G^{\alpha *} A_{\alpha 0}^{G0} + A_{0\alpha}^{0G} D_G^{\alpha}) . \qquad \text{(C4)}$$

The two terms in the first summand are equal; the two pairs of terms in the second and fourth summands cancel; on account of (3.26) and (3.30), the only terms remaining in the third summand are those for which *both* $\alpha = \beta$ *and* $G = F$, when the two terms in the summand are equal. We are left with

$$0 = 2 \sum_{G,\, G'} D_G^{\alpha *} A_{\alpha 0}^{G0} A_{0\beta}^{0G'} D_{G'}^{\beta} + 2 \sum_{F} |D_F^F|^2$$

$$- \sum_{G} (D_G^{\alpha *} A_{\alpha 0}^{G0} + A_{0\alpha}^{0G} D_G^{\alpha}) = Z , \qquad \text{(C5)}$$

which completes the proof.

References

1) J. B. Anderson, R. P. Andres and J. B. Fenn, in: *Advances in Atomic and Molecular Physics*, Vol. 1 (Academic Press, New York, 1965) p. 345.
2) J. P. Moran, M.I.T. Fluid Dynamics Research Laboratory Report T 68-1 (Feb. 1968).
3) D. R. O'Keefe, U.T.I.A.S. Report No. 132 (July 1968).
4) S. S. Fisher, M. N. Bishara, A. R. Kuhlthau and J. E. Scott, Jr., in: *Rarefied Gas Dynamics*, Suppl. 5, Vol. 2 (Academic Press, New York, 1969) p. 1227.
5) N. Cabrera, V. Celli and R. Manson, Phys. Rev. Letters **22** (1969) 346.
6) L. Trilling, in: *Fundamentals of Gas-Surface Interactions* (Academic Press, New York, 1967) p. 392.
7) R. E. Stickney, in: *Advances in Atomic and Molecular Physics*, Vol. 3 (Academic Press, New York, 1967) p. 143.
8) F. O. Goodman, J. Chem. Phys. **50** (1969) 3855.
9) R. M. Logan, Surface Sci. **15** (1969) 387.
10) E. C. Beder, ref. 7, p. 205.
11) P. Feuer and C. Osburn, ref. 4, p. 1095.
12) See the references given on pp. 288 and 289 of ref. 10.
13) See, for example, T. Y. Wu and T. Ohmura, *Quantum Theory of Scattering* (Prentice-Hall, Englewood Cliffs, N.J., 1962).
14) P. Morse, Phys. Rev. **34** (1929) 57.
15) R. J. Glauber, Phys. Rev. **98** (1955) 1692.
16) C. Strachan, Proc. Roy. Soc. (London) A **150** (1935) 456.
17) J. E. Lennard-Jones and C. Strachan, Proc. Roy. Soc. (London) A **150** (1935) 442.
18) R. Frish and O. Stern, Z. Physik **84** (1933) 430.
19) J. E. Lennard-Jones and A. F. Devonshire, Nature **137** (1936) 1069.
20) E. G. McRae, J. Chem. Phys. **45** (1966) 3258.
21) L. Van Hove, Phys. Rev. **95** (1954) 249.
22) J. E. Lennard-Jones and A. F. Devonshire, Proc. Roy. Soc. (London) A **158** (1937) **253.**

Biografía de D. Nicolás Cabrera Sánchez

por *Sebastián Vieira Díaz*

El siglo veinte, éste siglo que concluye, deja a la humanidad en una situación compleja y fascinante a la vez: De una parte con un conocimiento y control, impensables hasta hace bien poco, de nuestro mundo a escala molecular y atómica, y de otra con una conciencia de su insignificancia a escala de los espacios y tiempos en los que se extiende el Universo. A lo largo de mi vida, creo haber constatado que la gente, en general, digiere los más importantes logros científicos y técnicos, con idéntica falta de capacidad de asombro como con la que participa en la naturaleza. A menudo, pasamos al lado, sin darles mayor importancia, de los hombres y mujeres que han contribuido, como escribía Marcel Proust, "a levantar parcialmente en nuestro honor, el velo de miseria y de insignificancia que nos deja indiferentes ante el universo". Entre estos seres singulares, yo tuve la fortuna de conocer y tratar, y de gozar del afecto y la confianza, de un hombre de una extrema sencillez y caballerosidad, pero ante todo, un hombre con una gran capacidad y pasión por la creación científica. Voy a hablarles de D. Nicolás Cabrera Sánchez.

¿Quién fue D. Nicolás Cabrera? El apellido Cabrera es, con justicia, el que con tanto cariño ponderan y valoran sus paisanos lanzaroteños en la figura histórica de D. Blas Cabrera y Felipe, físico notable y personalidad señera, cuyas contribuciones permanecen en el no muy poblado acervo de la ciencia española. Blas Cabrera se casó con María Sánchez Real, siendo Nicolás el más pequeño de sus tres hijos: Blas, Luis y Nicolás. El ambiente de su infancia fue de una singular pujanza creativa. Científicos, artistas y otros creadores, visitaban asiduamente su casa de Madrid, circunstancia que dejó en su memoria recuerdos imborrables como fue la visita de Alberto Einstein. Tenía Nicolás nueve años, cuando su padre invitó a Einstein a una reunión en su casa, a la que asistía también el guitarrista Andrés Segovia, quien tocó algunas composiciones en honor del ilustre visitante. Este, pidió un violín y tocó también, causando la admiración de la audiencia por su virtuosismo. Esta anécdota la contaba D. Nicolás con una sonrisa admirativa y nostálgica en los labios. Un niño que tenía la posibilidad de participar en ambientes como el descrito era, en principio, un niño afortunado. Por eso D. Nicolás fue siempre agradecido con su pasado, y,

especialmente, a la figura de su padre. Gustaba recordar sus antepasados isleños, que se remontaban según sus datos, a Luis Cabrera Rodríguez, vecino de Garachico (Tenerife), quien se trasladó a Teguise en Lanzarote hacia 1750. Aquí nacieron y vivieron tres generaciones de Cabreras, personalizadas en Lorenzo Cabrera López, nacido hacia 1770. Juan Antonio Cabrera del Castillo, nacido en 1807. y Blas Cabrera Topham, nacido en 1851. Este último fue el padre de Blas Cabrera y Felipe, quien se estableció en Madrid donde estudió y trabajó como científico. La biografía de este físico notable, su importancia en el contexto histórico en el que se desarrolló, ha sido objeto de numerosos estudios, hechos por personas capaces, que dedican su esfuerzo a la historia de la ciencia y la técnica en España. Entre estas se encuentran mis amigos Francisco González de Posada y José Manuel Sánchez Ron, quienes escudriñan aquellas décadas de la primera parte del siglo, cuando España parecía dejar su estado de postración científica, lo cual se vio frustrado por una guerra que tantas cosas asoló. D. Nicolás se lamentaba de este fracaso con la siguiente reflexión: "Es difícil imaginar una iniciativa que haya tenido tanto éxito en su evolución, que prometiera tanto para su futuro, y que desapareciera en un corto periodo después de la guerra civil". Creo que la mayoría de las personas que trataron a D. Nicolás, se pudieron percatar del enorme respeto que tenía a la obra de su padre, y de su deseo de tender un puente que la conectase con un resurgimiento científico, en el que él, su hijo, iba a jugar un papel crucial. Es emocionante, así al menos lo siento yo, comprobar como aquel respeto y admiración, no lo llevaban a perder su capacidad de ponderar la labor científica. Ponderación que, en su mente, se hacía tomando como referencia el nivel de la comunidad científica internacional, la única posible, a la que su padre había pertenecido. Refiriéndose a un libro editado con motivo del homenaje que la Universidad de Canarias organizó para conmemorar el centenario del nacimiento de Blas Cabrera, en el que se recogía una selección de las publicaciones de éste, escribía D. Nicolás: "También en dicho libro se reproducen algunos de sus trabajos, once de ciento cincuenta, que a juicio del comité organizador del homenaje pueden ser más interesantes, ya por su valor intrínseco o bien como un ejemplo de lo que puede hacerse en un ambiente de tan escasa tradición científica como era el nuestro." Como decía anteriormente, me emociona la sobriedad en el elogio a la contribución científica de su padre, y la referencia implícita, llena de admiración, a su esfuerzo y capacidad de lucha, cualidades que heredó y que se hicieron patentes en momentos cruciales de su carrera.

He querido resaltar, a lo largo de mi exposición anterior, aspectos, en mi opinión ineludibles para profundizar en la semblanza de Nicolás Cabrera, referentes a la influencia que sobre él ejerció su padre. Dicho esto, vamos a dejar caminar sólo a nuestro protagonista que, como espero quede patente para aquellos de ustedes poco familiarizados con su obra, acumuló a lo largo de su vida méritos sobrados como para ocupar, en solitario, el lugar distinguido que le corresponde.

En el título de mi conferencia se pone énfasis en dos aspectos de la vida profesional de D. Nicolás: el aspecto de físico creativo y el aspecto de organizador de la investigación y la docencia de la física en el nivel universitario. Dado que las circunstancias históricas primero, y su interés profesional después, lo llevaron a cambiar de trabajo y de país, varias veces a lo largo de su vida, es posible relacionar dichos cambios, con las diversas etapas científicas y académicas en las que se puede dividir su biografía.

Es baladí, quizá, señalar que una obra tan vasta como la éste científico, no puede ser expuesta, con una mínima profundidad, en el tiempo de ésta conferencia. Los historiadores, estoy seguro, harán dicho trabajo con la profesionalidad requerida, de forma que, una vez sobrepasada la distorsión de la proximidad temporal, aparezcan el personaje y su obra en la dimensión que les corresponde.

Voy a desglosar, en primer lugar, diversos aspectos de la actividad científica de D. Nicolás. Posteriormente me referiré a su actividad como organizador de la docencia universitaria y de la investigación.

La primera orientación de nuestro personaje fue hacia los estudios de historia, aunque finalmente se decantó hacia los de ciencias. Hizo un año de ingeniería, pasando a continuación a cursar la carrera de física en la Universidad de Madrid, obteniendo el título de licenciado en 1935, cuando contaba veintidós años. Se inició a la investigación en física experimental, en los laboratorios del Instituto de Física y Química, centro de prestigio internacional, creado y dirigido por su padre. La tarea que se propuso fue extender a las temperaturas del helio líquido, las medidas de susceptibilidad magnética de los compuestos de tierras raras que Salvador Velayos había descubierto en su tesis. Estas medidas eran muy importantes para hacer comparaciones con los cálculos teóricos del profesor de Harvard J.H. van Vleck. Aunque como fruto de la investigación publicó su primer artículo, con su padre y Velayos como coautores, la guerra acabó, al igual que con tantas otras cosas, con éste esfuerzo ilusionado. Yo he dedicado mi

actividad científica a la experimentación a bajas y muy bajas temperaturas, campo en el que me considero un pionero en nuestro país. Pienso, a veces, lo que aquella empresa tuvo de grande. En 1935 se habían planteado adquirir un sistema para producir helio líquido, sistema que poseían muy pocos laboratorios en el mundo. ¡Qué gran visión de futuro se requería para lanzarse en esa dirección! Como consecuencia de la guerra todo aquello se vino a pique, planteándose diversas opciones a los jóvenes científicos que trabajaban en el Instituto de Física y Química. Entre éstas se encontraba la disyuntiva de emigrar o de quedarse en España. D. Nicolás se fue y lo recordaba así: " Del grupo de jóvenes hubo los que se quedaron como Velayos y los que nos fuimos. Me he preguntado muchas veces cuál debería haber sido idealmente la actitud más apropiada. Desde el punto de vista de la Universidad española fue siempre evidente que Velayos y su grupo tenían razón. Si se podía contribuir a la formación de los futuros científicos españoles había que intentarlo. Por otro lado, también es verdad que en tanto que científicos debemos intentar contribuir al progreso de la Ciencia donde mejor podamos hacerlo. Combinar los dos objetivos es a veces imposible, de modo que cada uno debe de tomar sus responsabilidades de acuerdo con las circunstancias. “Esta reflexión resume, mejor que cualquier otro comentario, la postura de D. Nicolás en su compromiso con la creación científica.

La familia Cabrera llegó, como refugiada, a París en 1938. El joven Nicolás encontró trabajo en la Oficina Internacional de Pesos y medidas. Su estancia en París, que se extendió hasta 1952, iba a ser decisiva en su vida. Se casó con Carmen Navarro, también de familia exiliada. se doctoró en Física, y, a pesar de su habilidad para la física experimental, como reconocía Salvador Velayos, supervisor suyo en Madrid, orientó su investigación hacia la teoría. Su talento natural para los estudios teóricos encontró una especial satisfacción, en la lectura del libro de Dirac de mecánica cuántica. Esa lectura le produjo un notable impacto que él solía recordar, tal como yo pude comprobar en su última etapa madrileña. Su tesis doctoral, que consistió en un estudio teórico de las transiciones de fase termodinámicas, tuvo la supervisión de dos físicos reputados, como fueron Louis de Broglie y Leon Brillouin. Al mismo tiempo, en el laboratorio, se interesaba en el efecto que la oxidación de los metales tiene en la metrología. Ello le condujo a hacer experimentos para entender el proceso de oxidación del aluminio, experimentos que, tal como se refleja en su currículum, cubrieron un número importante de aspectos. Ello da idea de su tenacidad como científico, que una vez abordado el problema quiere

penetrar hasta el fondo en su solución. Estudió la influencia de la luz, del grado de humedad, y de la temperatura, en el proceso de oxidación. Preparó muestras en forma de películas delgadas y las caracterizó por diversos procedimientos. Publicó en francés doce artículos sobre éstos temas, entre los que voy a comentar uno, el segundo de la serie, publicado en 1945. Es una nota breve en la que Cabrera discute la importancia de diversos mecanismos en el proceso de oxidación. El entonces, ya prestigioso físico Neville Mott, había propuesto una teoría de la oxidación de los metales, en la que ésta era comandada por el paso de electrones libres del metal a la banda de conducción del óxido, entre las que hay una diferencia de energía Φ, seguido de la difusión hasta la superficie óxido-aire. Φ define la altura de una barrera de energía cuya anchura viene determinada por el espesor del óxido. Para anchuras pequeñas de la barrera, como sucede en las primeras etapas de la oxidación, y a bajas temperaturas, el mecanismo más eficaz es el túnel cuántico de los electrones a través de la barrera. La activación térmica es otro mecanismo importante, sobre todo a altas temperaturas, y para valores bajos de la barrera. Los resultados experimentales de Cabrera, le llevaron a proponer un nuevo mecanismo precursor de la oxidación, que denominó fotoeléctrico, según el cual los electrones pasaban la barrera mediante el efecto fotoeléctrico. Admitido éste mecanismo los resultados experimentales, se podían explicar adecuadamente. Este, y los otros artículos citados, atrajeron la atención de Mott, el cuál invitó a Cabrera para trabajar con él, en el H.H. Wills Physical laboratory de la Universidad de Bristol. Allí pasó Cabrera los tres años que consideraba los más fructíferos de su carrera científica. Antes de pasar a desglosar éste período, avancemos que la estancia en París configuró el campo de la física del sólido al que Cabrera dedicó su trabajo científico: La física de las superficies. La interacción de un sólido y su entorno, se produce en la interfaz fronteriza a ambos. Procesos de extrema importancia, como es, por ejemplo, el de la oxidación de los metales se desarrolla en éstas regiones. Cabrera fue un pionero y una de las figuras más relevantes en el nacimiento y desarrollo de ésta rama de la física. La invención, en la segunda mitad de éste siglo, de técnicas potentes, especialmente las de ultra alto vacío, ha permitido profundizar en el estudio de fenómenos que se producen en superficies muy bien caracterizadas. D. Nicolás, fue siempre un impulsor y un semillero de ideas, para los físicos experimentales que se dedicaron a éste tema de investigación. Volvamos ahora a Bristol, pues ya hablaremos de esto, posteriormente, con más detalle. La capacidad creativa de nuestro personaje encontró allí la pujanza científica y el ambiente

adecuado, para dar lo mejor que llevaba dentro. Hay muchos trabajos que sería interesante comentar, pero me voy a limitar a los dos que son, sin duda, las perlas de su currículum. El primero que versa sobre la oxidación de los metales, lo hizo en colaboración con su mentor Sir Nevill Mott (1). En él se presenta la primera teoría cuántica del crecimiento del óxido. El segundo, que trata del crecimiento de los cristales y los estados de equilibrio de sus superficies lo escribió con F.C.Frank y W. K. Burton (2). Se expone en él la primera teoría del crecimiento cristalino que considera la interacción entre el crecimiento y las dislocaciones en el cristal. En éste artículo se propone, también por vez primera, que la fusión de la superficie puede preceder a la del volumen, fenómeno que se conoce como la transición rugosa.

Dichos trabajos, que la lógica brevedad de ésta conferencia no permite comentar, siguen teniendo plena vigencia, lo que es fácilmente comprobable haciendo una búsqueda de las veces que son citados en otros artículos científicos. En mayo de 1997, y con motivo de la entrega, por parte de la Fundación General de la UAM, a la Facultad de Ciencias y al Instituto Universitario de Ciencia de Materiales "Nicolás Cabrera" de sendos retratos al carboncillo que el pintor gaditano Hernán Cortés hizo de nuestro personaje, pronuncié unas palabras glosando su figura. Para éste fin encargué al servicio de documentación de la UAM, una relación de las citas que los dos trabajos habían tenido durante los diez años anteriores. Estas superaban las mil quinientas. Ello, considerando que había transcurrido casi medio siglo desde su publicación, es lo suficientemente significativo para mostrar la trascendencia científica de la obra de D. Nicolás. Obra sólida y bien construida, cuya permanencia le da una proximidad que ahuyenta a los alabadores de reliquias. Para expresar su solidez, yo sacaba a colación en mis palabras citadas, el motivo de una diapositiva que un ilustre profesor de mi universidad solía poner en sus charlas comentando obras perdurables. Era una señal de tráfico en la que se leía el siguiente aviso: "Camiones por el puente romano". Eso es lo que reflejan las citas. Hoy día en que llegan a todo el mundo, habida cuenta de la capacidad de difusión que se ha creado en nuestra sociedad, tal cantidad de opiniones vacuas, reiterativas, sin ningún tipo de contenido, cualquiera se puede percatar de lo difícil que es la permanencia. Eso pasa también en el mundo de la ciencia. Las revistas crecen almacenando experimentos y teorías que nadie considera. En la hemeroteca de mi departamento alguien puso, con gran sentido del humor, un cartel en el que se recogía una frase atribuida a Pauling, referida al crecimiento a lo largo de las estanterías de una revista determinada. Decía:

"En su crecimiento avanza por las estanterías a una velocidad superior a la de la luz, pero ello no contradice la teoría de la relatividad, porque no lleva información alguna." Como debe quedar claro no es éste el caso de la obra de D. Nicolás.

Sus trabajos de Bristol, hicieron que diversas instituciones se interesasen por los servicios de éste científico en plena madurez creativa. En 1952, aceptó una oferta de la Universidad de Virginia en Charlottesville, en los Estados Unidos. Los últimos meses de su estancia europea, los pasó en su laboratorio de París trabajando sobre las propiedades ópticas de capas múltiples alternadas. Habían nacido ya, sus hijos Blas y Cristina. No debe ser fácil dejar París, pero Cabrera era un hombre decidido. Sabía que en Estados Unidos sus posibilidades como científico eran muy superiores. Era consciente de su valía personal, y sabedor de que en aquel país, y en aquellos momentos, esa era su principal carta de presentación. Recuerdo que a él le sublevaba la aspiración, en el caso de la gente joven, de apalancarse cuanto antes en un puesto permanente. Consideraba que ello esterilizaba el empuje de la fuerza creativa cortando las alas de la creación. Sin duda, él era un buen ejemplo de lo acertado de su propio punto de vista. En Virginia, donde tuvo a su hija Carmen, permanecería hasta 1968. Allí encontró un ambiente que, estoy convencido, siempre había añorado. el ambiente universitario. D. Nicolás no era partidario de que los laboratorios y departamentos de investigación, estuviesen alejados de las aulas. Cuando hablaba, tras su vuelta a España, del Instituto Nacional de Física y Química del que su padre fue director, opinaba que "había sido un error no construir el Instituto en la Ciudad Universitaria de modo que la docencia y la investigación se mantenga como unidad, al estilo americano". Lamento no poder exponer aquí, por falta de tiempo, la actitud de D. Nicolás ante la docencia universitaria, y la enorme importancia que concedía a esa actividad, como acicate de la creación científica, ya que son sus logros más importantes en investigación durante la etapa americana lo que ahora me ocupa. Su contrato inicial fue de Associate Professor, pasando a Full Professor en 1954. En 1962 fue nombrado Director del Departamento de Física, puesto en el que pudo desarrollar su especial talento como organizador. Dirigió tesis doctorales a jóvenes que luego llegaron a ser científicos de primera fila, y que mantuvieron hacia él, como yo he podido comprobar, una actitud de admiración y respeto científico y humano, durante toda su existencia. Puestos a elegir, hay dos trabajos de ésta época que resumen lo más relevante de sus investigaciones. El primero, "Motion of a Frenkel-.ontorova dislocation in a one dimensional crystal", engarza

con su investigación en Bristol, y lo hizo en colaboración con Atkinson. El segundo "Theory of surface scattering and detection of surface phonons" (3), escrito en colaboración con V.Celli y R. Manson, significa la piedra angular de lo que iba a ser su mayor interés científico al final de su carrera. La utilización de la dispersión de átomos neutros por las superficies como método para obtener información sobre las propiedades vibracionales de ésta, prometía ser una herramienta de gran importancia. Como he comentado anteriormente, el desarrollo de las técnicas de ultraalto vacío, permitía obtener y caracterizar superficies cristalinas adecuadas, como para pensar en confirmar experimentalmente las teorías elaboradas por Cabrera y colaboradores. La física de la superficie, aparecía como algo en la que el objeto de la investigación, la superficie, adquiría con los nuevos métodos el perfil de los átomos, de sus ordenamientos y reconstrucciones, a los cuales se podía acceder con sondas adecuadas. Temas de importancia extrema estaban ahí esperando. D. Nicolás se trajo con ilusión a España, tras su vuelta en 1969, ésta línea de investigación como tema a desarrollar bajo su supervisión directa. En Virginia, Cabrera hizo una notable labor. Las responsabilidades que adquirió para hacer un buen departamento universitario de física, lo convencieron, posiblemente, de su capacidad para la tarea de organización y gestión. Sus contactos con colegas hispanoamericanos y españoles habían sido permanentes, y en él crecía la idea de ser útil impulsando la actividad científica en países como México o Venezuela. No podía, como persona agradecida que era, olvidar la acogida generosa que la Universidad Nacional Autónoma de México, dio a su padre en 1941. Al mismo tiempo, sus pensamientos estaban en España. Su padre había ocupado un lugar destacado en un esfuerzo que se había visto truncado por una guerra. La prostración científica de España había llegado a extremos impensables para aquellas generaciones, durante las décadas de los cuarenta y cincuenta. Los años sesenta, durante los que tantas cosas se movieron en Europa, también iban a traer aires nuevos a la universidad española. Gente joven y entusiasta, eligieron para su formación centros prestigiosos allende nuestras fronteras, en Europa y en Estados Unidos. En el Centro Europeo de Investigaciones Nucleares, se creaba un buen ambiente para físicos brillantes. D. Nicolás debía soñar en esos tiempos que, quizá él, podía, en el terreno de la física, contribuir a rehacer, y de forma irreversible, lo que su padre había comenzado. Como dije antes, valoraba de una forma singular, el esfuerzo de su padre " como un ejemplo- escribía- de lo que puede hacerse en un ambiente de tan escasa tradición científica como era el nuestro". Elegiría, como veremos, dedicar su última etapa profesional a un esfuerzo parecido al de su progenitor.

Si importante fue su labor organizativa en Virginia, más aún fue, posiblemente, la que hizo en Madrid. Pero, no quememos etapas y concluyamos primero lo referente a su carrera como investigador. D. Nicolás llega a la Universidad Autónoma de Madrid, UAM, en 1969, manteniendo su puesto de catedrático en Virginia hasta mayo de 1974. Por lo tanto, durante este primer período, el más importante por la cantidad de sucedidos con interés, su relación con la universidad americana fue muy intensa. Ello se refleja en su curriculum, en el que aparecen artículos de estos años firmados con sus colaboradores de allí. Aunque enviado a publicar en mayo de 1969, apareció en 1970 un artículo extenso y de gran importancia bajo el título de "Scattering of atoms by solid surfaces"(4), con la autoría de N.Cabrera, V. Celli, F.O. Goodman y R. Manson. Se expone en él una teoría mecanocuántica de la dispersión elástica de átomos por superficies sólidas, y se discute con brevedad la extensión de la teoría a procesos de dispersión inelástica, es decir, con intercambio de excitaciones de la superficie, los fonones de la superficie.

En aquellos comienzos madrileños Cabrera tuvo un colaborador muy activo, Javier Solana, que procedía de Virginia, donde había hecho el doctorado, en teoría de la materia condensada, en problemas relacionados con unas excitaciones muy interesantes del helio superfluido. Javier colaboró con D. Nicolás, y lo ayudó a entender diversos aspectos de los entresijos de la sociedad española de la época. No es posible olvidar, en éste último aspecto, a Antonio Trueba, que puso, con sacrificada ilusión, todo su esfuerzo, y su tiempo, en labores, no por menos vistosas, menos importantes. Sin embargo, su principal colaborador científico hasta su jubilación, fue Nicolás García, entonces joven impulsivo, que profesó siempre un respetuoso y admirativo cariño hacia la persona de Cabrera. Ambos publicaron en 1978 un artículo de gran interés, en el que se presentaba un método para resolver la dispersión de ondas por una superficie periódica dura. En los últimos años de su vida académica, D. Nicolás tuvo la satisfacción de ver publicado un artículo, en el que se mostraba la primera observación experimental directa de la transición de fase rugosa, en cristales de helio en equilibrio con el helio líquido superfluido. ¡Casi cuarenta años después de que Cabrera hubiese hecho la predicción teórica de éste tipo de transición! Voy a concluir este apartado sobre la carrera investigadora de D. Nicolás Cabrera, con unas frases que escribió el Prof. M.J.Yacamán de la Universidad Autónoma de México, en un artículo sobre la influencia de Cabrera en la ciencia iberoamericana, publicado en un libro homenaje a nuestro personaje. Escribía: "Yo siempre

recuerdo a D. Nicolás como un gran hombre en todos los respectos, con una tremenda intuición para la ciencia, un gran espíritu humano, y una personalidad afable con un gran sentido del humor. Espero que los trabajos presentados en este volumen representen un pequeño tributo a la figura de uno de los científicos iberoamericanos más grandes de todos los tiempos".

Voy a pasar a continuación a exponer algunos de los aspectos más destacables, en mi opinión, de la actividad de D. Nicolás como organizador de la docencia universitaria y de la investigación. Y hablo conjuntamente de docencia e investigación, porque para él ambas cosas debían estar íntimamente relacionadas. Yo lo he oído decir, que todo buen profesor tiene que ser buen investigador, aunque no todo buen investigador haya de ser buen profesor. Cuando Cabrera llegó a Virginia en 1952, llegó como miembro de un pequeño departamento de física, con solo cinco profesores, con el cometido de comenzar investigaciones en el campo de la física del estado sólido. Es posible hacerse una idea clara del ambiente universitario que se encontró Cabrera. Ese ambiente tuvo la suerte de ser inmortalizado por uno de los escritores más geniales de nuestro siglo: Vladimir Nabokov. De la mano de un modesto profesor emigrado, Timofey Pnin, podemos sumergirnos en la vida diaria de una universidad americana de tipo medio, de principios de los años cincuenta. Pronto obtuvo, D. Nicolás, reconocimientos por su labor investigadora y de formación, siendo doctorandos suyos de aquellos tiempos R.V. Coleman y P.B. Price, que han hecho en su carrera excelentes contribuciones a la física de la materia condensada. Se le nombró miembro de varios comités asesores de organismos con decisión en la política científica, y de centros nacionales de investigación. En 1962 fue nombrado jefe del departamento de física. Bajo su dirección el departamento de Virginia, llegó a ser un centro de primera categoría en investigación. El número de sus profesores creció hasta treinta, creciendo también de forma espectacular el número de licenciados, alrededor de cien, que se iniciaban en la investigación. Potenció el crecimiento de otras ramas de la física como la física nuclear y la física de bajas temperaturas. Su labor organizativa y su magisterio no se limitaron a Virginia. Su cariño hacia México y Venezuela, lo llevó a esforzarse en ayudar a investigadores y estudiantes de éstos países, para promover en ellos un mayor desarrollo científico. A México viajaba con frecuencia. Allí vivían su madre y su hermano Blas. D. Nicolás, según cuenta su hijo, viajó por vez primera a México en coche con toda la familia, en 1953. En aquél entonces, no existía el entramado de autopistas que existe actualmente, por lo que emplearon catorce días en el viaje, durante cada uno de los cuales D.

Nicolás estaba ocho horas al volante. Es posible, gracias a Nabokov también, recrear la dureza de los largos viajes a través de las carreteras y moteles estadounidenses, siguiendo la apasionada huida, u año antes, de Humbert Humbert con si nínfula. Desde ese primer viaje a México, las visitas de D. Nicolás se repitieron con frecuencia, dado que allí vivía una parte muy importante de su familia y allí se encontraban, también, colegas que habían ayudado y recibido, a su vez, el magisterio de su padre, durante los cuatro años que éste trabajó, hasta su fallecimiento en 1945, en el Instituto de Física y en la Facultad de Ciencias de la UNAM. La influencia que nuestro Cabrera tuvo en la física mejicana se pondera, de una manera muy cariñosa, en el artículo del Prof. Yacamán que cité anteriormente. Sus primeros contactos fueron con los profesores Manuel Sandoval Vallarta y Marcos Moshinsky, que habían sido estudiantes de Blas en los primeros cursos de física moderna que se dieron en la UNAM. A partir de entonces, además de las repetidas visitas de D. Nicolás, existió también, por su parte, un interés grande en apoyar las estancias de estudiantes mexicanos en la universidad de Virginia. En el transcurso del tiempo llegamos a 1967, año en el que Cabrera dio un curso de termodinámica de los sólidos en el Instituto Nacional Politécnico de México, dentro de la Escuela Latinoamericana de Física. Sus estudiantes, entre los que se encontraba Yacamán, se sintieron motivados y también sorprendidos. En palabras de éste: "Durante el curso dio unas clases excelentes que fueron grabadas por algunos estudiantes y distribuidas posteriormente entre los científicos del estado sólido. Estas notas fueron para la mayoría de los asistentes al curso, el primer contacto con la física de las superficies." También es interesante destacar los comentarios sobre la actitud de D. Nicolás hacia los estudiantes: "Comenzó su curso, -comenta Yacamán,- de una forma muy general alcanzando luego una gran profundidad. Con un respeto extraordinario a la inteligencia de la audiencia". También: "Los estudiantes apreciaron mucho el respeto y la preocupación que D. Nicolás manifestaba hacia ellos, algo que no habían apreciado en otros profesores extranjeros" En estos comentarios se pone de manifiesto una característica de Cabrera, que yo tuve la posibilidad de valorar también, su sincero respeto por la inteligencia de los demás. En el año 1969 D. Nicolás recibió, del Instituto Politécnico Nacional de México, la invitación como experto de la UNESCO, para pasar allí un sabático. Una vez incorporado dividió su tiempo ente el Politécnico y el Instituto de Física de la UNAM. Su liderazgo inteligente y entusiasta, contribuyó a dar un notable impulso, en dichas instituciones, a la física del estado sólido y de las superficies, impulso que se extendió a otras universidades y centros de investigación de

México y, también, de Venezuela, país en el que Cabrera había estado de sabático en 1963 invitado por el Prof. Gonzalo Castro Fariñas, de la Universidad de Caracas. Como se puede concluir de lo expuesto, su presencia en Latinoamérica tuvo un efecto muy positivo que se resume en una frase de su, ya varias veces citados, discípulo M.José Yacamán: " El Prof. Cabrera jugó un papel clave en el desarrollo de la ciencia de las superficies en Latinoamérica. Su influencia fue muy profunda y hubieron de pasar muchos años antes que su efecto fuese totalmente absorbido por la comunidad."

El recuerdo de España, como para la gran mayoría de los emigrados, no había desaparecido en D. Nicolás, y menos aún, si cabe, en Carmen, su mujer. Los contactos con otros científicos españoles, como Velayos y Bru, residentes en España, y otros, como Ochoa, residentes en Estados Unidos, eran frecuentes. Sus éxitos personales como científico y como organizador, eran conocidos y valorados en círculos diversos, entre los que se encontraban algunos que adquirieron, dentro del régimen de Franco, un peso notable en la década de los sesenta. El ministro Villar Palasí, fue, en mi opinión, un hombre sinceramente preocupado por la Universidad y consciente de la necesidad de que en ésta se impulsase la actividad investigadora. Supongo que debió llegar a la conclusión, que era muy complicado hacer un cambio profundo contando con las estructuras universitarias y de investigación existentes, y que sería más rápido y eficaz crear universidades nuevas en donde, al menos en algunas áreas, se pudiesen incorporar profesionales de prestigio, sorteando los efectos nocivos de los clanes, casi familiares, tradicionales en la universidad española. No sé si estas fueron las razones. A lo mejor fue necesario, para crear las universidades autónomas, convencer a los más recalcitrantes del régimen que sería bueno tener centros donde educar a los hijos de sus élites, lejos de los grandes centros masificados y políticamente conflictivos. Lo cierto es, que directamente y a través de asesores y amigos comunes, Villar Palasí tomó contacto con diversos científicos de relieve internacional, entre los que se encontraba Cabrera. Se le ofreció crear un departamento de física en la Universidad Autónoma de Madrid. Recientemente, José Manuel Sánchez Ron ha publicado un excelente libro, que bajo el título "Cincel, martillo y piedra", nos habla de las vicisitudes de la ciencia en España, durante los siglos diecinueve y veinte. En las últimas páginas del libro, como corresponde a su proximidad histórica, hay un apartado que bajo el título "Regresos y "Autonomías": El caso de Nicolás Cabrera" permite que nos acerquemos a aquel entonces. Sería presuntuoso por mi parte, escribir la

historia, cuando Sanchez-Ron, dedicado a la historia de la ciencia, ha reconstruido aspectos importantes de aquellos momentos, de forma muy acertada. Hay varios documentos que muestran tres aspectos que, por su relevancia, paso a destacar: el interés claro del ministro, por la creación de un nuevo tipo de universidad en el sentido apuntado previamente. La imposibilidad de obtener, por parte de los posibles candidatos a la incorporación, unas garantías de futuro razonables como para dejar situaciones estables y profesionalmente sólidas, en otros países; finalmente, la audacia de D. Nicolás Cabrera, convencido de que tenía un compromiso con el desarrollo de la física en España.

El primero de los aspectos mencionados, se recoge en una carta del propio Villar Palasí. El que fuera Catedrático de Química Inorgánica, y durante un tiempo Rector, de la Universidad Complutense, amén de Presidente del CSIC, Enrique Gutiérrez Ríos, había hecho diversas aproximaciones a Cabrera en la década de los sesenta. Consideraba Gutiérrez Ríos, y así se lo hacía saber a Cabrera en una carta fechada el tres de Junio de 1968, que la creación de una segunda universidad en Madrid, en la que los catedráticos podrían ser nombrados por designación directa, era una buena oportunidad, y que el ministro le había pedido que le hiciera, en su nombre, una serie de ofrecimientos para que se incorporase, cuanto antes, a la nueva universidad. A D. Nicolás le pareció muy interesante la proposición, por lo que contestó ilusionadamente, entre muchas otras cosas, lo siguiente: "Creo sinceramente que tanto fuera como dentro de España se podría reunir un número de científicos y humanistas sobresalientes que serían capaces de organizar una Universidad de primera línea en el plano internacional". Tras conocer la carta de Cabrera, el ministro le comentaba por escrito a Gutiérrez Ríos, que le había impresionado muy positivamente el párrafo citado de la carta de D. Nicolás. Para Villar Palasí, la recogida de científicos y humanistas sobresalientes, era el espíritu con que quería empezase la nueva universidad, "para que se crease -escribía el ministro- un cierto espíritu entre los catedráticos más acorde con la dedicación tal como lo entienden fuera y bastante diferente a como lo entendemos aquí". Los que hemos vivido aquellos tiempos sabemos lo difícil que era dar garantías sólidas para proyectos de futuro en un régimen, cuyo final empezaba a vislumbrarse. Importantes figuras de la ciencia, como Ochoa y Grande Covián, amigos personales de D. Nicolás, fueron contactados por las autoridades del Ministerio de Educación para que de una u otra forma se embarcasen en la aventura. Tal como consta en la documentación que Sánchez-Ron aporta, ambos científicos mantuvieron una interesante

correspondencia con Cabrera, en la que se vierten opiniones que ayudan a clarificar lo acaecido posteriormente. En noviembre de 1968, Ochoa le escribía a Cabrera. "Creo que puedo resumir mi impresión diciendo que definitivamente algo se está poniendo en movimiento y que, si no se pierde de vista el objetivo final y no hay equivocaciones, algo saldrá de ello. Mientras se tenga esperanza, continúo pensando que se debería ayudarles". Ya en junio de 1969, cuando D. Nicolás casi había decidido su venida, Grande Covián escribía sobre las dificultades que él veía: " Las dos más graves a mi juicio -decía Grande- son, la inercia de la organización universitaria y la reacción por parte de muchos de nuestros colegas, que, aunque digan otra cosa, están perfectamente satisfechos con la situación" Tanto Ochoa como Covián, consideraban de gran interés la venida de Cabrera como avanzadilla que permitiese a otros verificar la situación real.

Ochoa, con amistad y buen criterio, le aconsejaba aceptar la oferta española en principio por un tiempo limitado. "Mantener -le decía- tu posición aquí, con un permiso temporal, me parece esencial. Hoy por hoy, no aconsejaría a nadie que dejase de mantener un pie firmemente anclado aquí. En esas condiciones creo que podrás hacer el experimento y hasta me gustaría que lo hicieses por lo que ello supondría para España si .pitase. ". Grande Covián, también le animaba a dar el paso. "Temo mucho -escribía Grande a Cabrera- que una vez allí tuviese que perder la mayor parte del tiempo en luchar contra la oposición que vamos a encontrar. Creo que quizá tú, por ser los físicos gente más civilizada, podrías tener menos dificultades en este sentido.". Pienso que los puntos de vista recogidos aquí, y en otros documentos existentes, muestran a las claras cual era la situación desde el punto de vista de unos científicos prestigiosos que conocían bien el estado, en aquel tiempo, de las universidades y centros de investigación españoles. Como llegó a escribir Ochoa, "los primeros pasos deben ir encaminados a crear el personal científico y académico que prácticamente no existe". Considero, que el conocimiento de ésta época, agiganta la figura y la obra de D. Nicolás. Tuvo, como había hecho otras veces a lo largo de su vida, la audacia para lanzarse en pos de una reconstrucción en la que había soñado durante largos años, y el tesón para afrontar fracasos y vencer dificultades. Su labor en España, está ahí, para quien quiera verla. Yo he participado de forma directa, ya que me incorporé al Departamento de Física de la UAM en sus comienzos, en la apasionante aventura que Cabrera emprendió. Su capacidad de organización y liderazgo científico, hubieron de manifestarse a tope para contratar el personal necesario, de entre los científicos jóvenes que trabajaban en España y en el extranjero. Tenía una notable facilidad

para convencer y entusiasmar. Defendía la contratación temporal argumentando que un científico joven no debía nunca amarrarse a una situación fija. En los primeros tiempos, y mientras existió el soporte de Villar Palasí y del primer rector de la UAM, Sánchez Agesta, Cabrera dispuso de capacidad de maniobra como para crear un Departamento joven e ilusionado, en el que se vivía con pasión la aventura. Como es natural, a pesar de la inteligencia y capacidad científica de las personas que se incorporaron, quizás por ello, no faltaron los conflictos, ni las pequeñas mezquindades, pero eso no llegaba, al principio, a enturbiar el clima de efervescencia científica y creatividad que allí se respiraba. D. Nicolás estaba siempre presente. Visitaba los laboratorios en cualquier momento del día, sábados, y a veces domingos, incluidos. Los seminarios, uno o dos, todas las semanas, eran prácticamente de asistencia obligada. D. Nicolás se sentaba en primera fila, y era fácilmente detectable el respeto, a veces reverencial, que originaba en el conferenciante. Cualquier pregunta, por inocente que fuera, originaba tensión en el preguntado, que, sin duda, se devanaba los sesos tratando de adivinar qué reflexión profunda se escondía por ejemplo, en "qué es lo que había representado en el eje de las equis". Le agradaba comer con la gente joven del Departamento en los "chiringuitos" que se montaron al socaire de las obras en el campus de Cantoblanco, y posteriormente en los restoranes de las cercanías y comedores universitarios. Para muchos de nosotros, departir con una figura como D. Nicolás esos ratos de solaz, era una vivencia muy positiva. Se organizaron campeonatos de ping-pong, en los que él participaba con un gran entusiasmo. Esta sencillez en su comportamiento, no era muy frecuente en los estereotipos de catedrático de la época. Pero creo que, para la mayoría de nosotros, su postura afectuosa y sencilla, incrementaba nuestro respeto y admiración hacia su persona. Pienso que eso es algo que solo lo pueden mantener los grandes hombres y mujeres, que se nos aparecen como son, en su grandeza, sin necesidad de los parapetos de distanciamiento y la estudiada superioridad, que frecuentemente se encuentran en la gente que no alcanza la verdadera grandeza humana. Alguien escribirá algún día, sin el apasionamiento del que ha participado, la historia de aquel Departamento de Física, pero nada se podrá comprender sin aquella figura que componía D. Nicolás con su sombrero, sus singulares gafas de sol, y la cartera con la memoria anual del Departamento, como única arma, dispuesto a enfrentarse con colegas, autoridades y burócratas, en su lucha por hacer crecer, primero, y tratar de evitar su destrucción, después, el edificio que había construido con esfuerzo. Es imposible para mí, resumir la historia del Departamento, más tarde División, de Física de la UAM. Tal como

presumía Grande Covián, algunos sectores de la comunidad académica establecida, miraban con más recelo que complacencia, la empresa recién comenzada. Cabrera tuvo que ver pronto que algunos de los puntales de su proyecto, como Luis Bel y Oriol Bohigas se volvían a sus centros de procedencia en el extranjero. Las dificultades y trabas administrativas se potenciaban con los días de ebullición política que anunciaban el final de un régimen. Cabrera no tiró nunca la toalla, y fue extraordinaria su defensa de los miembros del departamento represaliados por motivos presuntamente políticos. Estaba convencido de que podía surtir efecto, incluso ante aquellas autoridades, la apelación a la calidad científica de los expedientados. Recuerdo, con cierta amargura, las reuniones en el despacho del rector Julio Rodríguez, a las que D. Nicolás acudía con algunos miembros del departamento, para protestar por los diversos motivos que hacían casi imposible la actividad académica en el campus. Y la actitud altiva, por no emplear otros términos, de aquel, sabedor de su próximo nombramiento como ministro. En aquellos tiempos, y a pesar de todos los desgraciados avatares que hubo de pasar, D. Nicolás estaba persuadido de que lo que había hecho no tenía marcha atrás, y que había acertado en su decisión de venir a España, en el momento y circunstancias que lo hizo. Es cierto, y así lo recoge su hijo Blas en una breve biografía de su padre, que en 1973 estuvo a punto de volverse a Estados Unidos. Las dificultades eran enormes, afectando incluso a su posición como catedrático contratado. Sin embargo, la tenacidad y espíritu de lucha que había heredado de su padre, le hicieron afrontar la situación, pensando, sobre todo, en la gente joven, para la que había creado un ambiente de investigación inédito, hasta entonces, en España. Uno puede pensar que aquella aventura tuvo un final. El ataque frontal por parte del sistema de alguno de sus aspectos fundamentales, como la capacidad de contratación por el jefe de departamento, era imposible de superar, ya que obligaba a la búsqueda de una cierta estabilidad a través de la vía general del funcionariado docente. Ello originó tensiones adicionales, dada la personalidad fuerte de muchos de los implicados en la "numerización". Al mismo tiempo se producían los grandes vaivenes y cambios políticos que nos depararon los setenta. Pero, pasando a través de esos tiempos convulsos, la semilla plantada en la ciencia española no dejaba de crecer, y se fueron destacando grupos activos en las distintas universidades y centros de investigación. Como había deseado Ochoa en la carta, antes mencionada, dirigida a Cabrera, el experimento había ‘pitado’, con todo lo que ello significaba para España.

Permítanme terminar con algunas apreciaciones más personales. Estuve próximo a D. Nicolás hasta el final de sus días en 1989. Fui testigo directo de su decadencia, de la cual era plenamente consciente, habida cuenta de la enfermedad hereditaria que sufría. "Dichosa entropía" decía, cuando se evidenciaban los huecos de su memoria. A lo largo de todos esos años, mi sensación ante su presencia fue la de estar ante un gran hombre. Es una sensación que no he sentido, de forma tan clara, ante ninguna otra de las personas que he tratado. Cabrera recibió reconocimientos y homenajes de diversa índole a lo largo de sus últimos años. Entre estos cabe destacar, por su carácter científico, el número especial que la revista Philosophical Magazine A le dedicó cuando cumplió setenta años, número al que contribuyeron con artículos originales algunos físicos eminentes. También en 1982, se celebró en la Universidad Menéndez Pelayo en Santander, un curso en su honor. La Universidad Autónoma le nombró Profesor Emérito, y recientemente le ha dedicado una calle. Desde hace siete años, se celebra en el mes de septiembre una escuela internacional sobre temas relacionados con la materia condensada, que lleva el nombre de Escuela Internacional "Nicolás Cabrera". Este evento, que organiza el Instituto de Ciencia de Materiales "Nicolás Cabrera", ha alcanzado un notable prestigio internacional. Creo que estas actividades contribuyen, como pequeñas muestras de gratitud a su obra, a que su memoria se mantenga viva en una comunidad que le debe tanto. En sus últimos años, no recibió, en mi opinión, los honores que merecía. Era un hombre sencillo y modesto al que le costaba incomodar a los demás. Quizá por eso fue fácil, para muchos, no sentir su olvido.

No buscaba el halago ni halagaba, y en su tumba está escrito: “Nicolás Cabrera Sánchez, FISICO, Científico de Gran Humanidad.”

Sebastián Vieira
Catedrático de Física de la Materia Condensada

Referencias de algunos artículos científicos, especialmente importantes, del Prof. Cabrera, que han sido comentados en el curso de la conferencia:

[1] Cabrera N and Mott N F, 1999, *Rep. Prog. Phys.* **12**, 63.

[2] Burton W C, Cabrera N and Frank F C, 1951, *Trans. Roy. Soc. (London)* **A243**, 299.

[3] Cabrera N, Celli V and Manson R, 1969, *Phys. Rev. Letters* **22**, 346.

[4] Cabrera N, Celli V, Goodman F O and Manson R, 1970, *Surf. Sci.* **19**, 67.

LISTA DE PUBLICACIONES DE DON NICOLÁS CABRERA

1. **CABRERA B.,** VELAYOS S, and CABRERA N**.**
Constantes magnéticas de algunos sulfatos octohidratados de las tierras raras.
Boletín Ac.Ciencias, Madrid **I**, nº 2, (1935) 1.

2. **CABRERA N.**
Sur la perturbation d'un problème de valeurs propres por déformation de la frontière.
Comptes Rendus **208**, 1175 (1938).

3. **CABRERA N.**
Sur la loi de multiplication des matrices representatives des operateurs différentiels linéaires.
Comptes Rendus **208**, 261 (1939).

4. **CABRERA N.**
Sur une modification de la méthode des franges de superposition pour mesurer des petites differences d'épaisseur des étalons optiques
Comptes Rendus **212**, 78 (1941).

5. **CABRERA N.** TERRIEN J**.**
Sur les franges de superposition de deux étalons optiques a lames parallelès.
Revue d'Optique **20**, 35 (1941).

6. **CABRERA N.**
Sur le retard d'un monomètre pour les basses pressions.
Revue Scientifique **80**, 317 (1942).

7. **CABRERA N.**
Problèmes de valeurs propes avec une frontière à distance finie. Perturbation de la frontière.
Bull. Analytique du C.N.R.S. Nº **7**, 15589 (1944).
(Diplôme de Docterur es Sciences Physiques).

8. **CABRERA N.**
Sur les propiétés optiques des couches minces d'aluminium, leur évolution dans l'air.
Comptes Rendus **218**, 994 (1944).

9. CABRERA N.
Sur l'oxidation de l'aluminium et l'influence de la lumière.
Comptes Rendus **220**, 111 (1945).

10. CABRERA N.
Sur les propiétés optiques des couches métalliques minces.
Journal de Physique **VI**, 248 (1945).

11. MOREAU H., CABRERA N.
Nouveau prototype pour les subdivisions du mètre.
Revue d'Optique **23**, 255 (1945).

12. CABRERA N., MOREAU H.
Etude de subdivisions du mètre prototype T_4.
Travaux et Mémoires du Bureau International des Poids et Mesures.
Sèvres., France **XXI**. (1945).

13. CABRERA N.
Sur la constante diélectrique des métaux.
Comptes Rendus **22**, 134 (1946).

14. CABRERA N.
Sur la structure des couches solides minces.
Comptes Rendus **222**, 950 (1946).

15. CABRERA N., TERRIEN J.
Retard d'un manomètre de Knudsen.
Revue Scientifique **84**, 224 (1946).

16. CABRERA N., TERRIEN J**.**
Obtention des couches métalliques minces.
Procès verbaux du Comité International des Poids et Mesures Paris **12**, 5 (1946).

17. CABRERA N., TERRIEN J**.**
Manomètre de Knudsen.
Mesures, Paris **12**, 5 (1946).

18. CABRERA N., TERRIEN J., HAMON J.
Oxydation de l'aluminium en atmosphère sèche.
Comptes Rendus **224**, 1958 (1947).

19. CABRERA N., HAMON J.
Oxydation de l'aluminium à haute temperature.
Comptes Rendus **224**, 1713 (1947).

20. CABRERA N., HAMON J.
Oxydation de l'aluminium en atmosphère humide.
Comptes Rendus, **225**, 59 (1947).

21. CABRERA N.
Perturbation des conditions aux limites.
Cahiers de Physique Paris. Nº **31-32**, 24 (1948).

22. CABRERA N.
Sur l'oxidation de l'aluminium à basse temperatura.
Revue de Métallurgie, Paris XLV, **86** (1948).

23. CABRERA N., TERRIEN J.
Sur la structure et les propiétés optiques des couches métalliques minces.
Revue d'Optique **28**, 635 (1949).

24. CABRERA N.
Oxidation of metals at low temperatures and the influence of light.
Phil.Mag., London **40**, 175 (1949).

25. CABRERA N., MOTT N.F.
Theory of the oxidation of Metals.
Reports on Progress in Physics, London XII, **163** (1949).

26. BURTON W.K., **CABRERA N.**,FRANK F.C.
Role of dislocations in crystal growth.
Nature, London **163**,398 (1949).

27. BURTON W.K., **CABRERA N.**
Crystal growth and Surface structure, I.
Discussions of Farady Society, London **5**, 33 (1949).

28. CABRERA N., BURTON W.K
Crystal growth and Surface structure,II.
Discussions of Faraday Society, London **5**, 40 (1949).

29. CABRERA N.
Surface diffusion in sintering of metallic particles.
J. Metals **188**, 677 (1951).

30. CABRERA N., MOREAU H.
Etalonnages et calibrages.
Travaux et Mémoires du Bureau International des Poids et Mesures.
Sèvres., Frances **XXI**, (1945).

31. VOLET C., **CABRERA N.**
Deux métodes interférométriques.
Revue d'Optique **30**, 169 (1951).

32. CABRERA N.
Evaporation and mobility of naphthalene molecules.
Nature **167**, 766 (1951).

33. BURTON W.K, **CABRERA N.,** FRANK F.C.
The growth of crystals and the equilibrium structures of their surfaces.
Phil. Trans. Royal Soc., London **243**, 299 (1951)

34. **CABRERA N.**
Structure des surfaces et leur absortion.
Zeit. für Elektrochemie **56**, 1043 (1952).

35. **CABRERA N.**
Propiétés optiques des couches multiples alternées.
Comptes Rendus **234**, 1043 (1952).

36. **CABRERA N.**
Propiétés optiques des couches multiples alternées en nombre limité.
Compes Rendus **234**, 1146 (1952).

37. **CABRERA N.**
Macroscopic spirals and the dislocation theory of crystal growth.
J. Chem. Phys. **21**, 1111 (1953).

38. **CABRERA N.**, LEVINE M.M. and PLASKETT J.S
Hollow dislocations and etch pits.
Phys.Rev. **96**, 1153 (1954).

39. **CABRERA N.**
On the dislocation theory of evaporation of crystals.
Phil. Mag. **1**, 450 (1956).

40. **CABRERA N.**
La germination des piqûres d'attaque et des germes d'oxide.
J. de Chimie Physique, Paris, p. 675 (1956).

41. **CABRERA N.**
The oxidation of metals.
En Semiconductor Surface Physics.
University of Pennsylvania Press (1957) p. 327.

42. COMENAR R.V., **CABRERA N.**
Properties of zinc and cadmium whiskers.
J.App. Physics **28**, 1360 (1957).

43. COLMENAR R.V., PRICE B. and **CABRERA N.**
Properties of zinc whiskers.
Growth and Perfection of Crystals. Doremus et al., editors (j. Wiley, 1958) p. 204.

44. VERMILYEA D. and **CABRERA N.**
The growth of crystals from solution.
Growth and Perfection of Crystals. Doremus et al., editors (J. Wiley, 1958) p. 393.

45. CABRERA N.
The structure of crystal surfaces.
(Kingston Discussion of the Faraday Society)
Paper nº 1, 16-22, Aberdeen Scotland, Faraday Society (1959).

46. CABRERA N.
On the role of dislocations in the reactivity of solids.
The Surface Chemistry of Metals and Semiconductors. H. Gatos, editor (J.Wiley & Sons, 1960) p. 71-81.

47. KINZER G.T. and **CABRERA N.**
Collision of atoms with crystal surfaces.
Bull. Amer. Phys. Soc.II. 6, 337 (1961).

48. CABRERA N.
Kinematic theory of crystal dissolution.
Reactivity of Solids. De Boer, ed. (Elsevier, Amsterdam, 1961) p.3.

49. CABRERA N. and COLMENAR R.V.
Theory of the crystal growth from the vapor.
Capítulo en the Art and Science of Growing Crystals. J.J. Gilman, editor (J.Wiley, N.Y. 1963) pp. 3-28.

50. ATKINSON W. and **CABRERA N.**
Theory of the motion of imperfections in lattices.
Bull. Amer. Phys. Soc. II. **8**, 204 (1963).

51. CABRERA N.
On the stability of the structure of crystal surfaces.
Symposium on Properties of Surfaces (ASTM Science Series nº 4, Special Publication nº 340). American Soc. for Test Materials, Philadelphia, 1963, pp. 24-31

52. CABRERA N.
Sur le processus de formation des couches minces et les déformations et tensions qui en résultent.
Mémoires Scientifiques Rev. Metallurg. **LXII**, 205 (1965).

53. ATKINSON W. and **CABRERA N.**
Motion of a Frenkel-Kontorowa dislocation in a one-dimensional crystal.
Phys. Rev. **138**, 763 (1965).

54. CABRERA N.
The equilibrium of crystal surfaces.
Proc. Int. Conf. on Phys. And Chem. (Brown University).
Surface Science **2**, 1967.

55. **CABRERA N.**
Algunas consideraciones sobre el estado actual de la Física del Sólido.
Primer Congreso Latinoamericano de Física, Oaxtepec. México, 29 de Julio al 2 de Agosto de 1968.

56. **CABRERA N.**, VELLI V. and MANSON R.
Theory of Surface scattering and detection of surface phonon.
Phys. Rev. Lett. **22**, 346 (1969).

57. **CABRERA N.**
Notes on Surface Science.
Lectures to the Latin American School of Physics. México, 1968, Libro Publicado (1969).

58. **CABRERA N.**
Sur la théorie de la dispersion superficielle des cristaux.
Colloques Int. CNRS, Nº 187, P. 141 (CNRS, Paris VII, 1970).

59. **CABRERA N.**, CELLI V., GOODMAN F.O. and MANSON R.
Scattering of atoms by solid surfaces I.
Surface Science **19**, 67 (1970).

60. **CABRERA N.**
On mixed volume and surface diffusion problems.
Contribución a la Conferencia on Crystal Growth, Whashington, D.C. Agosto 1969.
Publicado en J. Crystal Growth (1970).

61. GILMER G.H., CHEZ R. and **CABRERA N.**
An analysis of combined surface and volume diffusion process in crystal growth.
H. Cryst. Growth. **8**, 79 (1971).

62. **CABRERA N.**, GOODMAN F.O.
Summation of pairwise potentials in gas-surface interactions calculation.
*J. Chem. Phys. **56**, 4899 (1972).*

63. GOODMAN F, LIU W.S. and **CABRERA N.**
Model for the repulsive elastic scattering of atoms by solid surfaces.
J. Chemical Phys. **57**, 2698-2702 (1972).

64. SOLANA J, MARIN, **CABRERA N.**
The scattering of the atoms from solid surfaces.
Proceeding of the XIII Solid State Conference (Manchester, 1972).

65. GARCIA N., SOLANA J. and **CABRERA N.**
An alternative method to calculate surface states in crystals.
*Surf. Sci. **38**, 445-460 (1973).*

66. SOLANA J., and **CABRERA N.**
The vibrational properties and scattering of atoms from surfaces.
En Proc. Colloque de Physique et Chimie des Surfaces (Brest, 1973).

67. SOLANA J., and **CABRERA N.**
The vibrational elastic scattering from crystal surfaces.
En Int. Conf. on surface Phenomena (Madrid, 1973).

68. SOLANA J., **CABRERA N.**
Molecular beam scattering by surfaces.
Inter. School of Physics "Enrico Fermi" (Varenna, 1973). En Dynamics of Solid Surfaces, F.O. Goodman editor (Compositori, Bologne, 1975).

69. GARCIA N., KESMODEL L.L., SOLANA J and **CABRERA N.**
New interpretation of electron diffraction data for Al in terms of Lennard-Jones type surface states resonances.
Lawrence Berkeley Laboratory Bulletin 3764 (1975).

70. ROJO J.M., SOLANA J. and **CABRERA N.**
Diffusion des atomes neutres.
Congreso de la Sociedad Francesa de Física (Dijon, 1975).

71. GARCIA N., IBAÑEZ J., SOLANA J. and **CABRERA N.**
Analysis of the methods proposed for computing the scattering of atoms from a hard corrugated surface model He/LiF(001).
Surf. Sci. **60** 385-396 (1976).

72. GARCIA N., IBAÑEZ J., SOLANA J. and **CABRERA N.**
On the "quantum rainbow" in surface scattering
Solid St. Commun. **20**, 1159-1163 (1976).

73. GARCIA N. and **CABRERA N.**
On the exact solution to the scattering of atoms from a hard corrugated Surface: application to stepped surfaces.
Proc. 7th Intern. Vac. Congr and 3rd Intern. Conf. on Solid Surfaces, Vienna (1977).
Eds. R. Dobrozemsky et al. (Berger and Söhne, Viena 1977). Vol. 1 págs. 379-386.

74. GARCIA N., and **CABRERA N.**
New method for solving the scattering of waves from a periodic hard surface: solutions and numerical comparisons with the various formalisms.
Phys. Rev. B **18**, 576-589 (1978).

75. GARCIA N., CELLI V., HILL N.R. and **CABRERA N.**
Ill-Conditioned matrices in the scattering of Waves from hard corrugated surfaces.
Phys.Rev. **18**, 5184-5189 (1978).

76. GOODMAN F.O., GARCIA N. and **CABRERA N.**
Scattering of atoms by surfaces with one-dimensional periodicity on the stationary sinusoidal hard-wall model.
Surf. Sci. **77**, 94-100 (1978).

77. GARCIA N, and **CABRERA N**.
"Analysis of the scattering of He beams from random impurities on crystalline surfaces"
In "Rarefied Gas Dynamics" Ed. By Sam S. Fisher, Vol. 74 of Progress in Astronautics and Aeronautics, (1981).

78. GARCIA N, and **CABRERA N**.
Roughening transition in the interface between superfluid and solid ^{4} He
Phys. Rev. B (RC) **25**, 6057-6059 (1982).

79. IBAÑEZ J., GARCIA N., ROJO J.M. and **CABRERA N.**
Study of disordered adsorbate layers on Nickel (001) by helium scattering.
Surf. Sci. **117**, 23-32 (1982).

80. **CABRERA N.**, GARCIA N. and SAENZ J.J.
Termodinámica de la transición rugosa: aplicación a la interfase ^{4}He superfluido-^{4}He sólido.
Libro dedicado al Prof. A. Durán Miranda, 83-103 (1984).

81. **CABRERA N.**, SOLER J.M., SAENZ J.J., GARCIA N. and MIRANDA R.
Thermodynamics of the roughening transition of stepped surfaces.
Physica **127B**, 175-179 (1984).

82. GARCIA N., SAENZ J.J. and **CABRERA N.**
Cusp points in surface free energy: faceting and first-order phase transitions.
Physica **124B**, 251-254 (1984).

83. SOLER J.M., GARCIA N., MIRANDA R., **CABRERA N.** and SAENZ J.J.
Large finite-size effect on the critical temperature of adsorbed layers: Xe on Pd [8(100)x(110)].
Phys. Rev. Lett. **53**, 822-825 (1984).